*C*3 SYMMETRIC DESIGNER LIGAND SYSTEMS FOR USE IN LEWIS ACID CATALYSIS

By

PATRICK CHRISTOPHER HILLESHEIM

A DISSERTATION PRESENTED TO THE GRADUATE SCHOOL
OF THE UNIVERSITY OF FLORIDA IN PARTIAL FULFILLMENT
OF THE REQUIREMENTS FOR THE DEGREE OF
DOCTOR OF PHILOSOPHY

UNIVERSITY OF FLORIDA

2010

To my family and friends

ACKNOWLEDGMENTS

If someone were to ask me what was the most challenging aspect of writing a dissertation, I would have to say accumulating a list of people to thank. How can one truly put to paper the innumerable contributions people have made for me over the last five years? As a chemist I can appreciate how the smallest of molecules combine to buildup into something greater than the individual; for this I wish to thank all the people which will remain nameless in this section. Were I to make a comprehensive list of acknowledgements, I fear it would be longer than my dissertation itself.

I would like to thank my advisor Dr. Michael Scott for five years of providing insight and knowledge into the world of chemistry, and for five years of putting up with my constant questions. I would also like to thank all the professors on my committee for their commitment of time. I would like to thank the University of Florida and the Department of Chemistry, for providing me with an education and for five years of a stipend.

I would like to specifically thank Dr. Khalil Abboud. Dr. Abboud went above and beyond the requirements of his position to help me succeed. Dr. Abboud is a man of, from my experience, infinite patience and understanding. I would like to thank him for helping me discover the field of crystallography and teaching me all I know about crystallography and structure solution.

I would like to thank all the friends both in the lab and out of lab who have stuck with me for these years. First, I would like to thank the Scott Group members, past and present: Eric, Candace, Anna, Dempsey, Gary, Nate, Mikey, and Joe. You guys taught me a great deal of chemistry and provided a sympathetic ear when needed. For my non-chemistry friends Jereme, Lauren, Lindsay, Natalie, Mike, and Steven for

pretending to understand my technical ramblings and seemingly endless complaints about work. A special thanks for the “usual” lunch crew of Pam, Matt, Candace, and Gary. I know I would not have lasted long here without looking forward to lunch each day with you guys. Wherever I may end up, know that you all always have a friend and a free couch to sleep on. An encore thanks to the “Rock Band” Crew. I never knew what talent was until I heard you all singing some Bon Jovi.

TABLE OF CONTENTS

page

LIST OF TABLES

LIST OF FIGURES

Abstract of Dissertation Presented to the Graduate School
of the University of Florida in Partial Fulfillment of the
Requirements for the Degree of Doctor of Philosophy

*C*3 SYMMETRIC DESIGNER LIGAND SYSTEMS FOR USE IN LEWIS ACID CATALYSIS

By

Patrick Christopher Hillesheim

December 2010

Chair: Michael J. Scott
Major: Chemistry

Several novel ligands were synthesized for use in either multi-dentate or sterically demanding Lewis acid catalysts. Using the triphenoxymethane platform ligand to preorganize three binding pockets, a new family of C_3 symmetric ligands were synthesized and characterized for future use as ligands for Lewis acid systems. Derivatives of the multi-dentate ligand systems were synthesized with the hopes of establishing a well-defined reaction pathway that can lead to simple synthesis of C_3 symmetric ligands for use in poly-metallic systems.

Ligand sets bearing chiral moieties were synthesized with the hopes of developing stero- or regio- selective sterically demanding catalyst systems. A tris-aminomethyl ethane (TAME) scaffolding ligand was employed to tether three binol moieties leading to formation of a well-defined, rigid chiral ligand set for use in sterically demanding Lewis acidic catalysis. Novel derivatives bearing various alkyl chains and scaffolding ligands were synthesized to modulate overall structural properties.

CHAPTER 1
INTRODUCTION

Catalysts are of great importance to both the industrial and academic research community. Many common products, from plastics to medicine, would not be available without the aid of catalysts. [1-3] From the most complex enzyme in nature to the simplest mono-protic acid, catalysts are ubiquitous in today's world.[7,8] Highly dependant on the reaction medium and conditions in which they are employed, catalysts are continuously being modified and tested to optimize their reactivity, turn over number, functional group tolerance, selectivity, yield, and recently are the focus of "green" chemistry.[9]

Of specific importance to the chemistry are Lewis acid catalyzed reactions, which continue to be prevalent in synthesis in both the academic and industrial setting.[2,3] First described by Lewis in the early 1900's, a Lewis acid is generally defined as a lone pair acceptor.[6] This definition encompasses proton donors (Brønsted acids) wherein H^+ acts as an acceptor for a lone pair. Pearson further expanded upon the concepts of Lewis in 1963, introducing the idea of hard and soft acids and bases. Pearson gathered data and tracked trends in reactivity to develop the concept of hard-soft acid base theory.[5,6] Hard-soft acid base theory is based on several atomic and molecular trends. In general, ions that have a large radius, low charge, and high polarizability are considered soft, while the opposite characteristics apply to hard. Hard acids prefer to bind to hard bases while soft acids prefer soft bases.[5] While Lewis and Pearson provided useful concepts and ideas regarding reactivity of the active acidic species themselves, much of the selectivity and usefulness of modern Lewis acid catalysts arises from careful design of ligand systems rather than direct modification of the acidic sites.[2]

Lewis Acid Catalysis

There are a large number of well-known Lewis acid complexes that are readily employed in common synthetic schemes. The mechanism for how Lewis acids function is not always the same and varies on reaction conditions and which acid is employed.[1,2,13,16] One way in which Lewis acids function is by changing the electronics of the substrate. This is most often accomplished by simple binding of the Lewis acid to a nucleophilic center (Figure 1-2). This depiction is straightforward as there are numerous theories to consider when looking at which site will bind the Lewis acid. Steric, electronic, and statistical abundance are all factors that can influence the reactivity of the bound substrate. Simply changing the Lewis acid from an early transition metal to a late transition metal can cause a shift in binding affinity of the acid, which in turn can cause a shift in reactivity.[17] Additionally, changes such as oxidation state of transition metal acids have been shown to affect equilibria of these bound complexes.[2,13,17]

Figure 1-2 depicts several of the various binding modes which have been observed for Lewis acids. Each different binding mode can lead to a different preference for a product, making control of the reaction difficult. There are a few strategies for promoting selectivity in reactions: use of chirally modified reactants or use of a chiral catalyst. Of these possibilities, the more facile solution is usually the synthesis of a catalyst that is chiral and ideally reuseable and recoverable. Catalysts are often complex, as many factors are involved in the design of a successful catalyst. Ligand design needs to balance a number of concepts: ease of synthesis, a well-defined chiral pocket, and functional groups that can stabilize intermediates.

Ligand Systems in Catalysis

Ligand design has been a focus for catalysis, with particular emphasis on design of chiral ligands.[1-3,11,13,17] Of the numerous ligands synthesized, there are a select few ligands which have gained special status. Referred to as “privileged” ligands, they are templates that are ubiquitous within modern ligand design (Figure 1-3).

Privileged ligands tend to have C_2 symmetry with symmetric binding arms.[18,19] This design was employed to limit the complexity of the catalytic system. By simplifying the ligand a number of complexities can be eliminated by limiting isomeric metal structures and bound substrate complexes.[18,19] It is presumptuous to believe that one catalyst can function well in all reaction conditions, thus simplistic design and synthesis of ligands can aid in finding the correct balance of electronics and sterics for certain reactions. The SALEN and BOX ligand systems are exemplary of this concept, as both are synthesized cheaply from a variety of commercially available starting material.[18,19] There are many factors which contribute to design and synthesis of a novel ligand structure. The aspect which binds all the factors together is that careful screening and interpretation of data is needed for any optimized catalyst.[1-3,13-19] Though there exist many volumes of work written about the field of catalysis, serendipity still seems to play a major role in finding the next privileged ligand system.[19]

Lewis Acid Catalyzed Reactions

Friedel-Crafts Alkylations and Acylations

First discovered by Charles Friedel and James Crafts in the 1877, certain Lewis acids ($AlCl_3$, $FeCl_3$, BF_3) can be used to promote a condensation reaction between variously substituted hydrocarbons.[25] The reaction conditions and specifics have been studied and optimized over the past 130 years, which has led to the development of a

wide variety of reactions including coupling reactions, polymerizations, aminations, sulfonations, and numerous more.[25-27] While there are countless literature examples of Friedel-Crafts chemistry, they can be broadly classified as either alkylations or acylations.

A common issue with a Friedel-Crafts reactions is that the catalyst is often used in stoichiometric amounts. Studies into the effect of catalyst loading show some generalizations.[25-28] Some studies indicate that maximum yield and reactivity is obtained with 100 mol% catalyst, with excess catalyst inhibiting reactivity. This problem becomes a real concern on the industrial scale where reactions can be measured in tons rather than milligrams as in the traditional academic lab. Widely employed as a synthetic step in many processes, there is a necessity for more evolved catalysts. Alkylation and acylation reactions that are stereo- and regio- selective are an area of great interest.[25] Significant work has focused on developing catalysts that span a broad field of reactivity. Recent reviews[26] describe certain lanthanides, polymer encapsulated transition metal species, ligand bound transition metals, and zeolites are transitioning towards catalysts that can be employed in low mol% and yield stereo- and regio-selective products.

Zeolites have been of increasing use in the fine chemicals and academic laboratories for synthesis of various chemicals. As such, many on-going studies are looking into the reactivity and scope of application for zeolites.[26] Zeolites are well-studied microporous materials mainly composed of aluminum and silicon.[26,29] One advantage that zeolites provide is that they can be employed as heterogeneous catalysts, and as such they can be recovered and reused. Some promising results have

been reported for the use of zeolites as catalysts. While most ligand-based catalysts afford selectivity based on a combination of electronics and sterics, zeolites afford selectivity by pore and channel size. By designing zeolites with specific pores and channels, selectivity of certain reactions are affected (Figure 1-4). While zeolites do show promising reactivity in the area of Friedel-Crafts acylations, much remains to be studied regarding the selectivity and ideal reactions conditions.

Homogenous catalysis of Friedel-Crafts acylations has also been the focus of much research. Most common Friedel-Crafts reactions are carried out by using stoichiometric amounts of reagents such as $AlCl_3$, BCl_3, or $FeCl_3$. This approach is unfavorable for both large scale industrial processes and pharmaceutical chemistry as it produces large amounts of waste and employs toxic chemicals. Even for the academic laboratory these conditions can prove ill suited due to intolerance of functional groups and lack of stereo- and regio- selectivity.[11,25-27] These simple Lewis acids are still used in the laboratory setting, however, mainly due to their cheap costs and ease of use. The simplest starting point would be to find a Lewis acid that can be used in lower mole percent. The work of Bandini et al. show that lower catalyst loading can be employed with group 13 Lewis acid compounds, specifically $InBr_3$ (Figure 1-5).[27]

Studies also involved the pre-complexation of aluminum species with chiral substrates. Casiraghi et al. showed that reacting $AlClEt_2$ with (-)-menthol helped promote stereo selective Friedel-Crafts acylations to phenolic compounds (Figure 1-6) ;[30] however, this advance was offset by the need for using equimolar amounts of catalyst and chiral substrate.

To incorporate the results from the previous works, newer metal species were employed, which functioned in lower mol%, along with addition chiral substrates to aid in selectivity. Further efforts to promote regio- and stereo- selectivity with Friedel-Crafts reactions led to the combination of Lewis acidic metal centers with privileged ligand sets (Figure 1-7).[11]

Copper-based systems have been successfully employed with a number of ligands for use in Friedel-Crafts reactions. Since the first example of a copper-containing ligand (Figure 1-7) was shown to promote Friedel-Crafts reactions, much work has been put into optimization of certain reactions, in some cases reaching up to 99.5% enantiomeric excess (ee).[11] Building upon the success of the copper-based BOX catalyst, the trisoxazilone ligand was used by Tang et al. to optimize additions of malonates to indoles.[31] To generalize the findings of numerous bodies of literature from the area, ligand design and choice of active metal center is key for promotion of high yield and high ee reactions.

Diels-Alder Reactions

Another common example of a reaction that benefits from the use of catalysts is the Diels-Alder reaction. While the scope of the Diels-Alder reaction is broad, here the development of Lewis acid-assisted Diels-Alder reactions will be the focus. An ideal set-up for reaction involves an electronically deficient dienophile reacting with an electron rich diene or vice-versa. This electronic matching is not always feasible in synthesis, thus a Lewis acid catalyst can be used to help overcome the barrier of reaction.[2,8,13] There is debate as to how a Lewis acid actually promotes a Diels-Alder reaction. One theory is that the Lewis acid acts by abstracting an electron from the diene, forming a cationic radical. This radical then reacts with the dienophile and propagates the reaction

(Figure 1-8).[2] The other theory involves formation of a dienophile-Lewis acid adduct, which changes the electronics of the compound by lowering the energy of the LUMO.[2,17] By binding the dienophile, the energetic gap between the diene and the dienophile lowers, allowing for better orbital overlap.

One of the earliest examples of an asymmetric Diels-Alder reaction was investigated by Koga et al. in 1979.[17,32] Reaction of an aluminum species with (-)-menthol produced a bound chiral aluminum species, which promoted reaction of cyclopentadiene with methacrolein (Figure 1-9). The proposed transition state shows the blocking of one face of the dienophile by the isopropyl group on the bound menthol species, favoring formation of the endo product.

Efforts to promote selectivity and ee led to the synthesis of more sterically defined chiral ligand sets (Figure 1-10). Wuff et al. synthesized and analyzed a variety of BINOL derivatives as catalysts for the reaction of cyclopentadiene and methacrolein.[33] With surprisingly low catalyst loading (0.5 mol%), selectivity of up to 97.7% ee was achieved with 100% yield. Conclusions from the work of Wuff suggest that better defined chiral pockets help impart selectivity to product formation.

Conjugate Additions

Conjugate addition reactions, or Michael Additions, are a powerful method for not only formation of C-C bonds but also introduction of a stereocenter.[34,35, 36] Conjugate additions are broadly defined as the addition of a nucleophile to double or triple bonds. The reaction is often accomplished with the aid of certain transition metals acting as both the source of nucleophiles (organgocuprates and alkyl zinc reagents) and additional metal salts acting as catalysts (Figure 1-11). While the field has been well developed over the years,[35] there are still many areas that are being researched.

As shown in Figure 1-11, three broad methods are employed: diasteroselective addition (DCA), enantioselective addition (ECA) , and catalytic enantioselective addition (CEA).[34] Of these general reactions, both DCA and ECA function on the same principle. Either beginning with, or with the addition of a chiral substrate, the desired product is formed in accord with specific reaction conditions being met. On the other hand, CEA is the more difficult aspect of conjugate additions as not only does it require catalytic activity, but also formation of desired product in high yield.

Conjugate addition via organolithium reagents requires the use of copper(I) salts. While the simplest of setups involve just mixing a metal salt with the nucleophile, typically low yields and ee are observed for these reactions.[35] Chiral phosphine ligands have been studied as chiral auxiliaries for ECA reactions. As with the previously mentioned inclusion of (-)-menthol, addition of a chiral phosphine substrate can aid by binding to the active metal center and then promoting selectivity through both sterics and electronic effects.[34-37] Figure 1-12 depicts typical ligands and ee found with selected systems. Phosphine-based ligands, which are sterically demanding and are chiral, show promising results with regards to CEA reactions.

Focusing briefly on the concept of ligand design with regards to promoting selectivity, the work of Jansen and Feringa provide a good view as to how careful design leads to good results.[38] The reaction of i-PrMgBr with cyclohexene-2-one showed good yield albeit poor ee (Figure 1-13). Stabilization of the magnesium salt by the oxygen favors a setup where the 4 position on cyclohexene-2-one is adjacent to the nucleophile.

Research Objectives

The goal of our research was development and implementation of novel ligands for use in various fields of Lewis acid catalysis. Two specific classes of ligands were designed: one ligand for use in multi-dentate Lewis acid catalyst systems and another for chiral sterically demanding Lewis acids. The field of multi-dentate Lewis acid catalysis suffers from a lack of established ligand systems that incorporate tri-metallic species within their architecture. Our goal was to establish a simple and modular synthetic scheme for easy derivitization of a ligand which incorporates tri-metallic species. The field of sterically-demanding Lewis acid catalysis has several well-defined catalyst motifs, yet none incorporate chial moieties into the structure. Our goal was synthesis of a sterically demanding ligand system which contains chiral moities to probe the affects of chiral active sites on Lewis acid assisted reactions.

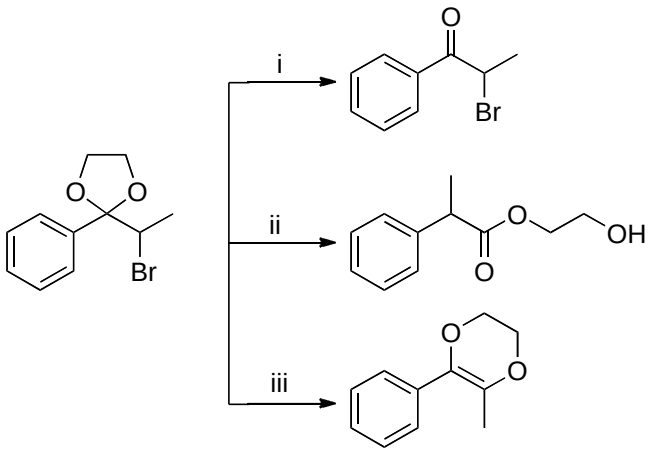

Figure 1-1. One starting molecule can yield various products depending on reaction conditions and reactive acidic species used. i) Brønsted acid ii) Hard Lewis acid iii) Soft Lewis acid.[2]

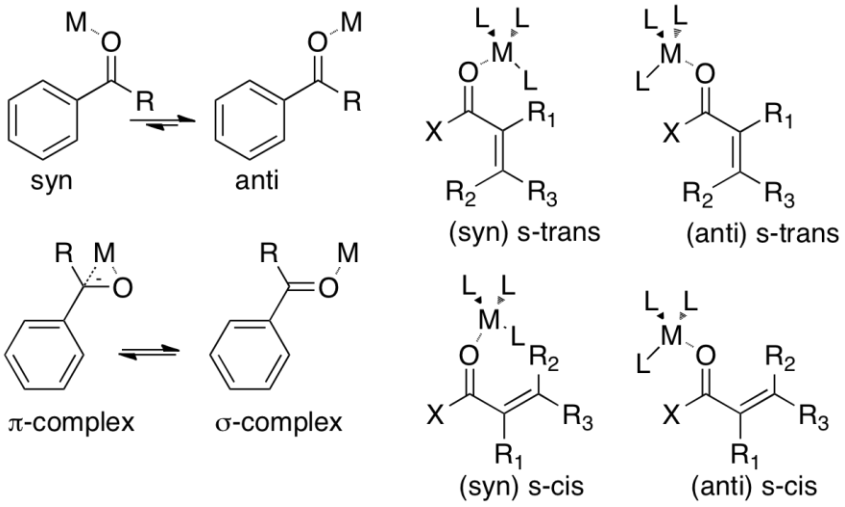

Figure 1-2. Lewis acids (M) bind to substrates in a variety of ways, changing both the reactivity and selectivity of certain reactions.[2,17] Varying ancillary ligands and functional groups (L, X, R) influences which form is preferred.

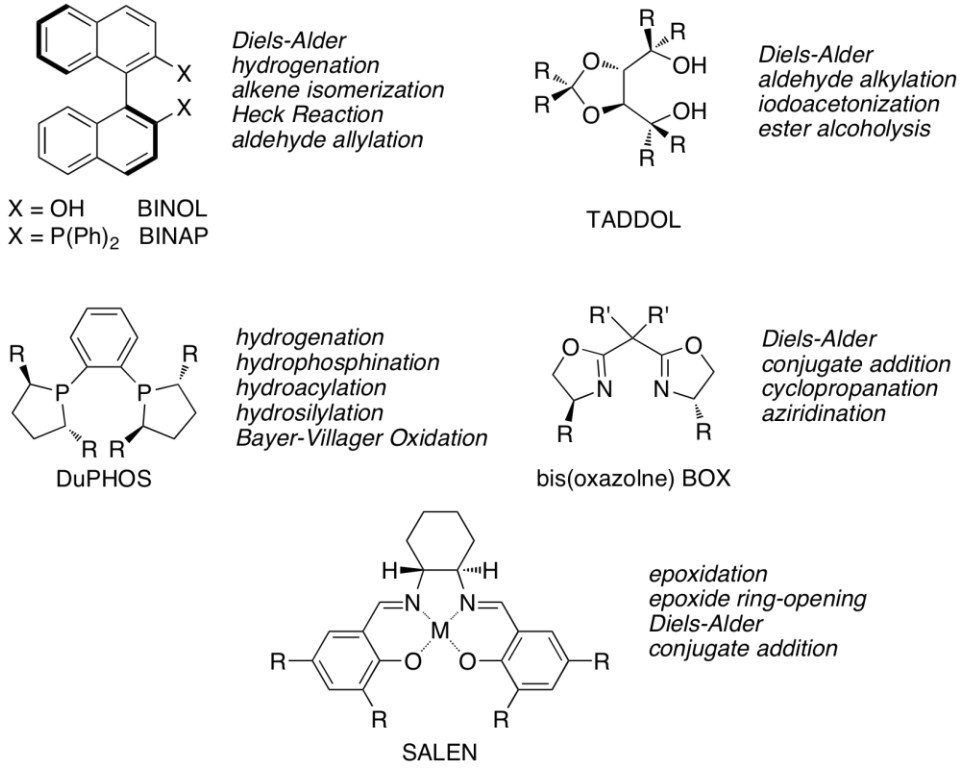

Figure 1-3. Examples of privileged ligand designs and common examples of reactions in which they are used.[18]

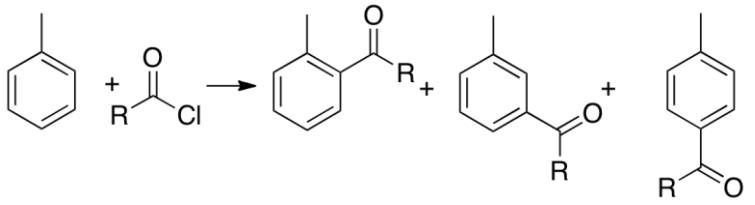

Figure 1-4. Friedel-Crafts acylation of toluene catalyzed by HBEA zeolite. Selectivity and yield is influenced by reaction conditions.[26,29]

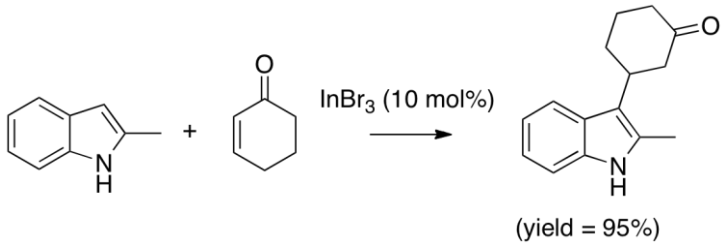

Figure 1-5. Alkylation of methyl indole with $InBr_3$.[27] Indium based catalysts can be used in smaller mol% than other group 13 species.

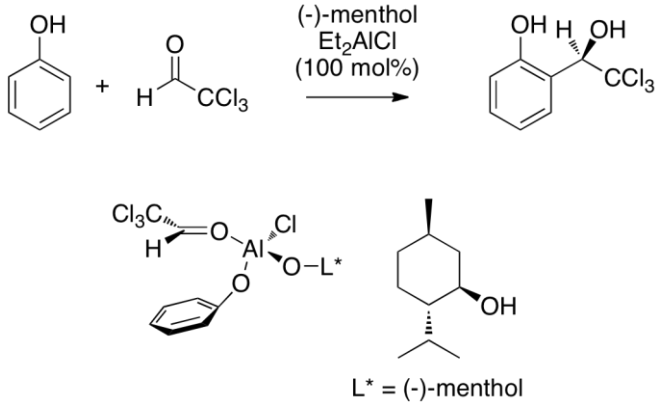

Figure 1-6. Coordination of (-)-menthol with a dialkylaluminum chloride showed surprising selectivity for alkylation of phenols.[11,30]

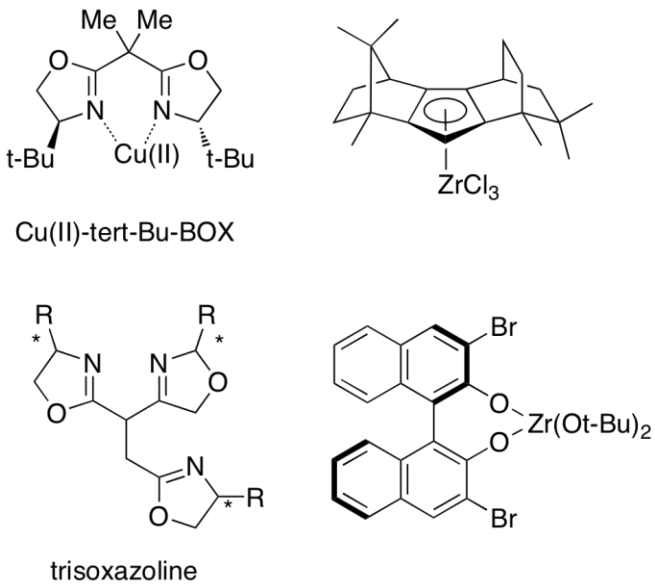

Figure 1-7. Ligands and catalysts used in selective Friedel-Crafts reactions.[11,30]

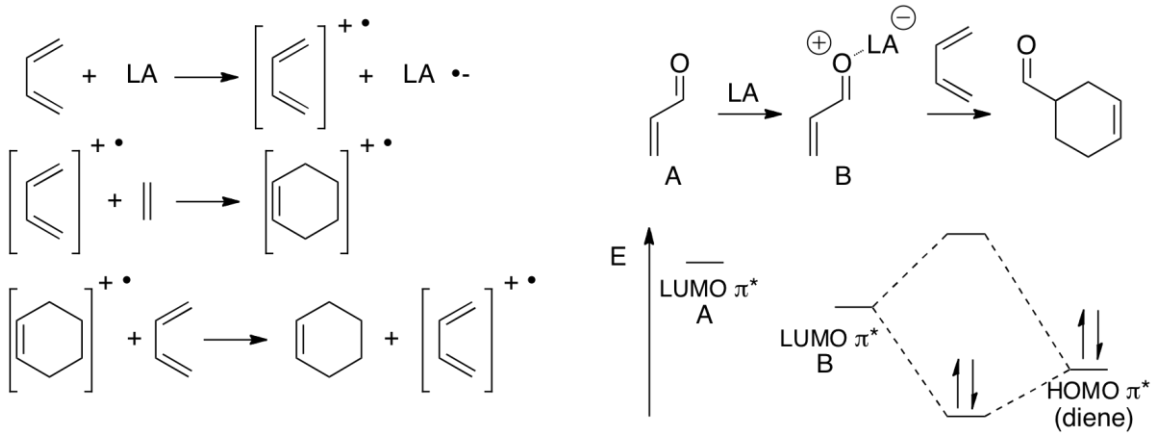

Figure 1-8. Depictions of both theories as to how Lewis acids act as catalysts for Diels-Alder reactions.

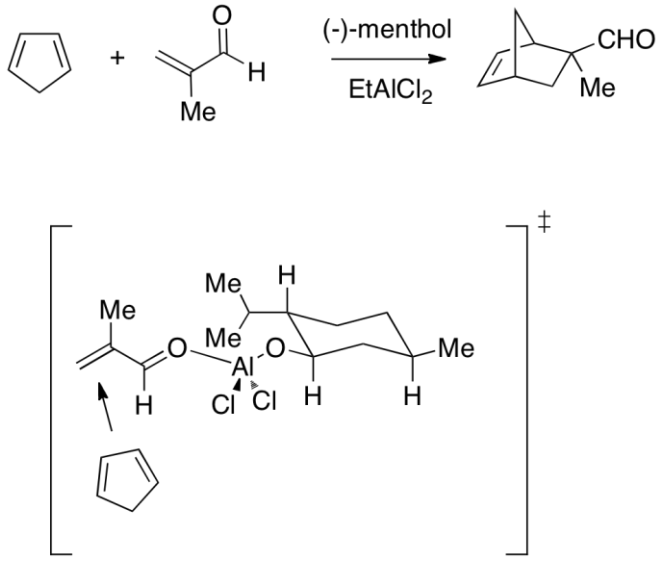

Figure 1-9. (-)-menthol bound to aluminum promotes selectivity via sterics.[17]

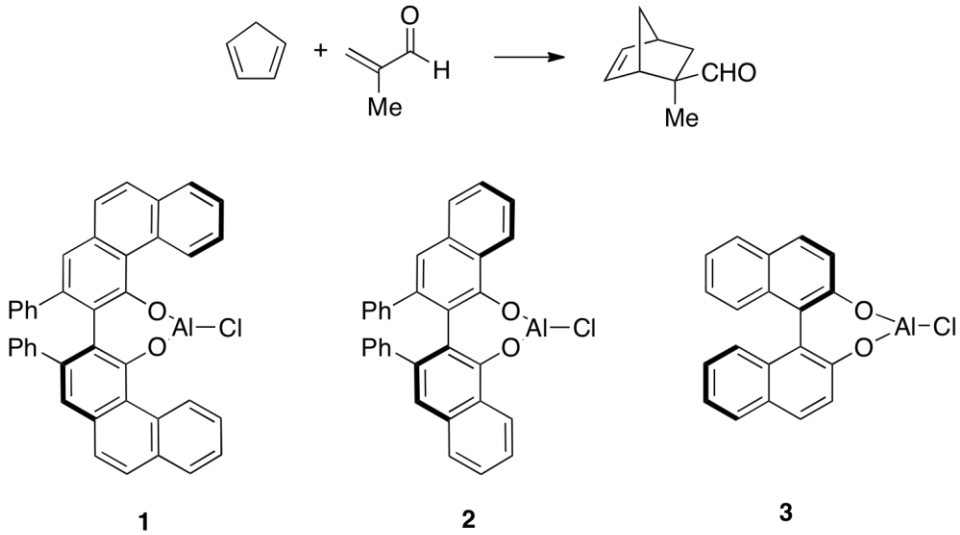

10 mol %	**1**	98/2 *exo/endo*,	97.8% ee, 100% yield
0.5 mol %	**1**	97/3 *exo/endo*,	97.7% ee, 100% yield
10 mol %	**2**	93/7 *exo/endo*,	5% ee, 84% yield
10 mol %	**3**	97/3 *exo/endo*,	23% ee, 99% yield

Figure 1-10. Series of chiral BINOL based ligands synthesized and studied by Wuff et al.[17]

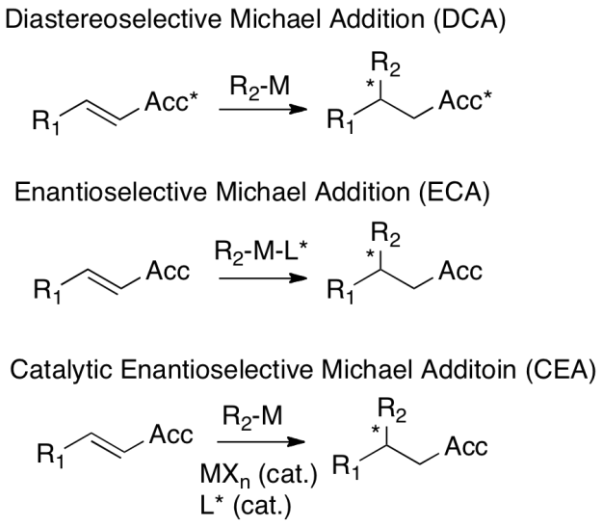

Figure 1-11. Strategies for stereoselective conjugate addition, where Acc is a conjugated group, and * refers to a chiral center.[34]

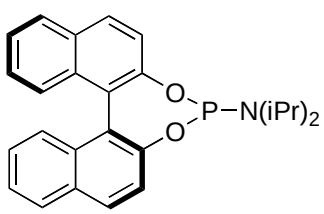

Feringa, 1996
L1.1

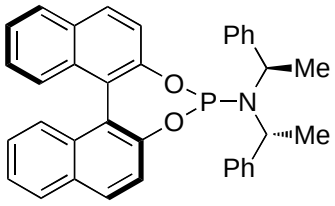

Feringa, 1997
L1.2

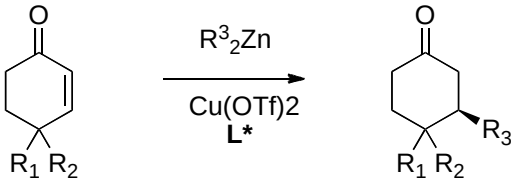

	Cu(OTf)2	R^3	L*		ee
$R_1 = R_2 = H$	3 mol%	Et	**L1.1**	6.5 mol%	63%
	2 mol%	Et	**L1.2**	4 mol%	> 98%
$R_1 = R_2 = Ph$	2 mol%	Et	**L1.2**	4 mol%	> 98%

Figure 1-12. Selected reactivities and phosphine based ligand sets employed for conjugate additions.[34]

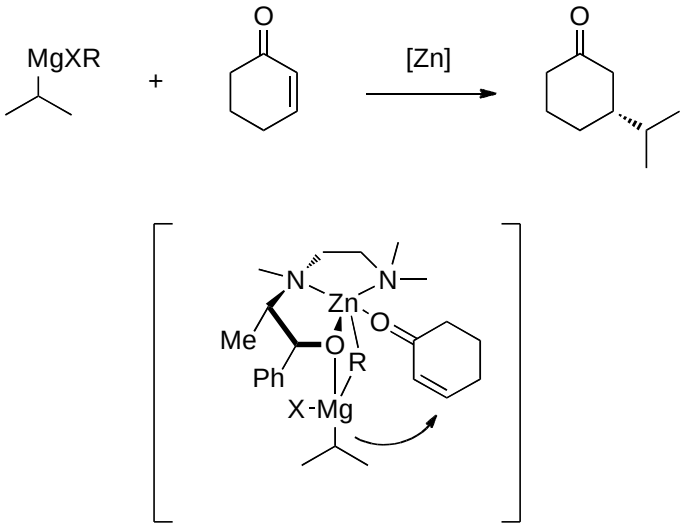

Figure 1-13. Stabilization of the incoming nucleophile by coordination to the ligand bearing a zinc atom helps promote selectivity.[35]

CHAPTER 2
BULKY DESIGNER LEWIS ACID CATALYSTS

Introduction

The pursuit of newer, more refined catalysts is a continuing area of research within both the academic and industrial setting. As discussed in the Introduction chapter, the recent focus of homogenous catalysis seems to be on ligand design which can promote stereo- and regio- specific reactivity in the substrate. In the late 1980's Yamamoto et al. began to expand the concept and utility of Lewis acid catalysts, beginning what is referred to as "Designer" Lewis acid catalysts.[12,64-67] Designer Lewis acid catalysts work on the principle that through careful modulation of sterics, unusual and "unfavored" reactivity can be promoted.

Designer Lewis Acid Catalysts

A great number of catalyst systems and research has been placed into elucidating the mechanism of action for "Designer" Lewis acid systems.[12] These sterically demanding Lewis acid catalysts employ the concept of sterics as a means to achieve new reaction pathways, in contrast to modulation of electronics to accomplish desired reactivity.[12,64,65] As a simple analogy, these bulky Lewis acid catalysts can be thought of as labile protecting groups, with a few considerations to be taken into account. First, most of these catalysts operate in an equimolar ratio with substrate. As such, the catalyst is not particularly appealing for industrial applications, as a significant quantity of catalyst would be required. In addition, the catalyst is not recovered at the end of the reaction, meaning that there is significant generation of waste with the reaction. This last issue is somewhat abated by the fact that the precursors for the catalysts are cheap and synthesis is only one step (Figure 2-1).

Bulky Designer Lewis Acid Catalysts: MAD and ATPH

Aluminum complexes in solution tend to exist as higher coordinate species, usually four, five, or six coordinate.[66] This is mainly due to the readily accessible open LUMO on the aluminum center and the ability of the ligands to form bridged complexes.[6] This property can be a hindrance, as in some cases the formation of the higher coordinate species can show a decrease in reaction rate.[66] Modulation of sterics by the coordinated ligand around the metal center can push the equilibrium to favor the monomeric species. Of particular interest with regards to this overview are phenoxides that contain sterically demanding groups in the two and six positions.

The compound $Al(BHT)_2Me$ (MAD, Figure 2-1) was first synthesized by Pasynkiewicz et al. in the late 1970's, but it was the work of Yamamoto[70] and Maruoka[69] which brought recognition to the unique reactivity of this class of sterically demanding aluminum complexes. [66,68] MAD is readily synthesized by the addition of $AlMe_3$ to two equivalents of BHT. Both NMR spectroscopy and crystallographic studies have shown that the complex remains as a monomer in solution and in the solid phase.[19] As mentioned previously, the unique reactivity arises from the steric demand around the aluminum centers. The usual electronic interactions between the metal center and the incoming base exist and have been studied;[19] however, the sterics are the key for the unusual reactivity (Figure 2-2, 2-3).

Steric interactions of the ligands with the axial groups on the cyclyhexyl ring only allow binding of the aluminum complex to the equatorial site. The incoming nucelophile must then attack the carbonyl carbon from what is usually considered the unfavored side, thus promoting exclusive formation of a single isomer. These sterically demanding catalysts can also be used to discriminate between carbonyls, allowing for selective

reactivity of functional groups. Again, invoking sterics, the aluminum complex preferentially binds to the less sterically encoumbered carbonyl group, leaving the more hindered site open for attack (Figure 2-3).

The next step in the field of designer Lewis acid catalysts is the ability to induce chirality. As discussed in the Introduction chapter, chirality can be introduced either via the substrate or through the modification of the catalyst itself. By modifying one of the discussed privileged ligands to bear sterically demanding ancillary groups, one could in theory harness the unique reactivity of the sterically demanding ligands while imparting chirality onto the substrate (Figure 2-4). Using these principles, the Yamamoto group has successfully synthesized and tested several designer Lewis acids containing chiral ligands.

Figure 2-5 depicts one of the binaphthol catalysts first employed by the Yamamoto group as a catalyst in Diels-Alder reactions. The incoming dienophile is bound by the Lewis acidic boron but is also stabilized by the pi electrons in the neighboring phenyl ring on the catalyst backbone. The phenyl ring also blocks the opposite face of the bound dienophile from attack by the diene, leading to higher ee.[64]

Using the same concept, a similarly designed aluminum-containing binol species has been synthesized and characterized (Figure 2-6).[76] The unique aspect of these catalysts is that they employ multiple metal centers. As expected, there are similarities between the aluminum and boron catalysts. In both cases, the dienophile is bound to the metal center and stabilized by the backbone of the ligand. One face of the dienophile is also blocked by the ligand, leading to high ee.[64]

Ligand Design and Synthesis

One of the keys for a successful chiral catalyst is the formation of a well defined chiral pocket. An ideal situation would be where chiral ligands are tethered in a way so as to limit degrees of freedom, making a more defined binding pocket. Working with the concepts put forth by Maruoka and Yamamoto, preorganization of binol rings to form a defined chiral pocket was set as a starting point. Simply tethering binol moieties together though is not the ideal situation, as there could still be rotation around certain bonds, thus increasing degrees of freedom of the molecule as a whole. To further restrict motion, binding a catalytically inert metal center within the tethered structure would help to further define the chiral pocket.

This concept of using a metal to define the orientation of ligands has been well documented within the literature.[71] Kläui tripodal ligands employ a kinetically inert metal center to define the binding mode of the ligands surrounding the cobalt center (Figure 2-7).[71,72] The bound Cp ring interacts with the incoming phosphate ligands, forcing them to orient in the same direction, with the oxygen pointing down. The cobalt center, being kinetically inert, inhibits lability of the ligands essentially locking them in place. Of note, within the literature there exists an example of using this same Kläui ligand design to form a ligand systems containing binol rings.[73]

The goal of our research was to design and synthesize a novel bulky-designer Lewis acid catalyst. Of the work presented by Maruoka and Yamamoto, there exist few examples of bulky ligands that contain defined chiral pockets. Incorporation of chiral moieties into the ligand sets should promote formation of regio- and stereo- selective reactions using the same properties observed in current designer Lewis acid systems.

Results and Discussion

A depiction of the target ligand is shown in Figure 2-8**.** Initial preorganization of the binol rings was accomplished by tethering the three moieties to a trisamino methyl ethane (TAME) scaffolding ligand. Subsequently, an inert metal was bound within the cavity of the ligand system to restrict motion of the binol rings and form an ideal binding pocket for a group 13 metal. Synthesis of the chiral binol-aldehyde (BINAL) moiety was accomplished using well established literature procedures.[79] The complete synthetic scheme for the ligand set is shown in Figure 2-8.

The first ligand, initially synthesized by former group member Nathan Strutt, was the Me-TAME-based ligand 2-3, the crystal structure of which is shown in Figure 2-9. The main concern with compound 2-3 is its poor solubility. The solid state structure of both 2-3 and 2-4 both show the phenolic oxygens pointed inwards, forming a C_3 symmetric cavity of oxygen donors, seemingly well suited for binding of a group 13 metal species. While compound 2-3 colors most solvents, it is only soluble in DMSO, DMF, and pyridine. Encouragingly though, the NMR spectrum of compound 2-3 in d_5-pyridine showed no evidence of decomposition, indicating that even in strongly coordinating solvents, the cobalt center remains bound. This poor solubility might be beneficial however. As discussed previously, the majority of the work done by Yamamoto and Maruoka employ the catalyst in stoichiometric amounts, with the catalyst being destroyed in the workup procedures. Compound 2-3 is sparingly soluble in most solvents, allowing for easy recovery via precipitation. Additionally, the compound is stable through aqueous workup, as evidenced by NMR spectroscopy and mass spectrometry. This property could potentially allow for recovery and further reuse. To further increase solubility of the ligand, the ethyl derivative of TAME (Et-TAME) was

used, yielding compound 2-4. Unfortunately the addition of the ethyl chain did not notably increase the solubility of the compound. The crystal structure of 2-4 is markedly similar to that of 2-3, showing that changes in the scaffolding ligand seem to have little affect on overall structure. To date, successful addition of a group 13 metal into the phenolic pocket has not been accomplished. This is mainly attributed to solubility issues encountered with the ligand system.

The next option that was explored was the use of a different scaffolding ligand, TREN**.** The Schiff base compound 2-5 was successfully synthesized and the crystal structure is shown in Figure 2-10. The phenolic oxygens in the solid-state structure of 2-5 are all oriented in different directions and do not form a well defined binding pocket Comparing this observation to the structures of 2-3 and 2-4 one can see that the phenolic moieties are well organized due to the cobalt ion. Molecules which are tethered by a TREN molecules form larger binding pockets than those made using TAME.[74] As such, a cobalt metal is not ideal for use in the TREN system. Larger M(III) ions, such as La and Lu, were used in an attempt to affect the same organization of the binol rings as with the cobalt systems. Several established literature procedures exist for incorporating metals into TREN-containing molecules; however, to date, all attempts have proven unsuccessful.

Current research efforts are focused on methods that will increase the solubility of the ligand. The two avenues which are being explored in synthesis of new derivatives of TAME and incorportation of a butylated derivative of binol **(**Figure 2-11). Preliminary work with the butylated binol derivative has yielded what is postulated to be the metallated ligand; however, overall yields for the ligand are low, being around 1%

through seven steps. Thus, to date a complete procedure and analysis for the compound has not been established. Work is focused on modification of synthetic procedures to increase the yield.

Experimental

General Considerations

Unless otherwise stated, all manipulations were carried out under an inert atmosphere of N_2. All NMR spectra were recorded on a Varian Mercury 300 MHz spectrometer at 299.95 and 75.47 MHz for the proton and carbon channels respectively. Chemical shifts (δ) are reported with reference to residual NMR solvent peaks. All chemicals were purchased from Sigma-Aldrich or Fisher Scientific and used as is without further purification. Mass Spectrometry data was done at the University of Florida using in house instrumentation. Each sample is dissolved in appropriate solvent and undergoes direct-injection through an autosampler, followed by ESI or APCI analysis with methanol (with or without 0.2% acetic acid) as mobile phase. For MALDI, the solution is usually added onto the matrix spot of dithranol, -cyano-4-hydroxycinnamic acid, dihydroxybenzoic acid or terthiophene. Solvent is used only when necessary for DART. The ions are detected with the Agilent 6210 TOF-MS while the data is processed with the MassHunter™ software. Methoxy Methyl Chloride (MOM-Cl)[78], 2,2'-dihydroxy-[1,1'-binaphthalene]-3-carbaldehyde (BINAL)[79], 2-(aminomethyl)-2-methylpropane-1,3-diamine (Me-TAME),[80,81] 2-(aminomethyl)-2-ethylpropane-1,3-diamine (Et-TAME), [80,81] were synthesized following known literature procedures.

Synthesis of 2-1

A 2.5g (8.0 mmol) sample of Me-TAME was dissolved in 50ml of ethanol. A 0.31g (2.7 mmol) sample of BINAL was added to the solution, and the reaction stirred

overnight at room temperature. The reaction was then cooled to 0℃ to promote precipitation of the product. The mixture was filtered and the resulting yellow solid was washed with cold methanol. Yield: 1.77g, 65%. ^{1}H NMR (300MHz ,CHLOROFORM-d) δ = 13.12 (br. s), 8.53 (s), 7.97 - 7.75 (m), 7.43 - 7.06 (m), 3.63 (br. s), 1.04 (s). ^{13}C NMR (75MHz ,CHLOROFORM-d) δ = 166.8, 155.4, 151.5, 135.4, 134.9, 133.6, 130.0, 129.2, 129.1, 128.2, 127.7, 126.5, 124.9, 124.7, 124.0, 123.3, 120.7, 117.8, 114.4, 113.7, 65.5, 40.2, 20.9. ESI-TOF-MS: calcd for $C_{68}H_{52}N_3O_6$ 1006.3851; found 1006.3879 $[M+H]^+$

Synthesis of 2-2

Compound 2-2 was synthesized using the same procedure as for compound 2-1. Yield: 1.51g, 55%. ^{1}H NMR (300 MHz, CHLOROFORM-*d*) δ = 13.14 (br. s.), 8.59 (s), 7.79 - 7.98 (m), 7.05 - 7.41 (m), 5.25 (br. s.), 3.61 - 3.76 (m), 1.46 - 1.62 (m), 0.92 (t, *J*=7.33 Hz). ^{13}C NMR (75MHz ,CHLOROFORM-d) d□=□166.7, 155.4, 151.5, 135.4, 134.9, 133.6, 130.1, 129.3, 129.1, 128.2, 127.7, 126.5, 124.9, 124.7, 124.0, 123.3, 120.7, 117.8, 114.4, 113.6, 63.1, 42.5, 25.6, 7.3. ESI-TOF-MS: calcd for $C_{69}H_{53}N_3O_6Na$ 1042.3827; found 1042.3847 $[M+Na]^+$

Synthesis of 2-3

A 1.0g (1.0mmol) sample of 2-1 was dissolved in of 20ml of THF. To this solution was added 15ml ethyl acetate, and 20ml of methanol. A 0.24g (1.1mmol) sample of cobalt(II) acetate tetrahydrate was added to the solution and a reflux condenser was fitted on the reaction vessel. The reaction was refluxed overnight under ambient atmosphere. The reaction was cooled to room temperature and filtered yielding the product as dark red solid. The mother liquor was reduced under vaccum and more methanol added yielding a second crop of product. Single crystals suitable for X-ray

diffraction were grown from slow evaporation of DMSO. Yield: 0.55g, 52% ^{1}H NMR (300 MHz, DMSO-d_6) δ = 7.76 (s), 7.58 (br. s.), 7.45 (d, *J*=8.21 Hz), 7.03 - 7.20 (m), 6.88 - 7.02 (m), 6.81 (d, *J*=8.80 Hz), 6.51 - 6.68 (m), 6.08 (d, *J*=8.80 Hz), 3.59 (d, *J*=12.31 Hz), 3.33 (br. s.), 0.91 (br. s.). ^{13}C NMR (75MHz ,DMSO-d_6) δ = 168.9, 157.9, 151.6, 136.9, 135.1, 133.1, 129.6, 128.3, 128.2, 127.2, 124.9, 124.4, 123.8, 123.1, 121.6, 120.0, 118.1, 117.6, 116.6, 66.9, 62.4, 25.1, 20.0. ESI-TOF-MS: calcd for $C_{68}H_{48}CoN_3O_6Na$ 1084.2767; found 1084.2794 $[M+Na]^+$

Synthesis of 2-4

Compound 2-4 was synthesized following the procedure of 2-3. Single crystals suitable for X-ray diffraction were grown from slow evaporation of acetone. Yield: 0.54g, 51% ^{1}H NMR (300 MHz, DMSO-d_6) δ = 7.78 (s), 7.74 (s), 7.43 - 7.53 (m), 6.92 - 7.19 (m), 6.80 (d, *J*=8.80 Hz), 6.55 - 6.63 (m), 6.06 (d, *J*=8.80 Hz), 3.44 - 3.71 (m), 1.40 - 1.53 (m), 0.85 (t, *J*=7.33 Hz). ^{13}C NMR (75MHz ,DMSO-d_6) δ = 168.9, 158.0, 151.6, 136.9, 134.9, 133.2, 129.6, 128.3, 128.2, 127.1, 125.0, 124.5, 124.4, 123.8, 123.1, 121.6, 120.0, 118.1, 117.6, 116.7, 60.7, 43.7, 26.8, 7.2. ESI-TOF-MS: calcd for $C_{69}H_{51}CoN_3O_6$ 1076.3104; found 1076.3115 $[M+H]^+$

Synthesis of 2-5

Compound 2-5 was synthesized using the same procedure as for compound 2-1, using TREN instead of TAME. Yield: 1.51g, 54%. ^{1}H NMR (300MHz ,CHLOROFORM-d) δ = 8.25 (s,), 8.12 (s), 7.91 - 7.79 (m), 7.45 - 7.03 (m), 6.55 (s), 6.20 (d, *J* = 8.2 Hz), 3.48 (m), 2.82 - 2.64 (m). ^{13}C NMR (75MHz ,CHLOROFORM-d) δ = 166.1, 155.4, 151.7, 135.1, 134.4, 133.7, 130.0, 129.8, 129.6, 129.2, 129.0, 128.3, 127.5, 126.4,

124.7, 123.6, 123.2, 120.5, 117.9, 114.9, 58.4, 55.7, 18.3. ESI-TOF-MS: clalcd for $C_{69}H_{54}N_4O_6Na$ 1057.3936; found 1057.3958 $[M+Na]^+$

Table 2-1. Crystallographic data for compound 2-3, 2-4 and 2-5.

	2-3	2-4	2-5
Total Reflections	14253	14639	20462
Uniq. Reflections/ Reflections $I \geq 2\sigma(I)$	14253/4654	14639/10023	13650/6851
Collection Range (°)	$1.05 < \theta < 27.50$	$1.61 < \theta < 27.50$	$1.57 < \theta < 27.50$
Formula	$C_{69}H_{50}CoN_3O_6$	$C_{68}H_{48}CoN_3O_6$	$C_{69}H_{54}N_4O_6$
M_r	1076.05	1062.02	1035.16
Crystal System	Monoclinic	Orthorhombic	Monoclinic
Space Group	$P2_1$	$P2_12_12_1$	$P2_1$
a (Å)	11.142(6)	14.8127(10)	14.4480(18)
b (Å)	38.74(2)	24.4490(17)	16.775(2)
c (Å)	14.411(8)	32.624(2)	14.6801(19)
α (°)	-	-	-
β (°)	101.141(11)°	-	118.034(2)°
γ (°)	-	-	-
V_c (Å^3)	6103(6)	11815.0(14)	3140.4(7)
D_c (g cm^{-1})	1.171	1.194	1.095
Z	4	8	2
F(000)	2240	4416	1088
μ[Mo-Kα] (mm^{-1})	0.344	0.344	0.070
$R_1[I \geq 2\sigma(I)$data]	0.0470	0.0396	0.0591
$wR_2[I \geq 2\sigma(I)$data]	0.1510	0.0734	0.0990
GoF	0.641	0.861	0.821
Largest peak, deepest trough (e Å^{-3})	+0.264, -0.271	+0.520, -0.412	+0.158, -0.174

Table 2-2. Selected bond lengths for compound 2-3

Atoms	Distance(Å)
Co1-N1	1.853(5)
Co1-N2	1.879(5)
Co1-N3	1.903(5)
Co1-O1	1.875(4)
Co1-O2	1.933(4)
Co1-O3	1.881(4)
Co2-N4	1.915(6)
Co2-N5	1.904(6)
Co2-N6	1.852(6)
Co2-O7	1.932(4)
Co2-O8	1.872(5)
Co2-O9	1.880(4)

Table 2-3. Selected bond lengths for compound 2-4

Atoms	Distance(Å)
Co1-N1	1.893(3)
Co1-N2	1.898(2)
Co1-N3	1.900(3)
Co1-O1	1.913(2)
Co1-O2	1.881(2)
Co1-O3	1.9340(19)
Co2-N4	1.896(3)
Co2-N5	1.896(3)
Co2-N6	1.892(3)
Co2-O7	1.883(2)
Co2-O8	1.913(2)
Co2-O9	1.881(2)

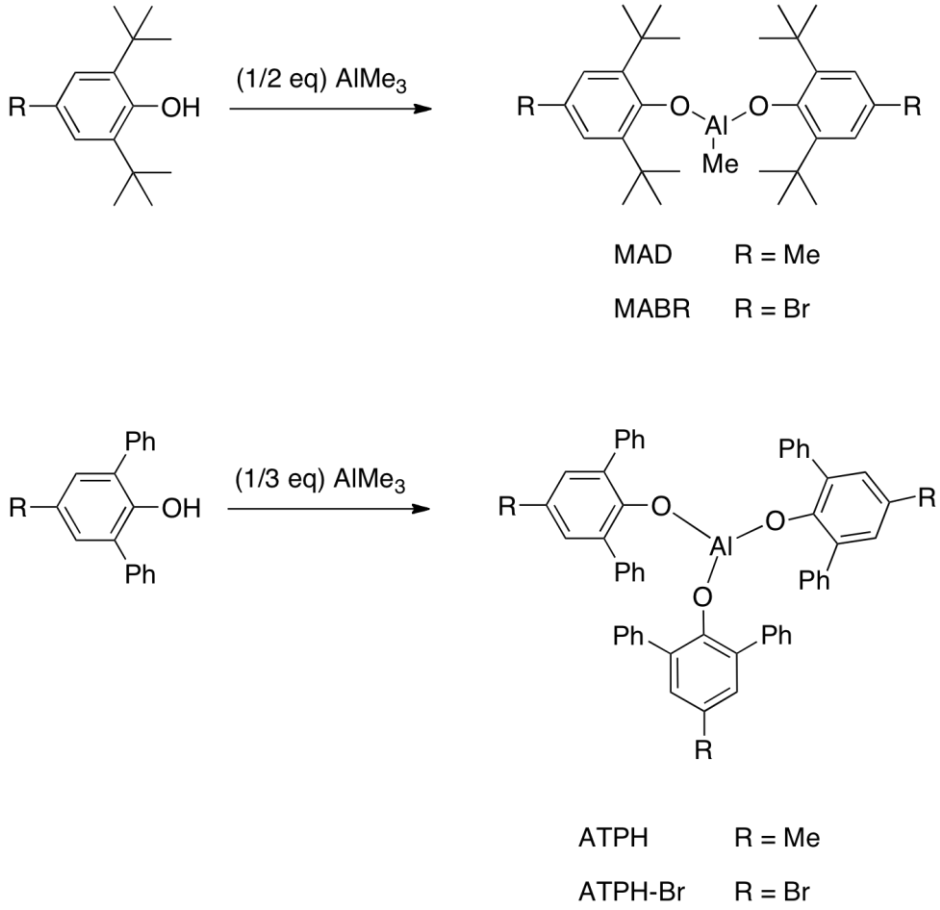

Figure 2-1. Synthesis of MAD and ATPH, two bulky designer Lewis acid catalysts.[70]

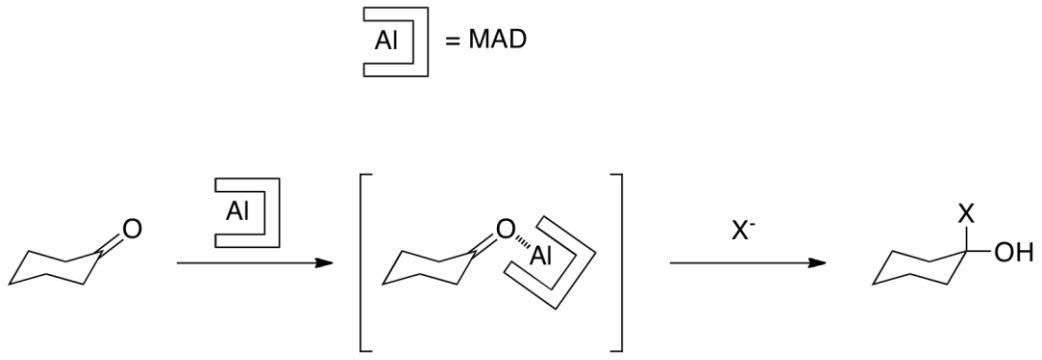

Figure 2-2. MAD binds to the carbonyl group of cyclohexanone, forcing the incoming nucleophile to attack from the less favored axial face.

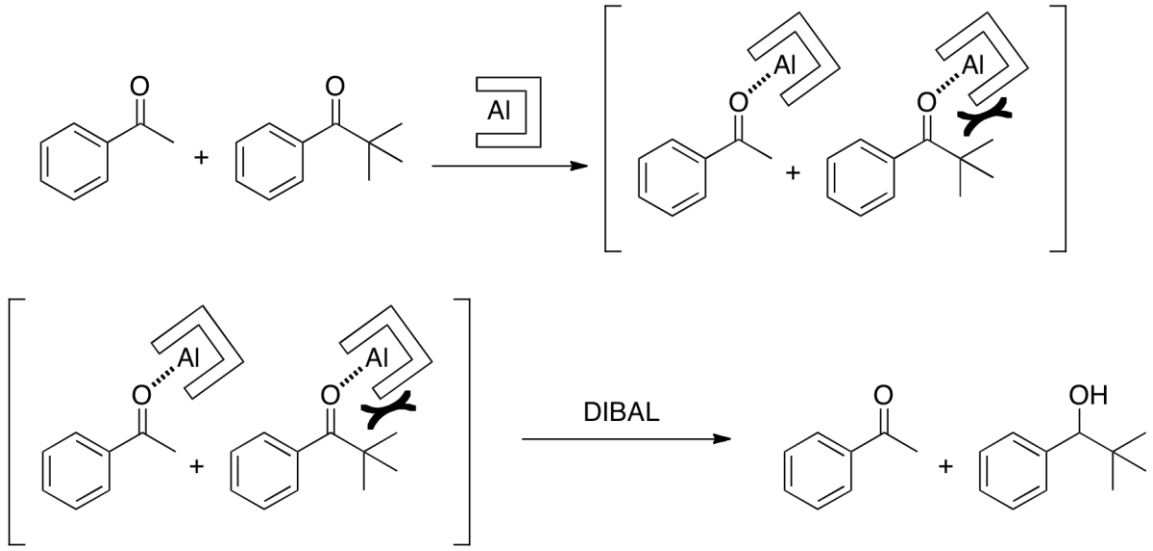

Figure 2-3. MAD selectively binds to less encumbered carbonyl groups allowing for selective reduction of functional groups.[70]

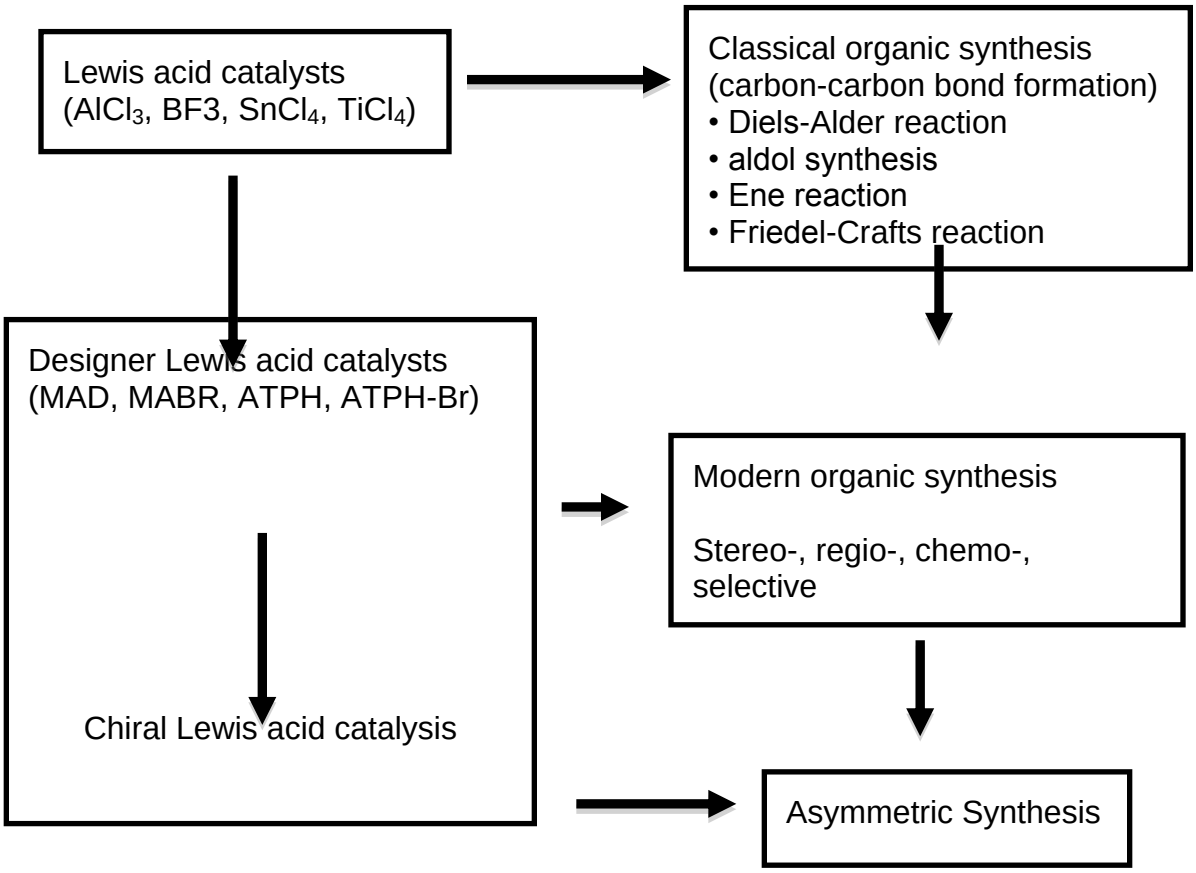

Figure 2-4. Combining previously studied concepts with careful modification of ligands can further enhance the field of designer Lewis acid catalysts.[70]

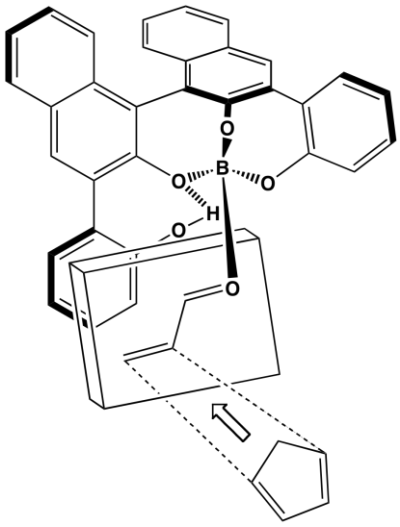

Figure 2-5. A boron-based catalyst studied by Yamamoto et al. shown binding to a dieneophile during the trasition state of a Diels-Alder reaction.[64]

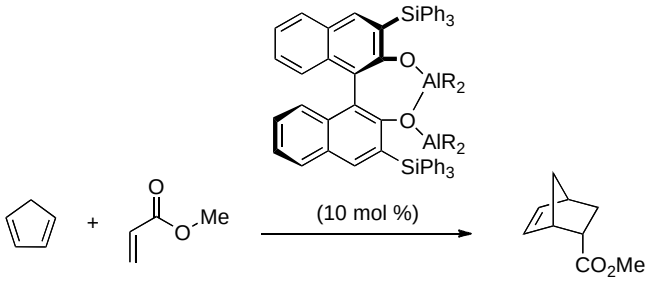

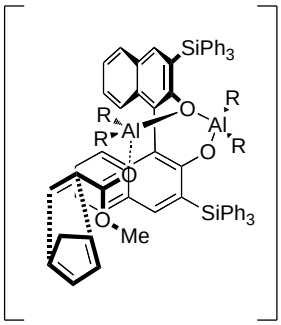

Figure 2-6. A Lewis acid catalyst bearing a binol ligand catalyzing a Diels-Alder reaction. The lower figure depicts the proposed transition state of the system.[64,76]

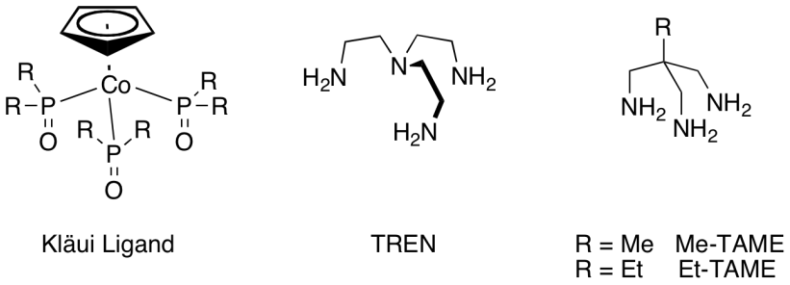

Figure 2-7. Representations of the Kläui ligand, TREN, and TAME scaffolding type ligands.

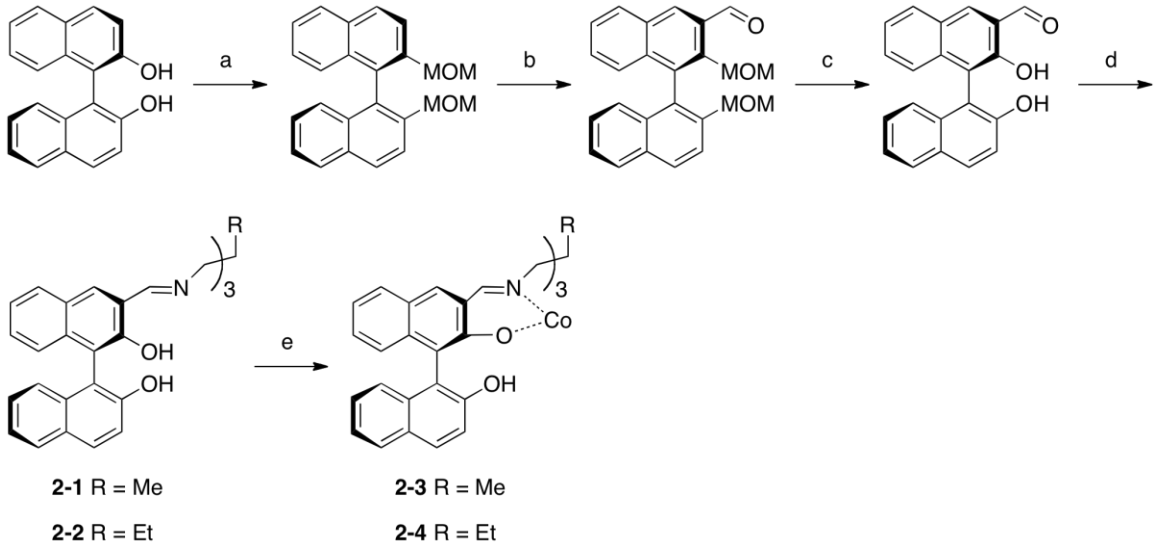

Figure 2-8. Synthetic scheme for synthesis of target ligands, 2-3 and 2-4. a) MOM-Cl, NaH b) DMF, n-BuLi c) HCl d) Me or Et-TAME, EtOH e) $Co(OAc)_2$

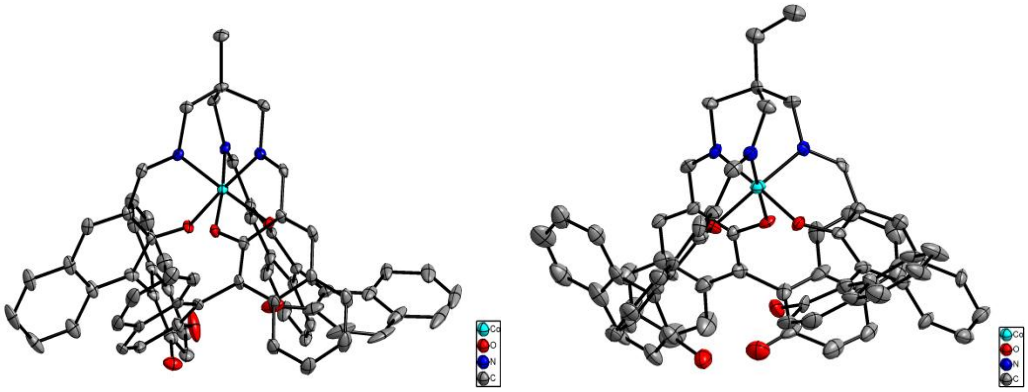

Figure 2-9. Solid state structures of compounds 2-3 (left) and 2-4 (right) shown at 30% probability ellipsoids. Hydrogen atoms are omitted for clarity.

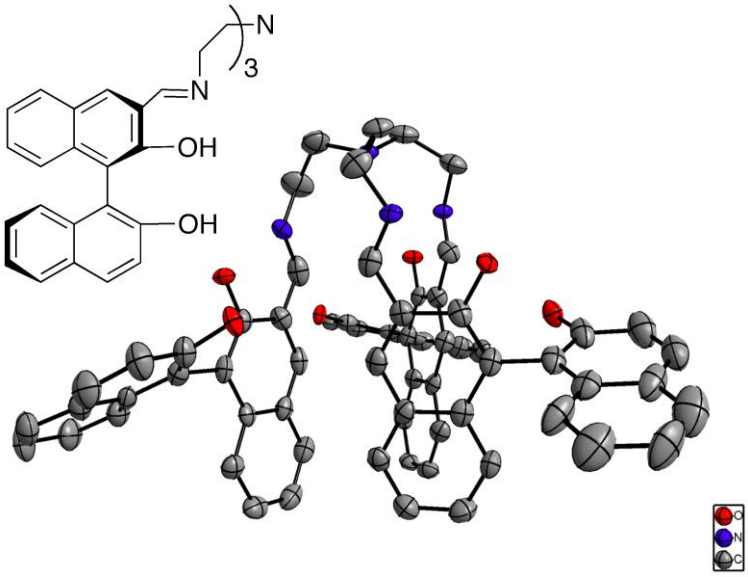

Figure 2-10. Solid-state structure of 2-5 shown at 30% probability ellipsoids. Hydrogens are omitted for clarity.

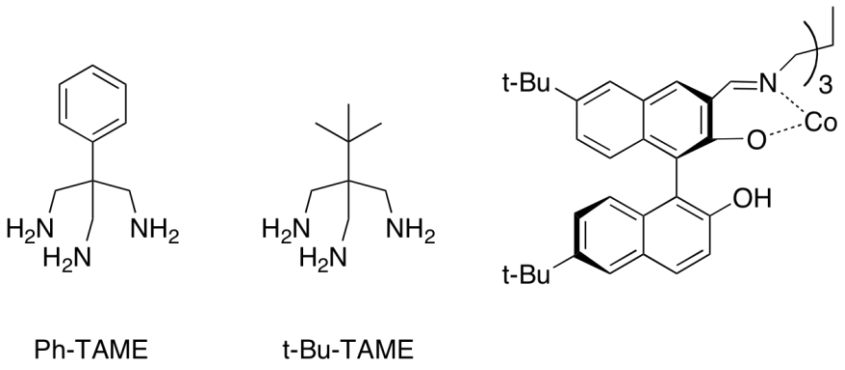

Figure 2-11. Several new derivatives of TAME are being synthesized to increase solubility of the tris-binol ligand

CHAPTER 3
MULTI-DENTATE LIGAND SYSTEMS BEARING COPPER ATOMS

Introduction

Lewis acid systems have been employed and studied in chemistry since their discovery in the 19th century. These studies largely focus on the use of a single metal center to bind and activate a substrate.[5,6,8,12] A more recent development in the area of Lewis acid catalysis arises from the idea of binding multiple Lewis acidic centers together to allow multiple coordination of a single substrate to multiple Lewis acid centers (Figure 3-1).[16]

Shriver and Biallas reported the first multi-dentate Lewis acid complex, 1,2-(Bis(difluoroboryl)ethane, in the late 1960s.[41] The diboryl compound was shown to cleave ethereal substrates, and bind the subsequent alkoxide products in a 2:1 ratio of boron to oxygen. While their work showed promise, the field did not receive much attention until the latter half of the 1980s.[16]

Wuest et al. began their fundamental work in the field of multidentate Lewis acid complexes by studying 1,2-phenylenedimercury dichloride and various derivatives thereof (Figure 3-2).[16,43] Through their studies into the coordination of carbonyl compounds to multidentate Lewis acids, many fundamental properties of the chemistry have been discovered. The mercury derivatives have been studied more than the newer aluminum-containing ligand sets, mainly due to the stability and tolerance of mercury compounds. While the area of multi-dentate Lewis acids is still under investigation, there is definitive evidence that coordination to multiple Lewis acidic sites shows a marked change in electronic and steric properties of the bound species.[16,38,40] In the work of Wuest et al., IR spectroscopy was used to show the shift in chemical stretches

between the monodentate and the bidenate mercury species with diethylformamide (DEF). The free carbonyl stretching frequency of DEF is 1668 cm^{-1} while the monodentate and the bidenate adducts showed frequencies of 1647 cm^{-1} and 1633 cm^{-1} respectively in CH_2Cl_2. Additional work led to the formation of a tetradentate DEF bound compound, identified by single crystal X-ray diffraction along with various spectroscopic methods. The IR spectrum of DEF, in Nujol, showed a carbonyl stretching frequency of 1689 cm^{-1} and a bound stretching frequency of 1648 cm^{-1}. Examination of the stretching frequency data presented by Wuest et al., multidentate Lewis acids show a significant shift in electronics as compared to the unbound substrate or mono adducts. Additional density functional theory (DFT) calculations and spectroscopic data show that the $\Delta H°$ for coordination of a second tethered Lewis acid site is roughly 30% that of the binding of the first.[16] These calculations also showed restricted rotation of the bound carbonyl species due to the simultaneous binding by two Lewis acidic metal centers. Wuest et al. postulate that this restricted rotation can lead to higher selectivity by reducing the number of possible reaction intermediates.[16]

The pioneering work of Shriver and Biallas and continuing work in the field has led to the discovery of many fundamental properties required for the ideal multidentate Lewis acids, though Wuest admits that there are significant issues regarding the synthesis of ideal ligand sets to maximize the effectiveness of the multiple metal sites.[16] Without proper alignment and spacing of the Lewis acidic metal centers, multiple binding modes can exist (Figure 3-3).

Expanding on the ideas developed by Wuest, Maruoka et al. developed a series of bidentate Lewis acid complexes.[59] Using a series of modified bisphenol ligands.

Maruoka demonstrated the concept of "double electrophilic activation," or the coordination of a single substrate to two Lewis acidic centers.[59] These 1:2 (substrate: Lewis acid center) complexes showed significant improvement in reduction of certain ketones under specific conditions, implying a change in electronic state of the bound substrate as compared to a 1:1 complex (Figure 3-4).

One complication that arises from the use of group 13 metal species with multi-dentate catalysts is the issue of dimerization.[6] Compound 1 (Figure 3-4) shows two aluminum species bound to a single ligand system. This depiction is deceptive as both in solution and in the solid-state this complex exists predominantly as a dimer.[59] Even as larger, more sterically demanding ligands are substituted for the methyl groups in the 2 and 7 positions, a dimer tends to be the favored geometry. Maruoka implies that given the inherent stability of these dimeric structures the monomeric bi-metallic system is responsible for the observed increase in Lewis acidic properties.[83]

Gabbaï et al. further expanded on the naphthalene based bidentate Lewis acid complexes incorporating many group 13 metals into the systems, synthesizing complexes containing boron, aluminum, gallium, and indium (Figure 3-5).[60,61] With a larger focus on investigating principals of the multidentate Lewis acid systems, Gabbaï et al. have examined how changing the metal centers within the ligand systems affects the anion binding and selectivity.[60,61] Through the use of modified, mixed metallic systems, Gabbaï et al. have developed anion selective Lewis acidic ligands, some showing a visual response to binding of the target anion.[60-63]

Ligand Design

As discussed earlier, the area of multidentate Lewis acidic compounds has been stunted by the difficulties associated with design and synthesis of ligands incorporating

multiple Lewis acidic sites.[16,39,40,61] There are a few examples of core ligand designs which have found success in use of multidentate Lewis acids.[38-40]

In addition to the structures shown in Figure 3-6, carborane-containing systems are also prevalent within the field.[38-40] Carborane-containing species can be problematic as they are expensive and have somewhat exotic reaction properties.[38,39] Also, the carborane containing structures require a serendipitous self-assembly into the desired tri- or tetra- metallic structure (Figure 3-7).

There were two main goals for our research. The first was to establish a defined synthetic route for synthesis of C_3 symmetric ligand sets. Given the noted difficulty associated with synthesis of ligands for multi-metallic systems, establishing a synthetic design that is easily tunable would benefit the field of multi-dentate Lewis acid catalysis.[16] Our second goal was to use the aforementioned ligands to bind three copper centers into a single ligand for use as a catalyst. The concept of copper as a Lewis acidic center in the laboratory setting is discussed in further detail in Chapter 1. Most transition metals can act as Lewis acid centers, and are ubiquitous throughout catalysis. Within the realm of biology, copper is employed as a Lewis acidic center in a variety of enzymes.[48] Nature readily employs the concept of multidentate metal centers incorporating copper.[48] The Multicopper Oxidase (MCO) class of enzymes contain three copper centers arranged in a C_3 geometry.[49] The three copper centers work in tandem to bind and reduce molecular oxygen to water.[50]

There are a few key features necessary for the target multidentate ligand system: C_3 symmetry, anionic binding pockets, and modular steric and electronic properties. The C_3 symmetry is necessary to force bring three bound metal centers together in an ideal

geometry. Tethering three symmetric binding arms to one central atom not only provides ideal control of stoichiometry but also reduces entropy by having one ligand bind three metal centers. An anionic binding pocket is needed to control the lability of copper species.[43] Copper species in both +1 and +2 oxidation states tend to be labile, yet the coulombic attraction of an anionic binding pocket to a cationic metal center would help minimize this. The most challenging aspect of synthesis is the modulation of sterics. Control of sterics is necessary for a number of reasons. First, the three binding arms not only must be held in close proximity to promote cooperativity, but also must be held far enough apart so that cooperativity of all three metallic sites is seen as opposed to binding by just one or two metal centers. Sterics is also used to control the coordination sphere of the bound copper species. The ideal setup would contain one binding arm bound to one metal center with no solvent of counter ion coordinating the other binding sites. The open coordination sites are needed so that incoming substrate is readily bound to the metal centers without having to displace some other bound species first.

There are a variety of C_3 symmetric scaffolding ligands that are found in the literature (Figure 3-8). The majority of these ligand systems are too flexible to be employed for this project. The triphenoxymethane ligand is a more rigid platform ligand and has been employed in the past to pre-organize three binding pockets for copper containing ligands.[43] While successful for binding copper and subsequent binding of O_2, there are few issues with the previously mentioned triscopper system, mainly the lability of the copper centers and degradation of the system by abstraction of the central methyne hydrogen.[43] Additionally, the binding arms were not sterically demanding and

thus not ideal for the current target system as evidenced by binding of acetonitrile moieties to the open coordination site. [43]

Taking into account all the required characteristics desired in the ligand set, two specific synthetic targets were designed using the triphenoxymethane platorform as a scaffolding ligand (Figure 3-9). Amidinates and diiminates were chosen as the binding pockets given their extensive use for formation of 1:1 adducts of metals to binding arms. The modular characteristics of both classes of ligands allow for tuning of both the steric and electronic aspects of bound metal species. Additionally, there are volumes of work regarding synthesis of both ligand sets.[44-47] In the previously mentioned work done by former group member Dr. Matthew Peters,[43] the binding pockets were attached to the "top" phenolic oxygens of the triphenoxymethane platform. In this work the target set of ligands will be attached to the "bottom" of the scaffolding ligand through an amine functionality. There are several key characteristics of the "bottom" functionalized triphenoxymethane platform that make it ideal for use with the target ligand sets. First, there is no observed ring flip by NMR spectroscopy or single crystal X-ray diffraction, thus the orientation of the rings remains consistent, with the phenols pointed "up." Multiple DFT optimizations have also confirmed that the arrangement with all of the phenol oxygens aligned in the same "up" direction to be of the lowest conformational energy. This rigidity implicates that any binding pockets attached to the bottom of the platform will always be aligned in the same direction. Second, since both the platform and ligand arms are rigid, minimal flexing and distortion of the binding pockets should be observed. Lastly, the spacing between the amines on the platform is approximately 7Å. This spacing is necessary to allow ample room not only to fit all three metal centers

within the ligand, but also allow for spacing between the metal centers to prevent formation of μ-oxo species.

Tris-Amine Platform Synthesis

Synthesis of the tris-amine triphenoxymethane platform is shown in Figure 3-10. Initial synthesis was focused on the methyl derivative of the ligand ($R_1 = R_2 = Me$), but has expanded to incorporate numerous new alkyl and alkoxy substituents. Synthesis of the platform ligands is accomplished by the methods first employed by Dinger and Scott.[51]

Initial synthesis and optimization was accomplished through work on the methyl derivate ($R_1 = R_2 =$ methyl). While the chemistry has been fairly well established at this point, there are still lingering issues with synthesis. The methyl derivative displays poor solubility. Of particular concern is the reduction of the tris-nitro to the tris-amine (step f, Figure 3-10). Isolation of the tris-nitro precursor is accomplished through precipitation by addition of methanol. Initial attempts at reduction of the tris-nitro compound used zinc in protic solvents, i.e. water or alcohol.[52-54] The nitro compound, however, is sparingly soluble in alcohols leading to a mixture of products. Reduction by zinc is known to yield a number of different products, the distribution of which is susceptible to reaction conditions (Figure 3-11).[55]

Even upon successful formation of product, as evidenced by NMR spectroscopy, isolation of clean product proved unsuccessful by all standard purification methods. Moving away from literature preps using protic solvent to mixed solvent systems showed formation of the desired product in higher yield but with formation of both calcium oxide and zinc oxide. Separation of the product from the metal salts was attempted but with little success. Subsequent reactions with crude tris-amine product

were conducted, yet unsurprisingly the yields of these reactions were low, irreproducible, and yielded impure product.

Reduction was eventually accomplished by using Raney Nickel in a mixture of THF and ethanol at room temperature for 48 hours under a hydrogen atmosphere, following the procedure established by Boehmer et al. While successful with some derivatives of the platform, solubility issues were encountered with other derivatives of the platform. The methyl version of the ligand platform (R_1 = R_2 = methyl) was initially screened as a comparison of reactivity between the zinc-based reduction system and the Raney Nickel system. The zinc-based reaction produced the expected mixture of products while the Raney Nickel-based system showed no measureable reactivity. The notable difference between the two reactions is the temperature at which the reaction is conducted. The zinc-based reactions are carried out at reflux, affording better solubility for the starting material and product; however, the Raney Nickel reaction was performed at room temperature lowering the solubility of the starting material. Reduction of the tris-nitro compound was successful with the more soluble derivatives of the complex. Five different derivatives were successfully and repeatably reduced to the corresponding tris-amine: 3-16, 3-17, 3-18, 3-19, and 3-20. The common characteristic between all the compounds is the notable increase in solubility due to larger aliphatic protecting groups substituted off the phenolic oxygens. In all cases, the reduction gave high yields and required minimal cleanup. Reduction of 3-11 was run on a five gram scale and showed similar yields and purity as compared with the previous reductions. Thus, successful reduction of the tris-nitro compounds has been established. Current efforts are focused on the synthesis and characterization of novel triphenoxymethane platform ligands

bearing larger alkyl and alkoxy groups to afford increased solubility. To date, five new ligand platforms suitable for the target compounds have been synthesized and characterized as their respective tris-nitro derivatives. Of these new compounds, all have been successfully reduced to the corresponding tris-amine (Figure 3-12).

Tris-diiminate Ligand Set

Results

Two synthetic pathways were devised to synthesize the target tris-dimminate ligand set (Figure 3-13). Simple Schiff base reaction with the tris-amine functionalized ligand platform and 2,4-pentanedione, followed by recrystallization from ethanol, yields the intermediate acetonamine. Initial reactions of acetonamine with primary amines failed to yield any significant quantities of the desired product. From here, synthetic pathway B was attempted. A number of simple monosubstituted dione derivatives were synthesized and reacted with the tris-amine, yet no significant quantities of product was isolated.

Discussion

In an attempt to better understand the difficulties with the synthesis, DFT studies were carried out by current Scott group member Dempsey Hyatt on the p-tolyl derivative of the target ligand to determine if there were any unforeseen steric issues with the structure. The results of the geometry optimization were surprisingly mundane. Upon inspection, there appears to be no obvious steric issues preventing the formation of the desired ligand system (Figure 3-14). The binding arms are spread out, showing no issues involving interactions of the binding arms with other arms in the system.

The chemistry of diiminates is a well established and ongoing area of research.[44] As such, there exist a great number of yet untested synthetic pathways that can be

used with the triphenoxymethane based ligand set. Aside from the previously mentioned Schiff base routes, numerous other synthetic schemes have been either devised or tested. The majority of these attempts have yielded either no visible product by spectroscopy or showed degradation of the starting material. Despite numerous attempts at synthesis of the tris-diiminate ligand set, to date there has been no product isolated.

Tis-amidinate Ligand Set

Results

Synthesis of the tris-amidinate ligand set was accomplished as shown in Figure 3-15. The majority of the work presented herein was accomplished using the methyl derivative of the ligand platform (R_1 = R_2 = methyl); however, there are significant problems to note. At the time when these experiments were carried out, the reduction of the tris-nitro compound was accomplished using zinc, which tended to yield impure tris-amine compounds. As such, the subsequent reactions using these impure starting materials were not consistently reproducible.

Condensation of the tris-amine platform with benzoyl chloride yields the tris-phenyl amide, which was converted into the corresponding imidoyl chloride using PCl_5. Reaction of the imidoyl chloride with aniline yielded the desired amidinate complex 3-21, albeit impure and in low yield. The tris-amidinate was then treated with butyl lithium and the appropriate copper salt. The compound was isolated and a single crystal grown by diffusion (Figure 3-16, Figure 3-17). To date the crystal, grown by former group member Maryline Beyler, remains the only example of the target ligand metallated with three copper ions.

The solid-state structure of compound 3-21 provides a wealth of practical information which is useful in optimizing our target compound. Of particular interest is the fact that the structure is dimeric, consisting of two tris-amidinate ligand sets binding three copper centers. This result is unsurprising as the majority of published monomeric amidinate structures incorporate more sterically demanding groups (Figure 3-18). The use of two phenyl rings as the ancillary groups within the target compound does not provide the necessary bulk needed to prevent dimerization and force a chelate binding mode as desired.

In the crystal structure, two of the copper ions are also seen binding to a chloride ion. The presence of a bound species within the Lewis acidic pocket shows that there is ample room within the ligand system to allow for substrate binding. Empirical geometrical calculations were performed on the dimerized amidinate complex to determine total binding area between the copper ions. Using the distances between each copper atom, a binding area of 9.88Å^2 was calculated. As a reference point, metal centers within enzymatic systems are separated[22] by roughly 4.5Å, making a smaller binding area of 8.77Å^2. This finding is promising as it further emphasizes the point that there should be adequate room within the structure to allow binding of incoming substrate.

Discussion

The more prominent issue with the diphenyl amidinate derivate is the problem arising form dimerization of the complex. By increasing the steric bulk at the 1 and 2 in the amidinate, the chelate binding mode should be preferred over the bridging. Additionally, increasing the steric bulk in the 2 position should deter the formation of dimer. To better understand how substitutions at the 1 and 2 positions affect the binding

arm and ligand system, semi-empirical and DFT geometry optimizations were employed to determine the optimal groups to incorporate within the system. Initially, structures were optimized using the PM6 methods as part of the MOPAC software package.[56] Structures that showed promising results were then optimized, by Dempsey Hyatt, using higher-level DFT to confirm the reliability of the semi-empirical calculations. As a large number of derivatives were optimized, semi-empirical methods were required to minimize calculation time. In total, 14 different structures were optimized by semi-empirical methods (Figure 3-19). Of those, six were further examined by DFT calculations. Since all alkyl and aryl groups tested are sterically demanding, the main feature that was examined is the torsion angle of the amidinate moiety with respect to the arene ring of the platform system. A complete list of torsion angles acquired from semi-empirical calculations is shown in Table 3-1. The torsion angle of the binding pockets with respect to the platform would help ensure correct positioning of the bound metal ions. An ideal angle of 180˚ would position that the binding pocket co-planar with the ring system. This conformation would ensure that the “top” face of the binding pocket would be occupied by the platform, while the “bottom” face would be protected by the appropriately substituted group in the 1 position. As the angle approaches 90˚ with respect to the arene ring, the sides of the copper ion become exposed and could cause issues with binding.

Of the structures examined, C3-1, C3-5, C3-7, and C3-8 had average torsion angles the closest to 180˚, making them ideal initial target ligands for synthesis. These compounds, and selected others, were then optimized using higher-level DFT studies to ensure reliability of the semi-empirical methods. A complete listing of the torsion angles

acquired from the DFT optimized structures are shown in Table 3-2. When comparing the average torsion angles of the semi-empirical methods to the DFT, there is a high degree of similarities between the two. Compounds C3-1 and C3-5 show little difference in average torsion angle between the two methods. From a synthetic view, compound C3-1, C3-5, and C3-8 would be the simplest to synthesize. Compound C3.7 did have an average torsion angle that was closest to 180˚; however, when the related compound C3.3 was optimized, significant deviations in the torsion angles were observed. From a practical view point, the idea of trying to fit two tert-butyl groups in such close proximity does not seem feasible, consequently the compound was eliminated from the synthetic targets list.

Geometry optimization of the potential ligand systems led to two important findings. First, the 2 position of the ligand system appears to be key in controlling the torsion angle of the binding pocket. As steric bulk increases, torsion angles trend towards the desired angle of 180˚. Second, a tert-butyl group in the 1 position seems to be ideal. Not only would this help favor the chelate binding mode, but it would also help prevent dimerization of the complexes.

Conclusions

Successful synthesis of a series of tris-amine functionalized ligand platforms for use as scaffolds has been completed. The tris-amine platforms are currently being employed in subsequent reactions in an attempt to successfully and repeatably synthesize both the tris-amidinate and tris-diiminate ligand sets. Several theoretical techniques have been used to help elucidate the ideal balance of sterics required to achieve the desired binding mode of copper atoms within the proposed systems. The theoretical studies have helped develop a series of target compounds that are currently

in the process of being synthesized, with the ultimate goal of employing the compounds as multi-dentate Lewis acid catalysts.

Experimental

General Considerations

Unless otherwise stated, all manipulations were carried out under an inert atmosphere of N_2. All NMR spectra were recorded on a Varian Mercury 300 MHz spectrometer at 299.95 and 75.47 MHz for the proton and carbon channels respectively. Chemical shifts (δ) are reported with reference to residual NMR solvent peaks. All chemicals were purchased from Sigma-Aldrich or Fisher Scientific and used as is without further purification. Mass Spectrometry data was done at the University of Florida using in house instrumentation. Each sample is dissolved in appropriate solvent and undergoes direct-injection through an autosampler, followed by ESI or APCI analysis with methanol (with or without 0.2% acetic acid) as mobile phase. For MALDI, the solution is usually added onto the matrix spot of dithranol, -cyano-4-hydroxycinnamic acid, dihydroxybenzoic acid or terthiophene. Solvent is used only when necessary for DART. The ions are detected with the Agilent 6210 TOF-MS while the data is processed with the MassHunter™ software. 6,6',6''-methanetriyltris(4-amino-2-methylphenol) was synthesized as described in the literature.[58] Butylated phenols were either purchased or prepared following a modified literature procedure.[57] DFT geometry optimizations were done with Gaussian[82] using B3LYP functional with the LANL2DZ basis set. Semi-empirical optimizations were carried out using MOPAC[56] with PM6 methods.

Preparation of 4-(tert-butyl) phenols

In a dried, well vented roundbottom flask, 0.1eq of annh. $AlCl_3$ was added to 1eq of the appropriate ortho substituted phenol. The reaction flask was fitted with an addition funnel and the suspension was stirred for 10 minutes after which 1.2eq of tert-butyl chloride was slowly added to the suspension. The reaction was allowed to stir overnight at room temperature. The resulting mixture was then poured onto a generous amount ice and stirred until all ice had melted. The mixture was transferred to a seperatory funnel and extracted with ethyl acetate (3 x 100ml). The combined organic phase was washed with saturated bicarbonate followed by brine. The organic phase was dried over sodium sulfate and the solvent removed under vacuum to yield a viscous oil. The crude oil was then distilled under full vacuum at 110-115˚ to yield pure product as clear oil.

Synthesis of 3-1

A 40.1g (97mmol) sample of 4-(tert-butyl)-2-secbutylphenol along with 74.26g (390mmol) of annh. $MgCl_2$, and 108ml (390mmol) of triethylamine were dissolved in 1000ml of acetonitrile. The mixture was stirred for 30 minutes, after which a 34.92g (580mmol) portion of paraformaldehyde was added. The reaction was refluxed overnight. The suspension was cooled to room temperature after which a 3M HCl solution was added until all solids dissolved. The aqeuous mixture was allowed to cool to room temperature and extracted with ethyl acetate (3 x 100ml). The organic phase was washed with 10% HCl (v/v), water, and brine successively. The solvent was removed yielding crude 3-(*sec*-butyl)-5-(*tert*-butyl)-2-hydroxybenzaldehyde as a yellow oil. The resulting yellow oil was dissolved into 80ml of methanol. The reaction vessel was fitted with an addition funnel and 100ml of thionyl chloride was added slowly over a period of several hours. The reaction was allowed to stir overnight, after which it was

filtered. The resulting solid was recrystallized from methanol and dried under vacuum yielding the product as a white solid. Single crystals suitable for X-ray diffraction were grown from slow evaporation of methanol. Yield: 21.9g, 36%. ^{1}H NMR (300MHz ,CHLOROFORM-d) δ = 7.14 (br. s, 3 H), 6.83 - 6.73 (m, 3 H), 5.85 (s, 1 H), 4.84 (br. s, 3 H), 3.08 - 2.92 (m, 3 H), 1.76 - 1.53 (m, 6 H), 1.25 (d, J = 7.3 Hz, 9 H), 1.20 (br. s, 27 H), 0.91 - 0.79 (m, 9 H). ^{13}C NMR (75MHz ,CHLOROFORM-d) δ = 149.3, 143.5, 133.8, 125.7, 123.6, 123.1, 41.9, 34.5, 34.2, 31.4, 29.9, 20.6, 12.2. ESI-TOF-MS: calcd for $C_{43}H_{64}O_3$ 628.4850; found 628.4848 [M^+]

Synthesis of 3-2

Compound 3-2 was synthesized in the same manner as 3-1. Single crystals suitable for X-ray diffraction were grown from slow evaporation of methanol. Yield: 35.9g 63% ^{1}H NMR (300MHz ,CHLOROFORM-d) δ = 7.19 (d, *J* = 2.1 Hz, 3 H), 6.81 (d, *J* = 2.3 Hz, 3 H), 5.87 - 5.81 (m, 1 H), 4.90 (br. s, 3 H), 3.31 - 3.14 (m, *J* = 6.8, 6.8, 6.8, 6.8, 14.0 Hz, 3 H), 1.26 (d, *J* = 6.7 Hz, 18 H), 1.20 (br. s, 27 H). ^{13}C NMR (75MHz ,CHLOROFORM-d) δ = 149.0, 143.5, 135.0, 125.6, 123.7, 122.2, 41.9, 34.3, 31.4, 27.5, 22.7. ESI-TOF-MS: calcd for $C_{40}H_{62}O_3N$ 604.4724; found 604.4730 [M+NH4]$^+$

Synthesis of 3-3

Compound 3-3 was synthesized in the same manner as 3-1. Single crystals suitable for X-ray diffraction were grown from an ethanol/ether diffusion. Yield: 10.9g, 22% ^{1}H NMR (300MHz, DMSO-d_6) δ = 8.84 (s, 3 H), 7.59 (s, 3 H), 6.59 (d, *J* = 2.3 Hz, 3 H), 6.48 (s, 1 H), 6.42 (d, *J* = 2.3 Hz, 3 H), 1.09 (s, 27 H). ^{13}C NMR (75MHz ,DMSO-d_6) δ = 143.6, 140.5, 139.2, 130.3, 117.7, 109.7, 35.3, 33.5, 31.4. ESI-TOF-MS: calcd for $C_{31}H_{41}O_6$ 509.2898; found 509.2913 [M+H]$^+$

Synthesis of 3-4

A 27.6g (200mmol) potion of K_2CO_3 along with a 30.2g (51.1mmol) portion of 3-1 were dissolved in 150ml of DMF and the reaction vessel fitted with a septum. A 12.4ml (200mmol) portion of iodomethane was injected into the reaction and stirred overnight at room temperature. The reaction was poured into 500ml of water, filtered, and the resulting white solid recrystalized from methanol. Yield: 20.6g, 64%. ^{1}H NMR (300MHz ,CHLOROFORM-d) δ = 7.09 (d, *J* = 2.3 Hz, 3 H), 6.59 (d, *J* = 2.6 Hz, 3 H), 6.41 - 6.39 (m, 1 H), 3.66 (s, 9 H), 3.37 - 3.25 (m, 3 H), 1.24 - 1.18 (m, *J* = 1.0 Hz, 18 H), 1.16 - 1.13 (m, 27 H). ^{13}C NMR (75MHz ,CHLOROFORM-d) δ = 152.6, 145.7, 140.6, 136.4, 125.4, 120.9, 61.4, 39.1, 34.3, 31.3, 26.4, 24.2. DART-TOF-MS: calcd for $C_{43}H_{65}O_3$ 646.5194; found 646.5183 $[M+H]^+$

Synthesis of 3-5

Compound 3-5 was synthesized using the same procedure as for 3-4, using bromoethane in place of iodomethane. Yield: 35.3g, 95% ^{1}H NMR (300MHz ,CHLOROFORM-d) δ = 7.06 (d, *J* = 2.6 Hz, 3 H), 6.76 (d, *J* = 2.6 Hz, 3 H), 6.58 (s, 1 H), 3.54 (q, *J* = 7.0 Hz, 6 H), 3.37 - 3.19 (m, 3 H), 1.29 (t, *J* = 6.9 Hz, 9 H), 1.21 - 1.17 (m, 18 H), 1.16 (s, 27 H). ^{13}C NMR (75MHz ,CHLOROFORM-d) δ = 152.1, 145.1, 140.6, 136.8, 125.7, 120.4, 69.3, 38.6, 34.3, 31.4, 26.6, 24.2, 15.7. DART-TOF-MS: calcd for $C_{92}H_{141}O_6$ 688.5663; found 688.5682 $[M+NH_4]^+$

Synthesis of 3-6

Compound 3-6 was synthesized using the same procedure as for 3-4. Yield: 8.8g, 44% ^{1}H NMR (300MHz ,CHLOROFORM-d) δ = 7.04 (br. s, 3 H), 6.65 - 6.57 (m, 3 H), 6.45 - 6.39 (m, 1 H), 3.69 - 3.56 (m, 9 H), 3.13 - 2.96 (m, 3 H), 1.67 - 1.49 (m, 6 H), 1.27

- 1.17 (m, 9 H), 1.16 - 1.10 (m, 27 H), 0.89 - 0.72 (m, 9 H). ^{13}C NMR (75MHz ,CHLOROFORM-d) δ = 153.3, 145.7, 139.4, 139.3, 136.5, 125.3, 121.0, 61.3, 39.3, 34.3, 33.3, 31.1, 22.1, 12.3. DART-TOF-MS: calcd for $C_{46}H_{74}O_3N$ 688.5663; found 688.5678 $[M+NH_4]^+$

Synthesis of 3-7

Compound 3-7 was synthesized using the same procedure as for 3-4. Yield: 17.2g, 80% ^{1}H NMR (300MHz ,CHLOROFORM-d) δ = 7.03 - 6.98 (m, *J* = 2.3 Hz, 3 H), 6.84 - 6.75 (m, 3 H), 6.63 - 6.58 (m, 1 H), 3.60 - 3.42 (m, *J* = 7.4 Hz, 6 H), 3.10 - 2.94 (m, 3 H), 1.63 - 1.48 (m, *J* = 4.2 Hz, 6 H), 1.33 - 1.23 (m, *J* = 2.8, 6.4, 6.4 Hz, 9 H), 1.22 - 1.19 (m, 9 H), 1.18 - 1.12 (m, *J* = 2.5, 2.5 Hz, 27 H), 0.83 - 0.72 (m, *J* = 5.4, 7.2, 7.2 Hz, 9 H). ^{13}C NMR (75MHz ,CHLOROFORM-d) δ = 152.7, 145.1, 139.4, 136.9, 125.6, 120.6, 69.1, 38.6, 34.3, 33.4, 31.4, 31.1, 22.0, 15.7, 12.4. DART-TOF-MS: calcd for $C_{49}H_{80}O_3N$ 730.6133; found 730.6177 $[M+NH_4]^+$

Synthesis of 3-8

Compound 3-8 was synthesized using the same procedure as for 3-4. Yield: 30.1g, 64% ^{1}H NMR (300MHz ,CHLOROFORM-d) δ = 6.99 (d, *J* = 2.5 Hz, 3 H), 6.82 (d, *J* = 2.5 Hz, 3 H), 6.62 (s, 1 H), 3.66 (q, *J* = 7.1 Hz, 6 H), 2.26 (s, 8 H), 2.31 - 2.21 (m, 9 H), 1.32 (t, *J* = 6.9 Hz, 8 H), 1.17 (s, 24 H). ^{13}C NMR (75MHz ,CHLOROFORM-d) δ = 153.3, 144.9, 136.4, 129.8, 125.8, 125.6, 68.0, 37.8, 34.1, 31.4, 16.8, 15.6. DART-TOF-MS: calcd for $C_{40}H_{62}O_3N$ 604.4724; found 604.4751 $[M+NH_4]^+$

Synthesis of 3-9

Compound 3-9 was synthesized using the same procedure as for 3-4. Yield: 27.9g, 56% ^{1}H NMR (300MHz ,CHLOROFORM-d) δ = 7.00 - 6.90 (m, *J* = 9.1 Hz, 6 H),

6.48 - 6.44 (m, 1 H), 4.23 - 4.08 (m, *J* = 6.1, 6.1, 6.1, 6.1, 6.1, 6.1 Hz, 3 H), 2.22 (s, 9 H), 1.17 (s, 27 H), 1.00 (d, *J* = 6.2 Hz, 18 H). ^{13}C NMR (75MHz ,CHLOROFORM-d) δ = 151.5, 144.1, 136.9, 130.3, 126.7, 125.1, 73.4, 38.6, 34.0, 31.4, 22.1, 18.2. DART-TOF-MS: calcd for $C_{43}H_{68}O_3N$ 646.5194; found 646.5164 $[M+NH_4]^+$

Synthesis of 3-10

A 20g (31.8mmol) sample of 3-4 was dissolved in 100ml of DCM. A 21.4ml (286 mmol) aliquot of TFA was added and the reaction vessel fitted with an addition funnel. 26ml (290 mmol) of nitric acid (70%) was slowly added dropwise to the solution and the reaction allowed to stir overnight. The solvent was removed under vacuum until a yellow slurry formed. 300ml of methanol was added and the mixture stirred for 10 minutes. The mixture was cooled to 0˚ and filtered yielding the product as a pale yellow solid. Single crystals suitable for X-ray diffraction were grown from a THF/pentane diffusion. Yield: 78% ^{1}H NMR (300MHz ,CHLOROFORM-d) δ = 8.16 (d, *J* = 2.3 Hz, 3 H), 7.56 (d, *J* = 2.5 Hz, 3 H), 6.59 (s, 1 H), 3.63 (d, *J* = 0.8 Hz, 9 H), 3.41 - 3.24 (m, 3 H), 1.28 (d, *J* = 6.8 Hz, 18 H). ^{13}C NMR (75MHz ,CHLOROFORM-d) δ = 160.4, 144.4, 136.8, 122.4, 122.2, 61.9, 38.9, 27.0, 23.5. ESI-TOF-MS: calcd for $C_{31}H_{41}N_4O_9$ 613.2894; found 613.2894 $[M+NH_4]^+$

Synthesis of 3-11

Compound 3-11 was synthesized following the same procedure for 3-10. Single crystals suitable for X-ray diffraction were grown from a chloroform/pentane diffusion. Yield: 10.9g, 81% ^{1}H NMR (300MHz ,CHLOROFORM-d) δ = 8.14 (d, *J* = 2.9 Hz, 3 H), 7.64 (d, *J* = 2.6 Hz, 3 H), 6.73 (s, 1 H), 3.53 (q, *J* = 6.8 Hz, 6 H), 3.36 - 3.21 (m, 3 H), 1.32 - 1.23 (m, 27 H). ^{13}C NMR (75MHz ,CHLOROFORM-d) δ = 159.7, 144.5, 144.3,

137.3, 122.5, 122.2, 70.5, 38.7, 27.1, 23.5, 15.4. ESI-TOF-MS: calcd for $C_{34}H_{43}N_3O_9K$ 660.2892; found 660.2870 $[M+K]^+$

Synthesis of 3-12

Compound 3-12 was synthesized following the same procedure for 3-10. Single crystals suitable for X-ray diffraction were grown from slow evaporation of methanol. Yield: 3.7g, 97% ^{1}H NMR (300MHz ,CHLOROFORM-d) δ = 8.15 - 8.07 (m, 3 H), 7.62 - 7.47 (m, 3 H), 6.55 (br. s, 1 H), 3.63 - 3.52 (m, 9 H), 3.14 - 2.97 (m, *J* = 6.9, 12.0 Hz, 3 H), 1.76 - 1.47 (m, 6 H), 1.28 (t, *J* = 6.7 Hz, 9 H), 0.80 (q, *J* = 7.4 Hz, 9 H). ^{13}C NMR (75MHz ,CHLOROFORM-d) δ = 161.0, 144.5, 143.4, 136.8, 122.6, 122.2, 61.8, 39.2, 33.9, 31.0, 21.5, 12.1. DART-TOF-MS: calcd for $C_{34}H_{47}N_4O$ 655.3338; found 655.3351 $[M+NH_4]^+$

Synthesis of 3-13

Compound 3-13 was synthesized following the same procedure for 3-10. Single crystals suitable for X-ray diffraction were grown from slow evaporation of methanol. Yield: 11.9g, 73% ^{1}H NMR (300MHz ,CHLOROFORM-d) δ = 8.17 - 8.04 (m, 3 H), 7.69 - 7.55 (m, 3 H), 6.76 - 6.66 (m, 1 H), 3.73 - 3.36 (m, 6 H), 3.12 - 2.93 (m, *J* = 3.4, 3.4, 7.0, 11.0 Hz, 3 H), 1.75 - 1.50 (m, 6 H), 1.31 (d, *J* = 1.4 Hz, 9 H), 1.27 (m, *J* = 2.7, 6.9 Hz, 9 H), 0.86 - 0.74 (m, 9H). ^{13}C NMR (75MHz ,CHLOROFORM-d) δ = 160.3, 144.3, 143.5, 137.3, 137.1, 122.4, 70.5, 38.9, 34.0, 30.9, 21.5, 15.5, 12.1. DART-TOF-MS: calcd for $C_{37}H_{53}N_4O_9$ 697.3807; found 697.3807 $[M+NH_4]^+$

Synthesis of 3-14

Compound 3-14 was synthesized following the same procedure for 3-10. Single crystals suitable for X-ray diffraction were grown from a dichloroethane/pentane

diffusion. Yield: 22.8g, 81% ^{1}H NMR (300MHz ,CHLOROFORM-d) δ = 8.06 (d, *J* = 2.6 Hz, 3 H), 7.56 (d, *J* = 2.6 Hz, 3 H), 6.64 (s, 1 H), 3.70 (q, *J* = 7.0 Hz, 6 H), 2.39 (s, 9 H), 1.26 (t, *J* = 7.0 Hz, 9 H). ^{13}C NMR (75MHz ,CHLOROFORM-d) δ = 161.0, 143.3, 136.6, 133.0, 126.3, 122.6, 69.0, 38.7, 17.0, 15.3. DART-TOF-MS: calcd for $C_{28}H_{35}N_4O_9$ 571.2399; found 571.2413 $[M+NH_4]^+$

Synthesis of 3-15

Compound 3-15 was synthesized following the same procedure for 3-10. Single crystals suitable for X-ray diffraction were grown from a THF/pentane diffusion. Yield: 23.7g, 54% ^{1}H NMR (300MHz ,CHLOROFORM-d) δ = 8.72 (d, *J* = 2.8 Hz, 3 H), 8.37 (d, *J* = 2.8 Hz, 3 H), 7.27 (s, 1 H), 5.16 (spt, *J* = 6.1 Hz, 3 H), 3.08 (s, 9 H), 1.75 (d, *J* = 5.9 Hz, 18 H). ^{13}C NMR (75MHz ,CHLOROFORM-d) δ = 159.7, 142.8, 136.7, 132.3, 126.3, 123.3, 75.0, 39.1, 22.2, 18.5. ESI-TOF-MS: calcd for $C_{31}H_{41}N_4O_9$ 613.2868; found 613.2890 $[M+NH_4]^+$

Synthesis of 3-16

A 3.1g (4.7mmol) portion of 3-11 was dissolved in 120ml of THF and 30ml of ethanol. A scoop of Raney Nickel was added and the reaction vessel sealed. H_2 was bubbled through the solvent for 8 hours, after which the reaction was stirred under an atmosphere of H_2 for 48 hours. The reaction was filtered and the catalyst washed with THF. The solvent was removed under vacuum and the solid dissolved in ether, filtered, and extracted with 10% HCl. The aqueous phase was washed with hexane and toluene sequentially. The aqueous phase was made basic using a 1M NaOH solution and extracted with chloroform. The solvent was removed in vacuo yielding the product as a pale yellow solid. Yield: 2.4g, 94% ^{1}H NMR (300MHz ,DMSO-d_6) δ = 6.39 (br. s, 1 H),

6.28 (br. s, 3 H), 6.13 (br. s, 3 H), 4.60 (br. s., 6 H), 3.30 - 3.16 (m, 6 H), 3.16 - 3.00 (m, 3 H), 1.10 (br. d, *J* = 5.9 Hz, 27 H). ^{13}C NMR (75MHz ,DMSO-d_6) δ = 145.7, 144.4, 141.7, 138.7, 114.6, 110.3, 69.3, 37.8, 26.5, 24.7, 16.1. ESI-TOF-MS: calcd for $C_{34}H_{50}N_3O_3$ 548.3847; found 548.3842 $[M+H]^+$

Synthesis of 3-17

Compound 3-17 was synthesized using the same procedure as 3-16. Yield: 1.98g, 76% ^{1}H NMR (300MHz ,DMSO-d_6) δ = 6.43 (s, 1 H), 6.23 (d, *J* = 0.9 Hz, 3 H), 6.19 - 6.12 (m, 3 H), 4.60 (br. s., 6 H), 3.30 - 3.06 (m, 6 H), 2.91 - 2.75 (m, 3 H), 1.45 (br. s., 6 H), 1.17 - 1.02 (m, 18 H), 0.83 - 0.69 (m, 9 H). ^{13}C NMR (75MHz ,DMSO-d_6) δ = 146.5, 146.4, 144.3, 140.6, 138.8, 114.7, 110.4, 69.2, 55.6, 33.5, 31.2, 22.6, 16.3, 13.1. ESI-TOF-MS: calcd for $C_{37}H_{56}N_3O_3$ 590.4316; found 590.4342 $[M+H]^+$

Synthesis of 3-18

Compound 3-18 was synthesized using the same procedure as 3-16. Yield: 1.1g, 61% ^{1}H NMR (300MHz ,DMSO-d_6) δ = 6.25 (br. s., 3 H), 6.09 (br. s., 1 H), 5.74 (s, 3 H), 4.64 (br. s., 6 H), 3.44 - 3.17 (m, 9 H), 2.85 (br. s., 3 H), 1.46 (d, *J* = 4.8 Hz, 6 H), 1.10 (d, *J* = 4.8 Hz, 9 H), 0.87 - 0.66 (m, 9 H). ^{13}C NMR (75MHz ,DMSO-d_6) δ = 147.2, 144.6, 140.5, 138.4, 114.6, 110.6, 61.3, 55.6, 33.4, 31.3, 22.6, 13.1. ESI-TOF-MS: calcd for $C_{34}H_{49}N_3O_3$ 548.3847; found 548.3866 $[M+H]^+$

Synthesis of 3-19

Compound 3-19 was synthesized using the same procedure as 3-16. Yield: 2.0g, 92% ^{1}H NMR (300MHz ,DMSO-d_6) δ = 6.23 (br. s., 3 H), 6.19 (s, 1 H), 5.99 (br. s., 3 H), 4.68 (br. s., 6 H), 3.59 - 3.42 (m, 6 H), 2.07 (s, 9 H), 1.27 - 1.08 (m, 9 H). ^{13}C NMR

(75MHz ,DMSO-d_6) δ = 146.4, 143.1, 137.8, 130.0, 114.5, 113.9, 67.4, 16.2, 15.4. ESI-TOF-MS" calcd for $C_{28}H_{38}N_3O_3$ 464.2908; found 464.2910 $[M+H]^+$

Synthesis of 3-20

Compound 3-20 was synthesized using the same procedure as 3-16. Yield: 1.8g, 77% ^{1}H NMR (300MHz ,DMSO-d_6) δ = 6.36 (br. s., 3 H), 6.28 (br. s., 3 H), 6.17 (s, 1 H), 5.75 (br. s, 6 H), 4.05 - 3.89 (m, 1 H), 2.07 (s, 9 H), 0.98 (d, *J* = 5.6 Hz, 18 H). ^{13}C NMR (75MHz ,DMSO-d_6) δ = 145.9, 139.5, 138.0, 131.1, 116.3, 72.9, 54.9, 22.0, 17.7. ESI-TOF-MS: calcd for $C_{31}H_{44}N_3O_3$ 506.337; found 506.3395 $[M+H]^+$

Table 3-1. Complete listing of torsion angles derived from semi-empirical optimizations using PM6 methods.

Compound	Angle 1	Angle 2	Angle 3	Average Angle
C3-1	160.6	138.6	163.7	154.3
C3-2	128.2	58.2	108.2	98.2
C3-3	101.8	111.0	113.0	108.6
C3-5	179.3	168.6	147.0	165.0
C3-6	111.8	118.6	53.4	94.6
C3-7	178.2	165.2	175.2	172.9
C3-8	161.7	163.2	164.1	163.0
C3-9	106.5	126.8	168.7	134.0
C3-10	105.3	121.9	108.5	111.9
C3-11	83.9	71.9	64.1	73.3
C3-12	119.7	107.8	122.5	116.7
C3-13	51.2	55.5	52.7	53.1
C3-14	117.2	94.5	111.9	107.9
C3-15	134.9	87.0	106.2	109.4

Table 3-2. Complete listing of torsion angles derived from DFT geometries optimizations using B3LYP functional and LANL2DZ basis set.

Compound	Angle 1	Angle 2	Angle 3	Average Angle
C3-1	152.2	164.6	179.2	165.3
C3-2	136.4	129.9	58.7	108.3
C3-4	138.1	140.7	144.8	141.2
C3-5	171.4	164.3	168.2	168.0
C3-6	120.9	59.0	136.4	105.4
C3-8	140.7	139.3	140.1	140.0
C3-12	122.3	119.6	116.9	119.6

Table 3-3. Crystallographic data for compounds 3-1, 3-2, 3-3.

	3-1	3-2 • 2 CH_3OH	3-3 • 2 C_2H_5OH
Total Reflections	38391	86584	55585
Uniq. Reflections/ Reflections $I \geq 2\sigma(I)$	2329/38402	9268/5795	16111/8065
Collection Range (°)	$3.83 < \theta < 65.90$	$1.74 < \theta < 27.50$	$1.75 < \theta < 27.50$
Formula	$C_{43}H_{64}O_3$	$C_{42}H_{66}O_5$	$C_{33}H_{46}O_7$
M_r	628.94	650.95	554.70
Crystal System	Cubic	Monoclinic	Triclinic
Space Group	$Pa\bar{3}$	$P2_1c$	$P\bar{1}$
a (Å)	20.0022(4)	14.2671(3)	10.8988(7)
b (Å)	-	14.9853(4)	17.1676(11)
c (Å)	-	19.0223(5)	19.0649(12)
α (°)	-	-	80.804(4)
β (°)	-	97.4831(1)	89.930(4)
γ (°)	-	-	84.543(4)
V_c (Å^3)	8002.6(3)	4032.27(17)	3505.0(4)
D_c (g cm^{-1})	1.044	1.072	1.051
Z	8	4	4
F(*000*)	2768	1432	1200
μ[Mo-Kα] (mm^{-1})	0.482	0.068	0.073
R_1[$I \geq 2\sigma(I)$data]	0.0856	0.0534	0.0617
wR_2[$I \geq 2\sigma(I)$data]	0.2471	0.1202	0.1463
GoF	1.105	1.039	0.895
Largest Peak, deepest trough (e Å^{-3})	+0.793, -0.451	+0.308, -0.287	+0.363, -0.415

Table 3-4. Crysallographic data for compounds 3-10, 3-11, 3-12.

	3-10	3-11	3-12
Total Reflections	21902	19737	27964
Uniq. Reflections/ Reflections $I \geq 2\sigma(I)$	7444/6621	8245/5833	5591/4612
Collection Range (˚)	$1.65 < \theta < 27.50$	$2.03 < \theta < 27.50$	$3.89 < \theta < 65.49$
Formula	$C_{31}H_{37}N_3O_9$	$C_{34}H_{43}N_3O_9$	$C_{34}H_{42}N_3O_9$
M_r	595.64	637.71	637.71
Crystal System	Triclinic	Triclinic	Triclinic
Space Group	$P\bar{1}$	$P\bar{1}$	$P\bar{1}$
a (Å)	9.4142(13)	10.0324(11)	12.4192(5)
b (Å)	12.7100(17)	13.1039(14)	12.6918(5)
c (Å)	14.1516(19)	14.3409(16)	13.1430(6)
α (˚)	95.651(2)	94.718(7)	65.881(2)
β (˚)	99.554(2)	103.108(6)	63.810(2)
γ (˚)	101.524(2)	98.706(7)	70.227(2)
V_c (Å^3)	1620.9(4)	1801.7(3)	1664.81(12)
D_c (g cm^{-1})	1.220	1.176	1.272
Z	2	2	2
F(*000*)	632	680	680
μ[Mo-Kα] (mm^{-1})	0.090	0.085	0.762
R_1[$I \geq 2\sigma(I)$data]	0.0400	0.0555	0.0686
wR_2[$I \geq 2\sigma(I)$data]	0.1101	0.1427	0.1774
GoF	1.090	1.087	1.040
Largest Peak, deepest trough (e Å^{-3})	+0.367, -0.234	+0.578, -0.490	+0.816, -0.539

Table 3-5. Crystallographic data for compounds 3-13, 3-14, 3-15.

	3-13	3-14	3-15
Total Reflections	26765	11086	21024
Uniq. Reflections/ Reflections $I \geq 2\sigma(I)$	8439/4661	11086/7581	7058/5478
Collection Range (˚)	$1.72 < \theta < 27.50$	$1.55 < \theta < 25.00$	$1.63 < \theta < 27.50$
Formula	$C_{37}H_{49}N_3O_9$	$C_{28}H_{31}N_3O_9$	$C_{31}H_{37}N_3O_9$
M_r	679.79	553.05	595.64
Crystal System	Triclinic	Triclinic	Triclinic
Space Group	$P\bar{1}$	$P\bar{1}$	$P\bar{1}$
a (Å)	12.604(2)	12.599(3)	11.0418(5)
b (Å)	12.654(2)	13.603(3)	12.2551(6)
c (Å)	12.928(2)	19.479(4)	12.4831(6)
α (˚)	100.926(3)	88.889(4)	89.941(3)
β (˚)	108.228(3)	78.549(4)	86.562(3)
γ (˚)	102.714(3)	74.711(4)	65.777(2)
V_c (Å^3)	1834.5(6)	3154.2(12)	1537.18(13)
D_c (g cm^{-1})	1.231	1.165	1.287
Z	2	4	2
F(*000*)	728	1166	632
μ[Mo-Kα] (mm^{-1})	0.088	0.088	0.095
$R_1[I \geq 2\sigma(I)$data]	0.0923	0.0773	0.0583
$wR_2[I \geq 2\sigma(I)$data]	0.2425	0.2231	0.1507
GoF	1.034	1.539	1.035
Largest Peak, deepest trough (e Å^{-3})	+1.806, -1.526	+0.920, -0.957	+0.919, -0.522

Table 3-6. Selected bond lengths for tripodal copper containing compound 3-21.

Atoms	Distance (Å)
Cu1-N1	1.934(6)
Cu1-N9	1.931(6)
Cu1-Cl1	2.680(2)
Cu2-N3	1.852(6)
Cu2-N7	1.866(6)
Cu3-N5	1.957(6)
Cu3-N11	1.963(6)
Cu3-Cl1	2.534(2)
N1-C26	1.304(9)
N2-C26	1.365(9)
N3-C39	1.315(9)
N4-C39	1.374(10)
N5-C52	1.272(8)
N6-C52	1.389(9)
N7-C65	1.331(9)
N8-C65	1.331(9)
N9-C78	1.272(9)
N10-C78	1.358(9)
N11-C91	1.313(10)
N12-C91	1.351(9)

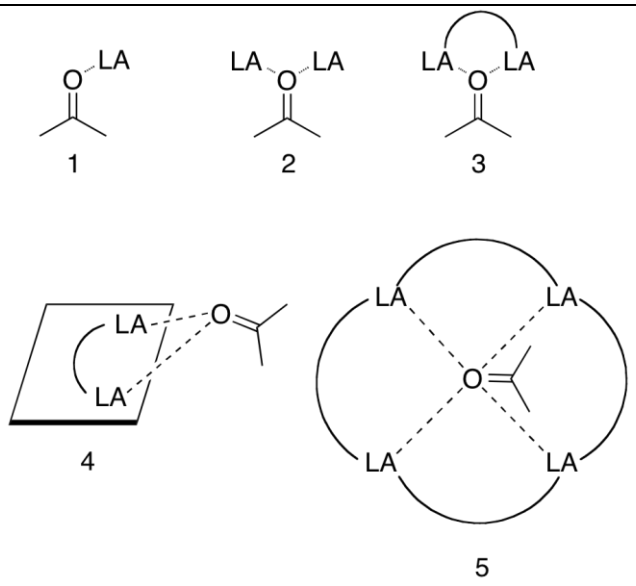

Figure 3-1. Coordination of multiple Lewis acids to a single base. Complex 1 represents the typical 1:1 Lewis acid : substrate binding mode, while complexes 2 – 4 show plausible multi-metallic binding modes.

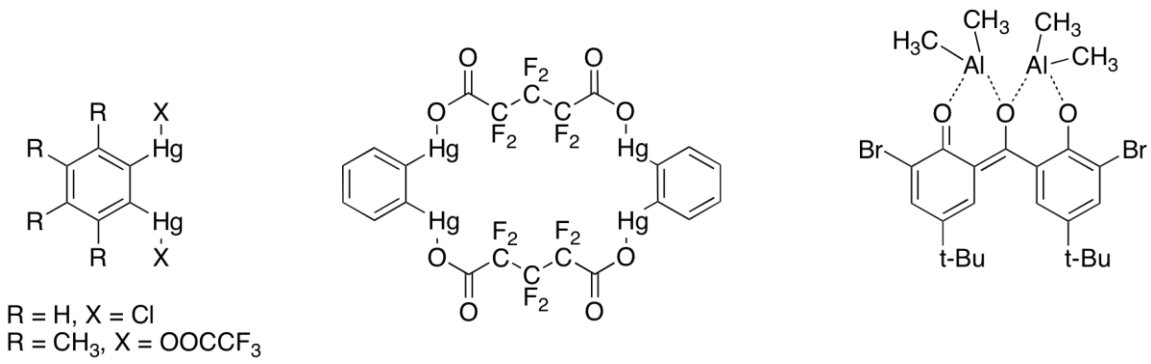

Figure 3-2. Multidentate Lewis acid complexes synthesized and studied by Wuest et al.[16]

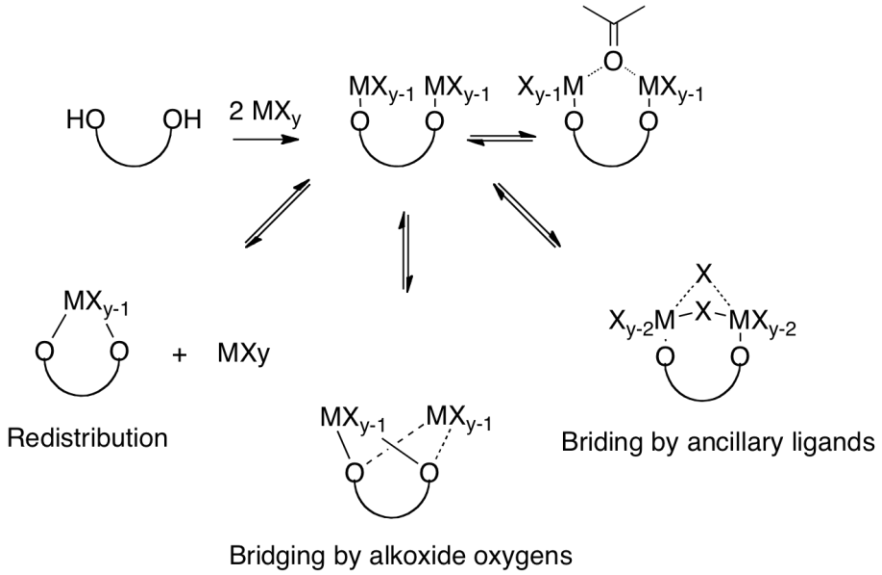

Figure 3-3. Plausible arrangements and binding between ligands and Lewis acid centers.

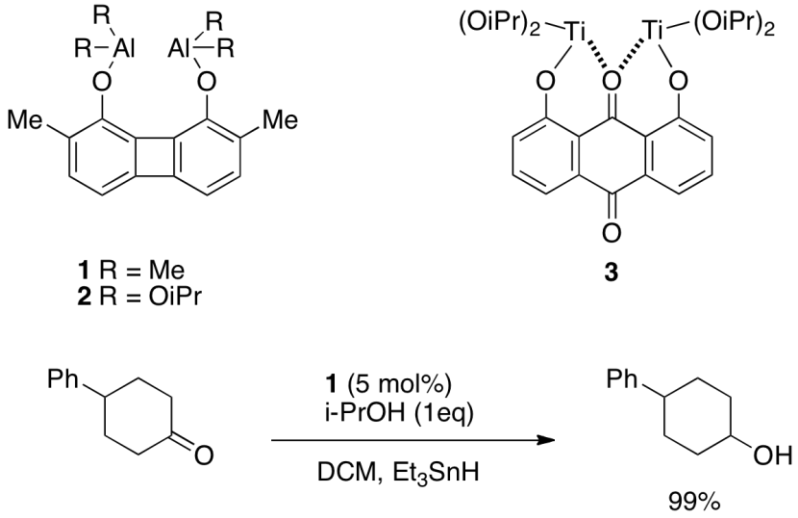

Figure 3-4. Compounds 1,2, and 3 were employed by Maruoka for reduction of carbonyls. Bidentate complexes showed a marked increase in reactivity from their monodentate counterparts.[59]

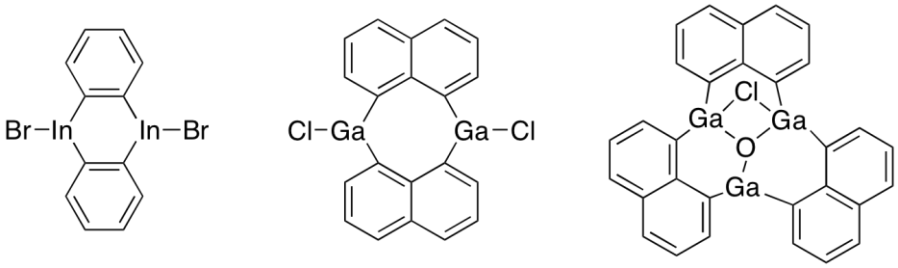

Figure 3-5. Several of the compounds synthesized by Gabbaï et al. for selective anion binding.[60]

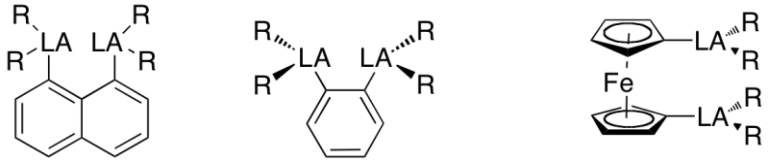

Figure 3-6. Common ligand motifs employed in multidentate Lewis acid systems. LA refers to a Lewis acid, typically B, Al, or Hg. R refers to some ancillary ligand, often perfluorinated.[16,39,60]

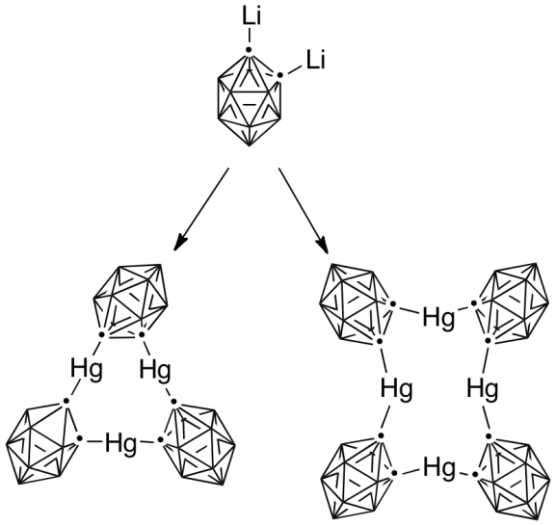

Figure 3-7. Mercurocarboranes have been shown to assemble into trimeric and tetrameric structures creating a binding pocket within the cavity of mercury ions.[38,40]

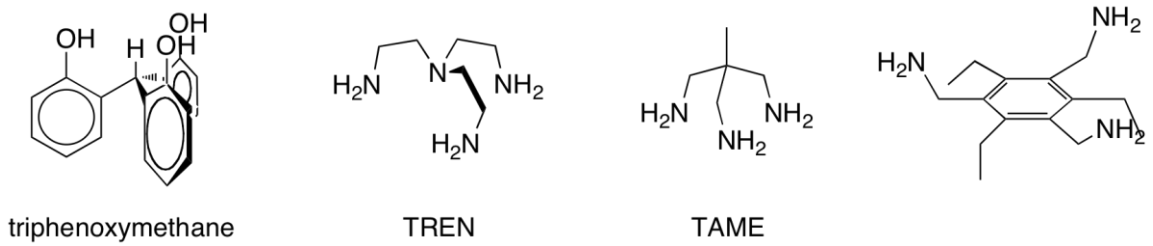

Figure 3-8. Several common C_3 scaffolding ligands that are found within the literature.

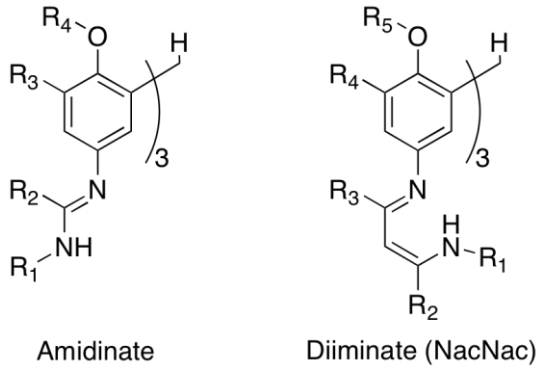

Figure 3-9. Depictions of the desired target ligand sets.

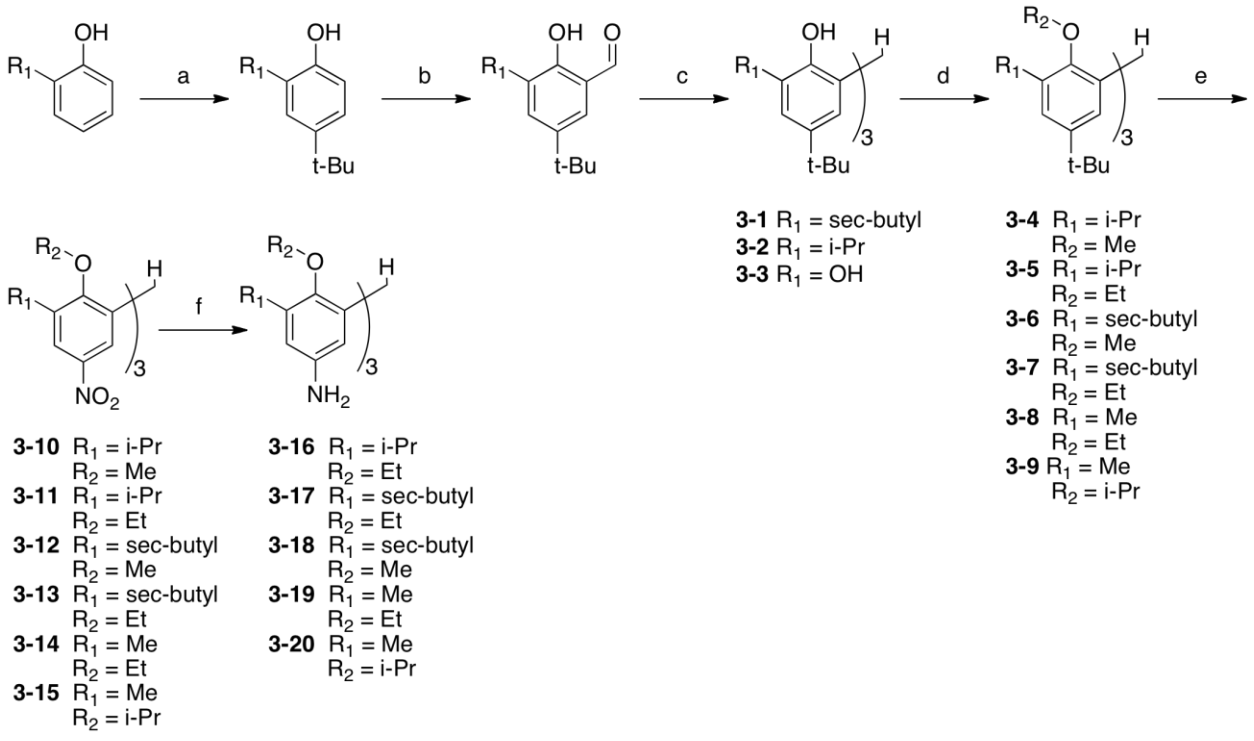

Figure 3-10. a) t-BuCl, $AlCl_3$ b) CH_2O, $N(Et)_3$, $MgCl_2$ c) $SOCl_2$, MeOH, butylated phenol d) alkyl iodide, K_2CO_3 e) HNO_3, TFA f) Raney Nickel, H_2

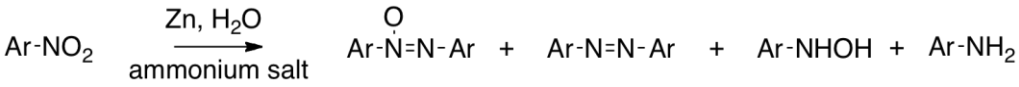

Figure 3-11. Mixture of reported products formed by reduction mediated by zinc.[55]

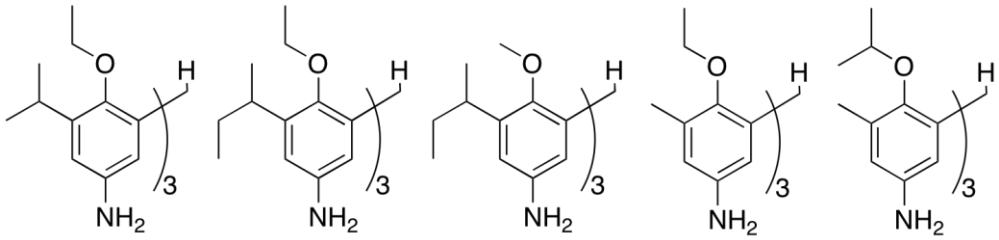

Figure 3-12. Successfully synthesized and isolated tris-amine scaffold ligands.

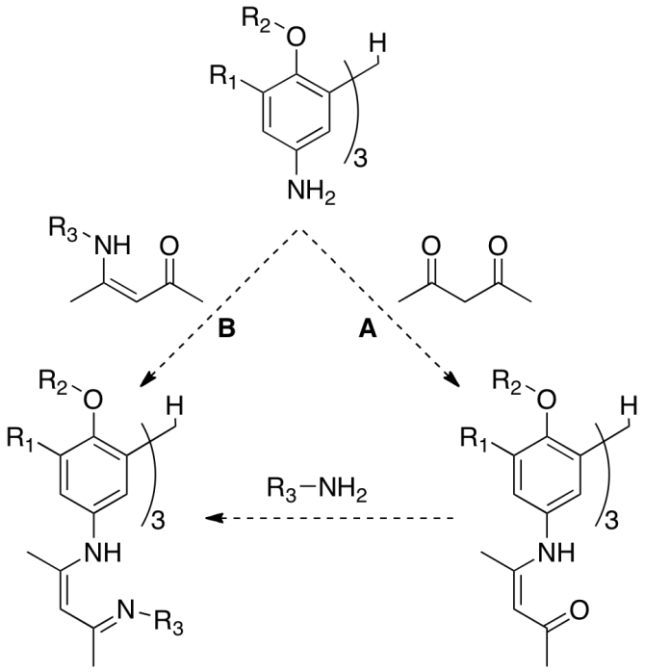

Figure 3-13. Proposed synthetic routes (A and B) leading to target tris-diiminate ligand set.

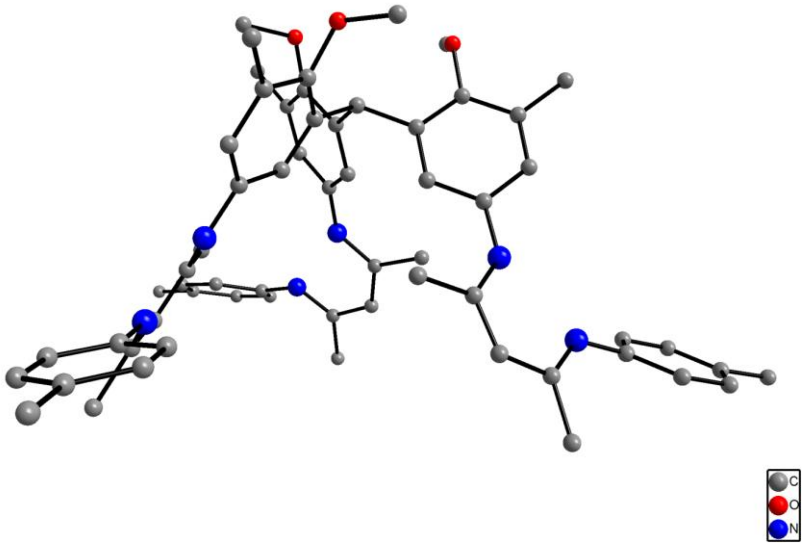

Figure 3-14. DFT optimized structure of the p-tolyl derivative of the diiminate ligand set.

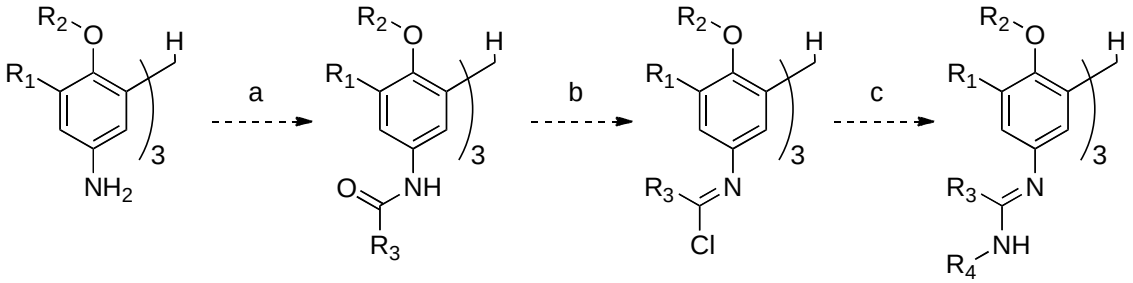

3-21

Figure 3-15. Proposed synthetic scheme of the tris-amidinate ligand set. a) alkyl/aryl acyl chloride b) PCl_5 c) alkyl/aryl amine

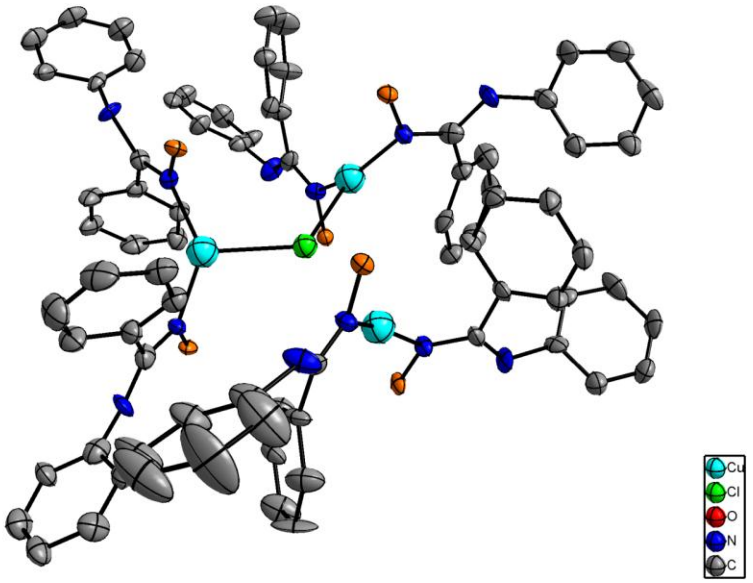

Figure 3-16. Core of the dimerized amidinate complex 3-21. Atoms in orange are carbons attached to the platform ligand. 30% probability ellipsoids, hydrogens and counter ions omitted for clarity.

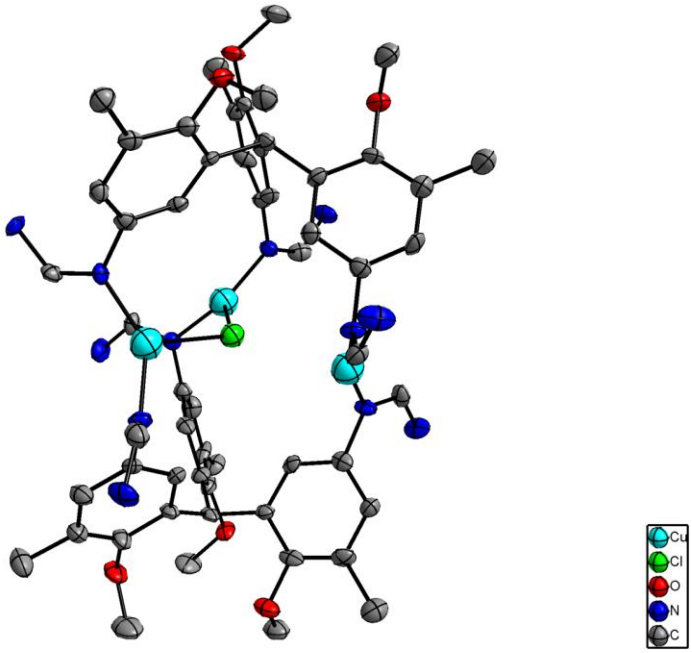

Figure 3-17. The dimerized amidinate structure(3-21) shown without ancillary phenyl rings. 30% probability ellipsoids, hydrogens and counter ions omitted for clarity.

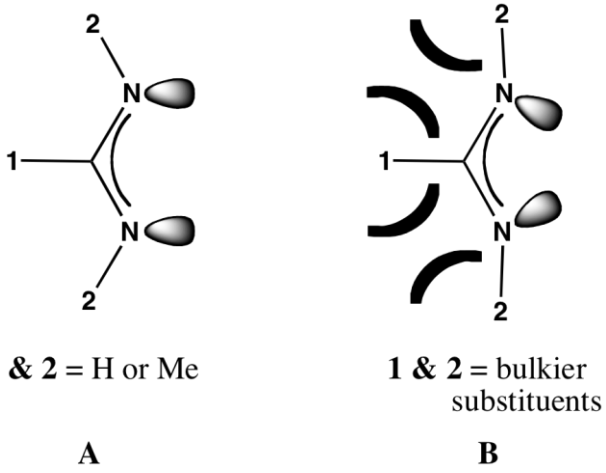

Figure 3-18. Less bulky substituents in the 1 and 2 positions allow for a bridging mode (A), while more bulky groups force a chelate binding mode (B).

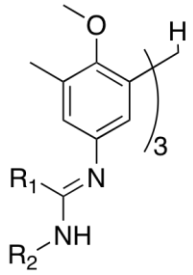

C3.1 R1 = 2,6-diisopropylphenyl
R2 = t-butyl

C3.2 R1 = phenyl
R2 = t-butyl

C3.3 R1 = t-butyl
R2 = t-butyl

C3.4 R1 = mesityl
R2 = t-butyl

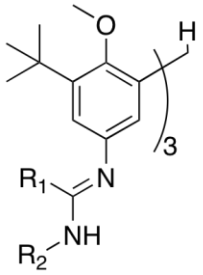

C3.5 R1 = 2,6-diispropylphenyl
R2 = t-butyl

C3.6 R1 = phenyl
R2 = t-butyl

C3.7 R1 = t-butyl
R2 = t-butyl

C3.8 R1 = mesityl
R2 = t-butyl

C3.9 R1 = 2,4-dimethylpentyl
R2 = t-butyl

C3.10 R1 = dibenzyl
R2 = t-butyl

C3.11 R1 = mesityl
R2 = 2,4-dimethylpentyl

C3.12 R1 = methyl
R2 = methyl

C3.13 R1 = methyl
R2 = t-butyl

C3.14 R1 = phenyl
R2 = isopropyl

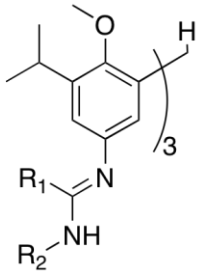

C3.15 R1 = phenyl
R2 = t-butyl

Figure 3-19. Complete list of structures which were optimized by either semi-empirical methods or DFT.

CHAPTER 4
SOLID-STATE STRUCTURAL PROPERTIES OF LIGAND SYSTEMS BEARING TRIPHENOXYMETHANE SCAFFOLDS

Introduction

The triphenoxymethane moiety has found success as both a pre-organized scaffolding ligand[86] and as a C_3 symmetric analogue for calixarene-based systems.[51] The triphenoxymethane platform has been employed successfully as an effective scaffold used to tether multiple binding arms for segregation of lanthanide and actinide metal ions.[87] These pre-organized species have been shown to produce an increase in selectivity between lanthanide ions from biphasic media. The data presented herein constitutes part of our efforts to better understand how substitutions on the platform moiety affect the formed binding pocket in the solid-state. It is theorized that subtle changes in the binding pocket can influence binding affinity of substrates through functional groups that are tethered through either the para-position or the phenolic oxygen of the platform (Figure 4-1).

Nitrated Derivatives of Triphenoxymethane

Several novel triphenoxymethane platforms have been synthesized bearing various alkyl and alkoxy chains. Complete synthetic discussion, spectroscopic data, and crystallographic tables for these compounds is presented in Chapter 3. Three compounds based off the methyl derivative (4-1), two based off the isopropyl derivative (4-2), and two based off the sec-butyl derivative (4-3) of the triphenoxymethane platform were synthesized and crystallized with varying alkoxy chains (Figure 4-2). The distances between the three nitrogens of the nitro groups (N1, N2, and N3) were set as a plane and the area of the formed triangle calculated. Table 4-1 lists relevant bond lengths and the corresponding calculated binding pocket size for all compounds

obtained from examination of the respective solid-state structures. Compound 4-5 contains two molecules in the asymmetric unit, each possessing a different binding pocket size. The average of the two molecules is used for comparisons.

Comparing the three ortho methyl-substituted compounds 4-4, 4-5, and 4-6 there is a significant decrease in binding area as steric bulk increases in the alkoxy position. A change of 1.98 $Å^2$ is observed as the alkoxy chain increases in steric demand from a methyl to isopropyl (Table 4-1). A negligible difference in binding pocket area is observed between 4-4 and 4-5. This difference is attributed to a minimal steric demand increase between a methyl and ethyl group and the interactions with the ortho substituted methyl group.

As the ortho substituted alkyl chains become more sterically demanding, it is expected that the substitution of the alkoxy group will have more of an impact in the area of the formed binding pocket. This idea is corroborated by the significant change in binding pocket size observed between compounds 4-6 and 4-7. Substitution of the alkoxy group from a methyl to ethyl derivative created a change of 1.00 $Å^2$ in the binding pocket.

Compounds 4-9 and 4-10 show deviation from the expected trends, with an observed increase in binding pocket dimensions as steric bulk decreases. Compound 4-9 has a binding pocket of 20.73 $Å^2$ while compound 4-10 shows a binding pocket of 20.67 $Å^2$. It is the author's opinion that as larger alkyl chains are placed into the ortho postion, these groups begin to dominate the overall steric effects, causing the alkoxy substituents to have less of an impact in the overall structure.

The modular capacity of the triphenoxymethane platform allows for careful tuning of the overall structural properties. The seven nitrated structures herein display an incremental increase in binding pocket area, allowing the possibility to synthesize supra-molecular structures which posses size-exclusion properties. The data also provides insight for tuning of nonadentate structures used for selective sequestration of lanthanide and actinide complexes.

Formylated Asymmetric Triphenoxymethanes

The modularity of the triphenoxymethane platform allows for simple substitution of alkyl groups located in the ortho and para positions of the aryl rings (Figure 4-1). Substitution of the ortho position with a carbonyl moiety allows for the triphenoxymethane ligand to be incorporated into larger structures via subsequent reactions via the carbonyl group. These triphenoxymethane-containing ligands have found potential applications for selective anion binding[88] and as catalyst motifs.[74] Two tripodal-aldehyde compounds have been crystallized to examine the structural characteristics of this class of ligands. Compound 4-11 bears a nitro moiety in the para position of one of the aryl rings, while compound 4-12 contains only alkyl substituents. These substitutions were chosen in an attempt to determine if electron withdrawing moieties impart any changes in structural aspects of the platform ligands.

Synthesis of the ligands was carried out using established literature procedures.[89] A para-substituted phenol was diformylated using standard Duff reaction conditions. The resulting dialdehyde was dissolved in a minimal amount of trifluoroacetic acid. A 2,4-substituted phenol was added to this slurry and the reaction allowed to stir overnight. The product was isolated by vacuum filtration and recrystalized from methanol (Figure 4-3).

Several properties of both structures were examined to determine if any noticeable change in geometry occurred with the inclusion of electron withdrawing groups (Table 4-2). Compounds 4-11 and 4-12 exhibit an average torsion angle of 35.9˚ and 48.2˚ respectively. Both compounds display consistent torsion angles with no large discrepancy in measured bond angles. The difference between the average torsion angles is 12.3˚. This significant deviation in torsion angles is attributed to steric effects arising from alkyl group substitutions in the para position.

The methine bond angle (Figure 4-1) and the binding pocket formed by the three phenolic oxygens were obtained in order to determine the affect of withdrawing groups on the structure. The methine bond angle was examined to determine if there was any observed “rocking” of the aryl ring bearing the nitro moiety. The bond angles of 4-11 and 4-12 were 105.9˚ and 106.0˚ respectively, while the area of the phenolic binding pocket for 4-11 and 4-12 are 7.686 $Å^2$ and 8.776 $Å^2$ respectively. The large difference in binding pocket area is directly related to the large change in torsion angles as mentioned previously.

Analysis of 4-11 and 4-12 shows no deviation in structure that can be attributed to any electronic affects observed in the solid-state. Both compounds exhibit strong correlation in both aryl ring torsional and bond angles. Sterics, rather than electronics, seem to affect a larger change in conformational changes. This finding further validates the binding pocket studies involving compounds 4-4 to 4-10, as sterics are the dominant factor for geometrical preference rather than the nitro functionalities.

Tri-phenolic Ligand Platforms

Triphenoxymethanes in their simplest, unmodified form bear three phenols which are all oriented in the same direction. Numerous spectroscopic and crystallographic

studies have shown that there is no observed ring-flip, meaning there is no inversion of the aryl rings within the structure. This property provides an advantage not observed in calixarene systems, which have a propensity for ring inversion.[90] These tris-phenolic platforms provide ideal scaffolds for synthesis of C_3 symmetric ligand systems with applications to selective metal ion sequestration,[87] anion binding,[88] or enzyme active site models.[86] Two novel derivatives of a tris-phenolic triphenoxymethane platform have been synthesized and examined using X-ray diffraction.

Synthesis of the new derivatives of the triphenoxymethane platform is discussed in complete detail in Chapter 3. The new derivatives, compounds 4-3 and 4-13, were synthesized using established literature procedures.[51] Synthesis of the *iso*-propyl derivative (4-2) has been optimized from previously reported procedures.[43] Compound 4-3 was synthesized in hopes of elucidating observed steric interactions between ortho alkyl chains on the platform and ligands which are tethered to the phenolic oxygens.[87] Compound 4-13 is the first reported example of a catechol based triphenoxymethane ligand (Figure 4-4).

Compounds 4-2, 4-3, and 4-14 were examined to determine what affect substitution of larger alkyl chains in the ortho position has on the overall platform geometry. Several examples of unsubstituted triphenoxymethane ligands have been reported in the literature and will be used as points of comparison for the novel structures presented herein. Compounds 4-13 and 4-14 contain two molecules in the asymmetric unit. Unless otherwise noted, the average values obtained from both molecules are used for comparisons. Compound 4-3 crystallized in a cubic lattice, containing one third of the triphenoxymethane ligand within the unit cell. Relevant bond

lengths and angles were obtained by application of symmetry elements to observed atoms to generate the complete molecular unit.

Compound 4-13 contains significant hydrogen bonding, both to solvent ethanol molecules and extended bonding interactions to other ligands in the lattice. Intramolecular hydrogen bonding is also observed between vicinal phenols. Several of the phenolic hydrogens occupy multiple positions, extending the possibility for further hydrogen bonding interactions. The binding pockets formed by oxygens O1—O2—O3 for each molecule in the asymmetric unit is 7.395 $Å^2$and 7.354 $Å^2$. While the methine bond angles show strong correlation intramolecularly, the other molecule in the asymmetric unit shows significant deviation (Table 4-3). Given the large amount of hydrogen bonding observed in this system it is plausible that intermolecular bonding to other molecules in the lattice is one cause for this observed deviation in angle. This theory is further evidenced by the observed deviation in torsion angle of one aryl ring. In each of the molecules in the asymmetric unit, one ring shows a deviation in torsion angle of roughly 10˚. Attempts to grow single crystals of 4-13 suitable for X-ray diffraction from non-hydrogen bonding solvents have proven unsuccessful.

Compounds 4-2, 4-3, 4-13 and 4-14 provide an opportunity to examine how subtitutions in the ortho position of the triphenoxymethane ligand affect structural properties. Compound 4-2 shows an unusual disparity in torsion angles, with a deviation of 37.1˚ between rings. This large difference in torsion angle is attributed to interactions of the aryl ring with a methanol molecule hydrogen bound to the adjacent phenol. This hydrogen bonding interaction causes the methanol to align in a position directly above the adjacent ring, necessitating an increase in torsion angle to alleviate steric

interactions. The methine bond angles for 4-2 are 107.31˚, 107.49˚, and 107.46˚ with a binding pocket of 7.486 Å^2.

Compound 4-3 crystallizes in a cubic lattice with one third of the triphenoxymethane in the unit cell. Because of this high symmetry lattice, significant disorder is present in the sec-butyl and tbutyl group. Compound 4-3 exhibits intermolecular hydrogen bonding to other triphenoxymethane molecules in the lattice. The methine bond angle is 107.0˚ with a binding pocket of 8.414 Å^2.

Compound 4-14 was previously synthesized and crystallized by the Scott group, referred to as 4-15.[51] The data presented herein has been collected at a lower temperature to provide a more precise structure solution. Both compounds 4-14 and 4-15 have two molecules in the asymmetric unit. While compound 4-15 shows little disparity in measured angles and distances, compound 4-14 displays a larger range of values (Table 4-3). Despite showing significantly different torsion angles, compounds 4-14 and 4-15 have similar average binding pocket areas of 8.55 Å^2 and 8.57 Å^2 respectively. The larger variation in measured properties can be attributed to solvent effects. Residual electron density was located between both molecules in the unit cell of compound 4-14. This density was partially modeled as a diethyl ether molecule, but a proper model could not be established. Since the ether molecule was not interacting with the phenolic hydrogens, its contribution to the solution was removed using SQUEEZE.[94]

One aspect that must be addressed with the phenol containing molecules is the extended hydrogen bonding interactions that are observed in some of the structures. Comparing compounds 4-14 with the previously discussed compound 4-15, both exist

as dimers in the solid-state. Both compounds 4-14 and 4-15 were crystallized from non-hydrogen bonding solvents, diethyl ether and benzene respectively. To probe the affects of coordinating solvent on the solid-state structures of compound 4-15, a crystal was grown from DMSO by previous Scott group member Maarten Dinger.[51] Compound 4-15•DMSO exhibits coordination of a DMSO molecule to the hydrogen of the phenolic moiety of the triphenoxymethane platform. The torsion angles for 4-15•DMSO show a significant disparity due to corrdination of the DMSO molecule, similar to the occurrence in compound 4-2. The coordinated DMSO molecule hydrogen bonds to a phenolic hydrogen which then arranges the DMSO molecule to sit over the adjacent arene ring causing a distortion in the torsion angle. As expected, coordination of the DMSO solvent broke the intermolecular hydrogen bonding between triphenoxymethane platforms, causing them to exist as monomers in the solid-state; however, no reliable data can be drawn with respect to changes in binding pocket size due to the large distortion imparted by the coordinated DMSO molecule. Given the significant change in the aggregation of the triphenoxymethane platforms when changing solvents, it must be taken into account that changes in solvent will impact the size of the formed binding pockets.

Substitutions in the ortho position of the triphenoxymethane platform have an effect in control of binding pocket area. A linear increase in binding pocket area is observed as steric bulk is increased in the ortho position (Table 4-3). The affect of the ortho position is significant as evidenced by the large difference in binding pocket observed in compounds 4-16 and 4-17 (Figure 4-16) which were previously reported by Dinger et al.[51] Substitution of a t-butyl group for a methyl group in the ortho position

affected an increase in binding pocket area of 1.55 $Å^2$. Current studies are into synthesis and characterization of cycloalkane containing derivatives of the triphenoxymethane platform.

Triphenoxymethane-based Ligand Systems for Use in Selective Metal Sequestration

As world-wide demand for energy increases, an ever increasing percentage of energy is being provided with nuclear power.[84] The dominant issue with nuclear waste is the storage and handling of the generated waste. The ultimate goal of nuclear waste remediation would be the selective separation of actinides (Ac) from lanthanides (Ln) followed by transmutation of the actinides to reduce their half-life.[84] While this goal may seem relatively simple, there are a number of obstacles which must be overcome to achieve selective separation of Ln and Ac. First, with some exceptions, the preferred oxidation state for both groups of metals is +3. This limits selectivity derived from charge balance principles. Second, both groups share similar preference for coordination sphere, with tricapped trigonal prismative being the most common geometry. Finally, the ionic radii for the metal ions show limited changes in size across the periodic table due to lanthanide contraction. While both sets of metal ions are classified as hard acids,[5] actinides display more covalent bonding than lanthanides due to increased interactions with their radially extended f-orbitals, especially for U, Np, and Pu.[91] To exploit this electronic difference, binding pockets containing softer donors are used to increase selectivity for actinides over the more oxophillic lanthanides. Further enhancement of separation factor is obtained through preorganization of binding arms into a single ligand system.[84] Our research focused on synthesis and characterization of terdentate and nonadenate hetero-cyclic donors containing nitrogens. Single crystal X-ray

diffraction was used to examine structural properties of the ligands in an effort to better understand the functionality of the overall system.

Terdentate Ligand Systems

To examine structural affects imparted by tethering of binding pockets to a ligand platform, a series of terdentate ligand were crystallized as analogues of nonadentate systems discussed in subsequent sections. Two symmetric bis-1,2,4-triazine pyridine (BTP) based ligands and one picolinamide-triazine ligand were synthesized by current Scott group member Gary Guillet (Figure 4-6). Bond distances, intramolecular torsion angles, and twist angles were examined in an effort to correlate terdenate and nonadentate ligands systems bearing this class of binding arms. As mentioned previously, the most common geometry for lanthanides and actinides is tricapped trigonal prismatic, possessing D_{3H} symmetry (Figure 4-5). In an ideal coordination environment, the six molecules that comprise the prism are eclipsed. It is postulated that deviation from this eclipsed conformation causes a less desirable coordination, which would correlate to less favorable binding and subsequently poorer separation.

The two BTP-based compounds, 4-18 and 4-19, differ only by substitution in the ancillary position of the triazine rings. Compound 4-18 contains a single phenyl ring, while 4-19 contains one phenyl ring in each position. Structurally these phenyl rings provide three main functions. First, they offer extended pi systems which have been shown to absorb and diffuse ambient gamma radiation which is present in the waste stream.[92] Second, BTP based ligands with alpha hydrogens have been shown to degrade under the caustic conditions present in the unrefined waste. Substitution with phenyl rings replaces these alpha positions providing addition stability.[92] Lastly, the

phenyl rings provide the additional benefit of allowing for electronic tuning of the ligand systems via substitutions on the phenyl ring.

The counter ion for each compound was varied to probe if any counter ion affects would be observed within the solid-state structures. There is limited literature evidence indicating that subtle changes in counter ion would have an effect of bond distances.[85] Compound 4-18 contains nitrate counter ions while 4-19 contains triflates. In the case of compounds 4-18 and 4-19, however, there is no observed change in structure which can be attributed to a change in counter ion. Compound 4-18 crystallized in a trigonal space group, with one third of the molecule contained in the asymmetric unit. As such, all relevant bond distances are symmetric within the unit. Compound 4-19 crystallized in a triclinic space group, and the reported bond distances are given as the average for each position (Table 4-4). The N1—Yb bond distance for 4-18 and 4-19 are 2.465(3) Å and 2.483(2) Å respectively. Two things may cause the subtle change in bond distance. First, there is the possibility that the electron withdrawing properties of the additional phenyl created a “softer” triazine donor, increasing the bond length. Another possibility is that addition the additional phenyl ring caused inter or intra molecular steric hinderance causing a less favorable orientation of the rings, decreasing orbital overlap. This theory is evidenced by the large disparity in torsion angles observed in 4-19. The average torsion angle for 4-19 is 5.312˚ while compound 4-18 has a torsion angle of 4.300˚; however, the average torsion angle of 4-19 is deceptive, as the range of observed angle varies significantly.

Two examples of an un-metallated BTP complex exists in the literature (Figure 4-7);[92] however, the torsion angle derived from compound BTP1[93] does not give useful

comparisons for our structures. Compound BTP1 has an observed ring flip, with the four position oriented to form the internal binding pocket. BTP1 exhibits torsion angles of 27.22˚ and 28.77˚, likely due to the sterically demanding tetramethyl cyclohexyl group bound in the 5,6 positions. Compound BTP2[94] exhibits the proper ring orientation, but N1 from each of the triazine rings is seen hydrogen bonding to a water molecule. The average torsion angle for BTP2 is 16.57˚.

Several other examples of metallated BTP ligands have been synthesized and analyzed by crystallography. Compounds BTP3 and BTP4 were selected as comparisons to 4-18 and 4-19. BTP3 contains a lanthanum metal, providing an example of an early f-block element as a comparison. BTP4 is a ytterbium containing complex bearing n-propyl groups in the 5,6 positions. The average N1—Yb bond distance in BTP3 and BTP4 is 2.631(7) Å and 2.466(9) Å respectively. Bond distances observed in 4-18 and 4-19 correlate well with BTP4, showing an average bond distance difference of only 0.01 Å and 0.011 Å respectively. Compound 4-19 displays the largest average torsion angle of all the compounds, lending further evidence to steric effects imposed by the two phenyl rings.

Compound 4-20 was synthesized as a comparison for the similarly substituted nonadenate complexes discussed in subsequent sections. As of writing, 4-20 is the only reported complex of a picolinamide-triazine complex observed in the crystallographic database. The average N1 and N_{py} to metal bond distances are 2.474(2) Å and 2.471(2) Å respectively. The average metal-oxygen bond distance is significantly shorter at 2.271(2) Å, as expected by the more oxophillic lanthanide ions (Table 4-5). Compounds 4-18, 4-19, and 4-20 display twist angles of 10.756˚, 10.475˚, and 9.942˚

respectively. The twist angles in the BTP based ligands show a linear increase potentially associated with the increase in sterics, while the picolinamide ligand shows a decreased twist angle potentially arising from more flexible ligand system or increased bonding interactions.

Compounds 4-18, 4-19, and 4-20 provide a useful point of comparison for tethered nonadentate ligand systems. The symmetric BTP based ligands 4-18 and 4-19 provided useful comparisons arising from changes in steric bulk in the 5,6 positions of the triazine rings. Several structural changes seem to be sterically induced, such as the observed increase in torsion angle. As expected, these BTP ligands show longer bond distances when compared to oxygen containing ligands such as 4-20. Further studies involving modulation of electronics via substitution of the ancillary phenyl rings is currently underway.

Preorganized Nonadenate Ligand Systems

Preorganization of binding pockets has been shown to improve selectivity towards certain lanthanides.[84] Using the triphenoxymethane ligand platform, three terdenate binding pockets were tethered together to form a nonadenate ligand. Gary Guillet and Dempsey Hyatt of the Scott group synthesized the compounds presented herein. A total of nine novel nonadentate ligands were synthesized and characterized by single crystal X-ray diffraction. Systematic changes in the ligands were chosen to examine structural changes in the overall system. Steric affects of alkyl substitutions in the ortho position, flexibility of the linker, and changes in the tethering mode were all examined in our efforts to improve selectivity for metal ions (Figure 4-8). Relevant data for the subsequent chapters is summarized in Table 4-6.

Ortho alkyl effects

Three nonadenate ligands (4-21, 4-22, 4-23) bearing the same triazine-picolinamide binding pocket were synthesized, varying the alkyl chain in the ortho position of the ligand platform. Compound 4-21 bears a t-pentyl chain, 4-22 a t-butyl, and 4-23 a methyl group. Alkyl substituents in the ortho positions of the platform have shown interactions with the linker chain, as evidenced by numerous NMR spectroscopy studies preformed in the Scott group. Significant broadening of the methylene hydrogens has been observed with more sterically demanding groups present in the ortho position. Furthermore, CHECKcif, part of the PLATON crystallographic software suite, often indicates unexpectedly short interactions between carbons in the ortho position and those in the linker chain observed in the solid-state. Compounds 4-21, 4-22, and 4-23 were synthesized to examine the structural affects these ortho alkyl substituents have on the overall system.

As expected, all three compounds show a strong correlation in average bond distances (Table 4-6). A slightly shorter O—Yb bond of 2.279(1) Å is observed in 4-22, which is 0.03 Å shorter than 4-21 and 4-23.This is attributed to crystallization affects though, as 4-22 crystallizes in a cubic lattice while both 4-21 and 4-23 are triclinic. There is an observed linear decrease in the twist angle of the compounds as steric strain in the ortho position is mitigated. As the alkyl substituent is changed from a t-pentyl group in 4-21 to a methyl group in 4-23, a change of nearly 11%, or 1.39˚, is observed. Given the observed broadening of the methylene hydrogens and noted CHECKcif errors, it is probable that the alkyl ortho groups are interacting with the linker carbons affecting the twist angle of the overall structure. An exact measurement of the

distance between the ortho position and the linker chain is difficult, as these groups are often disordered in the solid-state.

Twist angle correlation

The twist angle of the nonadentate ligands is thought to relate proportionally to extraction efficiency. Using the nonadentate triazine-picolinamide ligand, three complexes were crystallized with lanthanum, erbium, and ytterbium to examine structural effects. All three compounds have similar average bond distances (Table 4-6), indicating that the observed extraction trends arise from structural rather than thermodynamic effects. Compound 4-24, containing lanthanum, displays the highest average torsion angle of 22.07˚. Of particular note is that 4-24 contains a methyl group in the ortho position which has been shown to produce lower twist angles, as discussed previously. Compound 4-25, containing erbium, and 4-22, containing ytterbium, display twist angles of 12.81˚ and 12.48˚ respectively indicating minimal difference in extraction efficiency.

Triazine Linked Nonadenate Ligands

Two novel nonadentate ligands bearing triazole moieties as linkers were synthesized by Gary Guillet and Dempsey Hyatt. Compounds 4-26 and 4-27 were synthesized in an effort to incorporate softer nitrogen donors into the binding pockets of the ligand systems. Depictions of the structures and relevant data for all compounds are shown in Figure 4-9 and Table 4-7. The twist angles for 4-26 and 4-27 are 10.65˚ and 8.90˚ respectively. The twist angle of 4-27 is the lowest observed twist angle of the triazine bearing ligand sets indicating that the incorporation of the softer triazole nitrogens should lead to better extraction efficiency.

To gain a better understanding of the benzimidazole series of ligands, Dempsey Hyatt synthesized compound 4-28 bearing an amide as the tethering bond. Compound 4-28 has an average twist angle of 9.079˚ showing a negligible increase in twist angle when compared to the all nitrogen based donor set of 4-27; however, it is probable that the twist angle of 4-28 is affected by the longer tethering chain used for this complex. Both compounds 4-26 and 4-27 display longer $N_{triazole}$—Yb bond distances than the O—Yb distances as is observed in similar complexes.

Conclusions

Novel nonadenate ligands for use in selective actinide partitioning have been synthesized and characterized by single crystal X-ray diffraction. The large volume of data gathered from these studies allows insight into development of more selective ligand systems as well as correlations to extraction efficiency. Future work is focused on incorporation of additional softer nitrogen based donor moieties as well as anionic ligand sets.

Experimental

X-Ray intensity data was collected at 100 K on either a Bruker DUO or Bruker SMART diffractometer using MoKα radiation (λ = 0.71073 Å) or CuKα (λ = 1.54178 Å) and an APEXII CCD area detector. Raw data frames were read by program SAINT and integrated using 3D profiling algorithms. The resulting data was reduced to produce hkl reflections, intensities, and estimated standard deviations. Structures were solved and refined in SHELXTL6.1, using full-matrix least-squares refinement. Where necessary, the program SQUEEZE, a part of the PLATON[93] package of crystallographic software, was used to calculate the solvent disorder area and remove its contribution to the overall intensity data.

Table 4-1. Relevant distances and binding areas for nitrated triphenoxymethanes.

Compounds	N1—N2 (Å)	N1—N3 (Å)	N2—N3 (Å)	Binding Pocket Area (Å^2)
4-4	6.109	7.166	6.869	19.28
4-5 (1)	6.802	6.373	6.719	19.00
4-5 (2)	6.571	6.805	6.753	19.48
4-6	6.048	6.491	6.449	17.30
4-7	6.700	7.603	7.069	21.79
4-8	6.572	7.085	6.708	19.79
4-9	6.761	7.082	6.894	20.67
4-10	6.637	7.567	6.680	20.73

Table 4-2. Relevant distances and angles for triphenoxymethane-aldehydes.

	4-11	4-12
O1—O2 (Å)	4.195	4.456
O1—O3 (Å)	4.117	4.419
O2—O3 (Å)	4.336	4.544
Torsion Angle 1 (˚)	38.3	46.9
Torsion Angle 2 (˚)	36.4	48.7
Torsion Angle 3 (˚)	33.0	48.9
Methine Angle (˚)	105.9	106.0
Binding Pocket Area (Å^2)	7.686	8.776

Table 4-3. Relevant distances and angles for tris-phenol triphenoxymethanes.

	4-13 (1)	4-13 (2)	4-2	4-14 (1)	4-14 (2)	4-3
O1—O2 (Å)	3.781	3.771	4.069	4.337	4.401	4.408
O1—O3 (Å)	4.262	4.239	4.801	4.369	4.384	4.408
O2—O3 (Å)	4.434	4.435	3.809	4.577	4.626	4.408
Torsion Angle 1 (˚)	37.3	33.4	30.6	44.5	45.0	42.7
Torsion Angle 2 (˚)	34.9	37.9	24.6	48.3	52.8	42.7
Torsion Angle 3 (˚)	24.7	23.5	61.7	46.1	45.5	42.7
Methine Angle 1 (˚)	106.59	108.39	107.31	103.82	105.68	107.00
Methine Angle 2 (˚)	107.87	105.85	107.49	105.90	106.02	107.00
Methine Angle 3 (˚)	106.92	106.88	107.46	107.33	104.87	107.00
Binding Pocket Area (Å^2)	7.395	7.354	7.486	8.470	8.637	8.414

Table 4-4. Relevant distances and angles for compounds for terdentate BTP ligands.

	4-18	4-19	BTP2	BTP4
$N1_a$—M (Å)	2.465 (3)	2.449 (2)	2.655 (7)	2.493 (10)
$N1_b$—M (Å)	2.465 (3)	2.518 (2)	2.616 (6)	2.458 (8)
$N1_c$—M (Å)	2.465 (3)	2.490 (2)	2.628 (6)	2.483 (9)
$N2_a$—M (Å)	2.465 (3)	2.459 (2)	2.651 (8)	2.479 (9)
$N2_b$—M (Å)	2.465 (3)	2.489 (2)	2.609 (7)	2.472 (10)
$N2_c$—M (Å)	2.465 (3)	2.488 (2)	2.624 (6)	2.469 (9)
N_{py1}—M (Å)	2.446 (19)	2.457 (2)	2.686 (6)	2.481 (10)
N_{py2}—M (Å)	2.446 (19)	2.472 (2)	2.675 (7)	2.474 (8)
N_{py3}—M (Å)	2.446 (19)	2.452 (2)	2.646 (7)	2.462 (9)
Avg. N1—M (Å)	2.465 (3)	2.483 (2)	2.631 (7)	2.466 (9)
Average Torsion(˚)	4.3	5.3	4.4	3.0
Twist Angle (˚)	10.76 (5)	10.48 (6)	-	-

Table 4-5. Relevant distances and angles for compound 4-20.

	4-20
$N1_a$—M (Å)	2.467 (2)
$N1_b$—M (Å)	2.469 (2)
$N1_c$—M (Å)	2.487 (2)
N_{py1}—M (Å)	2.462 (2)
N_{py2}—M (Å)	2.459 (2)
N_{py3}—M (Å)	2.490 (2)
Avg. N1—M (Å)	2.474 (2)
O1—M (Å)	2.238 (2)
O2—M (Å)	2.293 (2)
O3—M (Å)	2.281 (2)
Avg. O—M (Å)	2.271 (2)
Avg. Torsion (˚)	16.10
Twist Angle (˚)	9.942 (1)

Table 4-6. Relevant data for compounds nonadentate compounds. *Compound 4-25 contains two molecules in the asymmetric unit. The average of both molecules is used for simplicity.

	4-21	4-22	4-23	4-24	4-25 (a)	4-25 (b)
$N1_a$—M (Å)	2.503 (3)	2.512 (1)	2.517 (1)	2.686 (1)	2.519 (5)	2.521 (5)
$N1_b$—M (Å)	2.543 (2)	2.512 (1)	2.535 (2)	2.693 (1)	2.530 (5)	2.539 (5)
$N1_c$—M (Å)	2.548 (3)	2.512 (1)	2.516 (1)	2.727 (1)	2.530 (5)	2.541 (5)
N_{py1}—M (Å)	2.472 (3)	2.472 (1)	2.478 (2)	2.692 (1)	2.489 (5)	2.510 (5)
N_{py2}—M (Å)	2.495 (3)	2.472 (1)	2.459 (2)	2.686 (1)	2.478 (5)	2.464 (5)
N_{py3}—M (Å)	2.460 (3)	2.472 (1)	2.477 (2)	2.696 (1)	2.502 (5)	2.498 (5)
Avg. N1—M (Å)	2.531 (3)	2.512 (1)	2.471 (2)	2.702 (1)	2.530 (5)*	2.530 (5)*
O1—M (Å)	2.296 (2)	2.301 (1)	2.318 (1)	2.495 (1)	2.311 (4)	2.327 (4)
O2—M (Å)	2.303 (2)	2.301 (1)	2.292 (1)	2.446 (1)	2.311 (4)	2.341 (4)
O3—M (Å)	2.303 (2)	2.301 (1)	2.289 (1)	2.420 (1)	2.334 (4)	2.335 (4)
Twist Angle (˚)	12.97	12.48	11.58	22.07	12.81*	12.81*

Table 4-7. Relevant data for compound 4-26, 4-27 and 4-28. * 4-28 contains one and a third molecules in the asymmetric unit.

	4-26	4-28 (a)	4-28 (b)*	4-27
$N1_a$—M (Å)	2.446 (3)	2.528 (9)	2.507 (9)	2.485 (7)
$N1_b$—M (Å)	2.487 (2)	2.523 (8)	2.507 (9)	2.473 (6)
$N1_c$—M (Å)	2.463 (3)	2.586 (9)	2.507 (9)	2.472 (6)
N_{py1}—M (Å)	2.498 (2)	2.474 (8)	2.508 (8)	2.498 (6)
N_{py2}—M (Å)	2.481 (3)	2.501 (10)	2.508 (8)	2.499 (7)
N_{py3}—M (Å)	2.494 (2)	2.488 (9)	2.508 (8)	2.532 (6)
N_{tri1}—M (Å)	2.428 (2)	2.328 (7)	2.300 (7)	2.445 (6)
N_{tri2}—M (Å)	2.436 (2)	2.317 (7)	2.300 (7)	2.488 (7)
N_{tri3}—M (Å)	2.398 (2)	2.275 (7)	2.300 (7)	2.458 (7)
Avg. N1—M (Å)	2.465 (3)	2.526 (9)	2.526 (9)	2.477 (6)
Avg. N_{py}—M (Å)	2.491 (2)	2.498 (8)	2.498 (8)	2.510 (6)
Avg. N_{tri}—M (Å)	2.421 (2)	2.303 (7)	2.303 (7)	2.451 (7)
Twist Angle ˚	10.65	9.079	9.079	8.895

Table 4-8. Crystallographic data for compound 4-18, 4-19, 4-20.

	4-18(NO_3)	4-19$(CF_3SO_3)_3 \cdot (CH_3OH)_3\ H_2O$	4-20$(CF_3SO_3)_3$
Total Reflections	27563	66571	37661
Uniq. Reflections/ Reflections $I \geq 2\sigma(I)$	3307/2406	23419/20736	12824/12386
Collection Range (°)	$1.63 < \theta < 27.50$	$1.50 < \theta < 27.50$	$3.17 < \theta < 66.50$
Formula	$C_{69}H_{45}N_{23}O_6Yb$	$C_{111}H_{81}F_9N_{21}O_{13}S_3Yb$	$C_{90}H_{93}F_9N_{15}O_{12}S_3Yb$
M_r	1465.32	2357.19	2017.01
Crystal System	Trigonal	Triclinic	Monoclinic
Space Group	$P\bar{3}1c$	$P\bar{1}$	Cc
a (Å)	14.4423(10)	13.6476(9)	24.8539(6)
b (Å)	-	16.3938(10)	13.9870(3)
c (Å)	23.723(2)	23.0054(14)	28.8206(6)
α (°)	-	88.036(1)	-
β (°)	-	89.204(1)	104.791(1)
γ (°)	-	82.558(1)	-
V_c (Å^3)	4285.2(6)	5100.5(6)	9687.0(4)
D_c (g cm^{-1})	1.136	1.071	1.383
Z	2	2	4
F(*000*)	1476	2394	4132
μ[Mo-Kα] (mm^{-1})	1.147	1.071	3.088
R_1[$I \geq 2\sigma(I)$data]	0.0273	0.0347	0.0284
wR_2[$I \geq 2\sigma(I)$data]	0.0731	0.0847	0.0679
GoF	1.050	1.022	1.055
Largest Peak, deepest trough (e Å^{-3})	+0.629, -0.496	+1.713, -1.219	+0.747, -0.695

Table 4-9. Crystallographic data for compound 4-21, 4-22, 4-23.

	4-21$(CF_3SO_3)_3$	4-22(NO_3)	4-23Yb$(NO_3)_5NO_3$
Total Reflections	125559	5536	18761
Uniq. Reflections/ Reflections $I \geq 2\sigma(I)$	31899/22963	5536/4482	9684/8278
Collection Range (°)	$1.52 < \theta < 27.50$	$1.48 < \theta < 27.50$	$1.01 < \theta < 18.76$
Formula	$C_{121}H_{127}F_9N_{15}O_{15}S_3Yb$	$C_{112}H_{112}N_{18}O_{15}Yb$	$C_{105}H_{103}N_{21}O_{26}Yb_2$
M_r	2471.60	2123.24	2421.16
Crystal System	Triclinic	Cubic	Triclinic
Space Group	P1	$P2_13$	$P\bar{1}$
a (Å)	14.8807(3)	23.7722(9)	17.6026(14)
b (Å)	20.2373(4)	-	17.8227(15)
c (Å)	24.8721(6)	-	20.5821(17) Å
α (°)	95.009(2)	-	81.5270(10)
β (°)	101.027(2)	-	81.6540(10)
γ (°)	107.138(1)	-	88.4920(10)
V_c (Å^3)	6942.5(3)	13434.1(9)	6318.9(9)
D_c (g cm^{-1})	1.182	1.050	1.273
Z	2	4	2
F(*000*)	2554	4400	2456
μ[Mo-Kα] (mm^{-1})	0.790	0.753	1.542
$R_1[I \geq 2\sigma(I)$data]	0.0469	0.0582	0.0557
$wR_2[I \geq 2\sigma(I)$data]	0.1025	0.1662	0.1583
GoF	0.914	1.079	1.095
Largest Peak, deepest trough (e Å^{-3})	+0.980, -1.133	+1.436, -0.632	+2.185, -1.223

Table 4-10. Crystallographic data for compound 4-24, 4-25, 4-26.

	4-24$La(NO_3)_6$	4-25$(NO_3)_3$	4-26$Yb(NO_3)_5NO_3$
Total Reflections	40185	54385	94402
Uniq. Reflections/ Reflections $I \geq 2\sigma(I)$	22967/20200	30261/22824	31754/24891
Collection Range (˚)	$1.12 < \theta < 25.00$	$0.79 < \theta < 22.50$	$1.66 < \theta < 27.50$
Formula	$C_{103}H_{97}La_2N_{21}O_{24}$	$C_{103}H_{97}ErN_{18}O_{15}$	$C_{121}H_{127}N_{27}O_{21}Yb_2$
M_r	2290.84	1994.25	2641.58
Crystal System	Triclinic	Triclinic	Triclinic
Space Group	$P\bar{1}$	$P\bar{1}$	$P\bar{1}$
a (Å)	18.2537(10)	21.310(2)	13.8162(15)
b (Å)	18.390(1)	21.575(2)	13.9131(16)
c (Å)	20.7899(12)	25.924(2)	40.956(5)
α (˚)	74.209(1)	82.036(2)	96.233(3)
β (˚)	89.492(1)	86.570(1)	91.615(3)
γ (˚)	87.577(1)	84.975(1)	117.197(2)
V_c (Å^3)	6709.5(6)	11744.8(19)	6933.9(14)
D_c (g cm^{-1})	1.134	1.128	1.265
Z	2	4	2
F(*000*)	2336	4116	2700
μ[Mo-Kα] (mm^{-1})	0.693	0.776	1.410
R_1[$I \geq 2\sigma(I)$data]	0.0395	0.0575	0.0576
wR_2[$I \geq 2\sigma(I)$data]	0.1082	0.1535	0.1174
GoF	1.101	1.089	1.096
Largest Peak, deepest trough (e Å^{-3})	+1.800, -1.233	+1.959, -1.351	+2.631, -6.333

Table 4-11. Crystallographic data for compounds 4-27, 4-28

	4-27$(CF_3SO_3)_3$	4-28$_{1.3}(CF_3SO_3)_4$
Total Reflections	50337	17922
Uniq. Reflections/ Reflections $I \geq 2\sigma(I)$	19530/15188	17922/12086
Collection Range (˚)	$1.49 < \theta < 25.00$	$1.54 < \theta < 27.50$
Formula	$C_{103}H_{118}F_9N_{18}O_{12}S_3Yb$	$C_{106}H_{130}F_9N_{12}O_{18}S_3Yb$
M_r	2240.37	2300.44
Crystal System	Triclinic	Rhombohedral
Space Group	$P\bar{1}$	R3c
a (Å)	13.9187(16)	42.262(3)
b (Å)	14.9433(18)	-
c (Å)	29.236(4)	45.351(3)
α (˚)	90.593(2)	-
β (˚)	91.506(2)	-
γ (˚)	114.085(2)	-
V_c (Å^3)	5548.0(11)	70148(8)
D_c (g cm^{-1})	1.341	1.307
Z	2	24
F(*000*)	2314	28632
μ[Mo-Kα] (mm^{-1})	0.979	0.933
R_1[$I \geq 2\sigma$(I)data]	0.0796	0.0577
wR_2[$I \geq 2\sigma$(I)data]	0.2013	0.1443
GoF	1.027	1.089
Largest Peak, deepest trough (e Å^{-3})	+4.588, -1.802	+1.081, -0.817

Table 4-12. Crystallographic data for compounds 4-11, 4-12

	4-11	4-12
Total Reflections	20026	25421
Uniq. Reflections/ Reflections $I \geq 2\sigma(I)$	7427/6334	8125/4188
Collection Range (˚)	$1.90 < \theta < 27.50$	$1.33 < \theta < 27.49$
Formula	$C_{69}H_{45}N_{23}O_6Yb$	$C_{38}H_{50}O_5$
M_r	505.59	586.78
Crystal System	Trigonal	Triclinic
Space Group	$P\bar{1}$	$P\bar{1}$
a (Å)	9.074(2)	10.6410(8)
b (Å)	11.381(3)	11.4721(9)
c (Å)	16.709(4)	16.1099(13)
α (˚)	103.646(13)	72.367(2)
β (˚)	95.729(14)	88.946(2)
γ (˚)	102.204(14)	71.739(2)
V_c (Å^3)	1618.4(7)	1773.5(2)
D_c (g cm^{-1})	1.037	1.099
Z	2	2
F(*000*)	540	636
μ[Mo-Kα] (mm^{-1})	0.072	0.071
R_1[$I \geq 2\sigma(I)$data]	0.0467	0.0531
wR_2[$I \geq 2\sigma(I)$data]	0.1319	0.1207
GoF	1.077	0.876
Largest Peak, deepest trough (e Å^{-3})	+0.375, -0.586	+0.425, -0.236

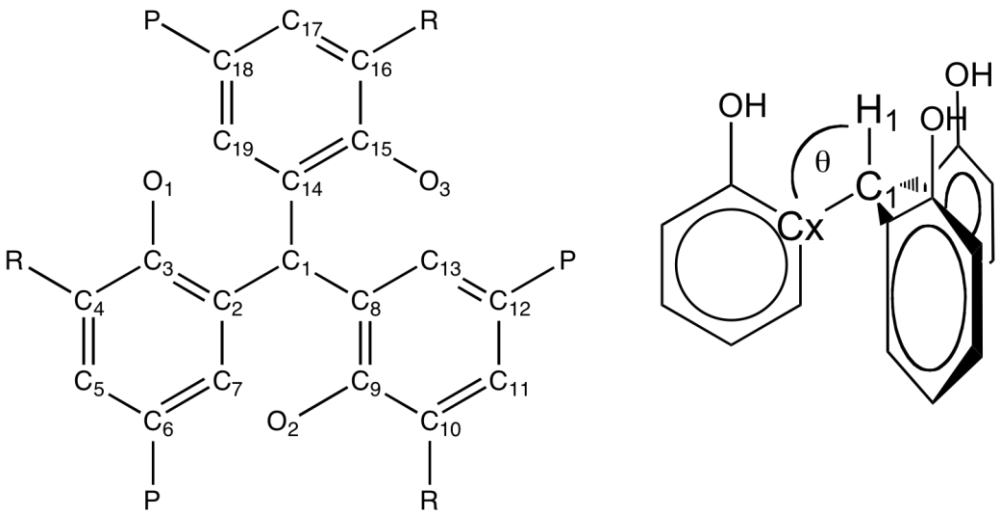

Figure 4-1. (left) Labeling scheme used for triphenoxymethane structures. R and P refer to ortho and para positions respectively. (right) Methine bond angle measured for structural comparison.

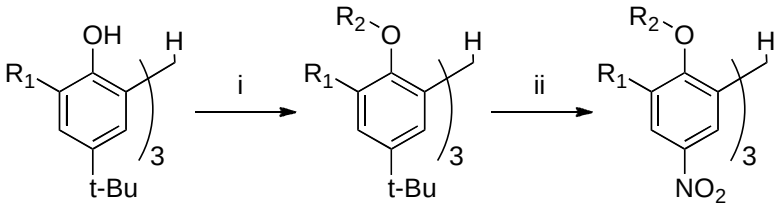

4-1 R_1 = Me
4-2 R_1 = i-Pr
4-3 R_1 = s-Bu

4-4 R_1 = Me, R_2 = Me
4-5 R_1 = Me, R_2 = Et
4-6 R_1 = Me, R_2 = i-Pr
4-7 R_1 = i-Pr, R_2 = Me
4-8 R_1 = i-Pr, R_2 = Et
4-9 R_1 = s-Bu, R_2 = Me
4-10 R_1 = s-Bu, R_2 = Et

Figure 4-2. Synthesis of nitrated derivatives of the triphenoxymethane platform. i) alkyl iodide, K_2CO_3 ii) TFA, HNO_3

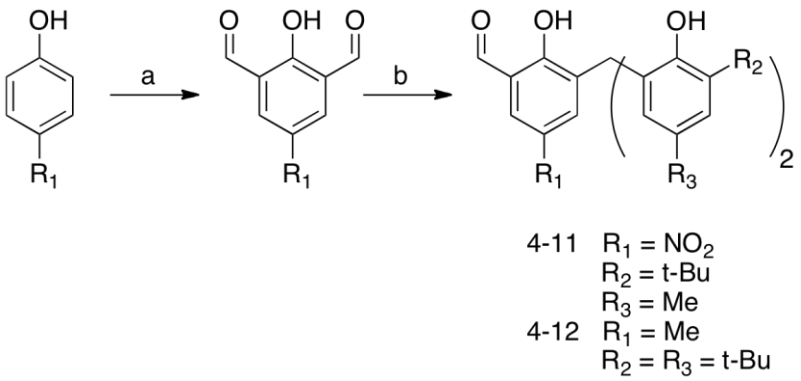

Figure 4-3. Synthetic scheme for carbonyl containing triphenoxymethanes.[88] a) TFA, HMTA b) 2,4-dialkylphenol, TFA

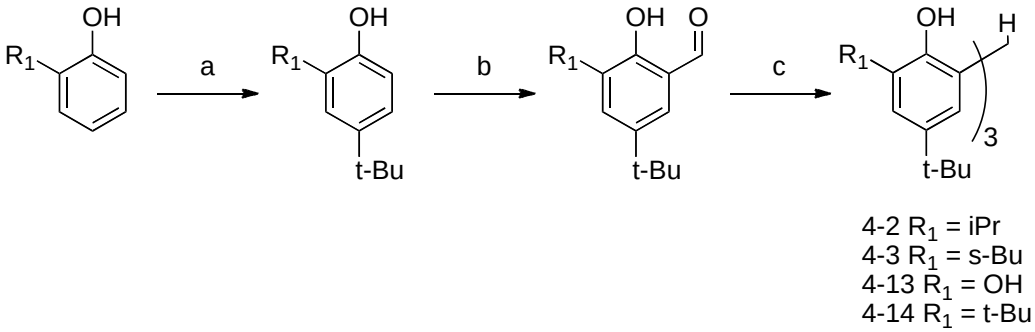

Figure 4-4. Synthesis of tris-phenolic triphenoxymethane ligands.
a) t-BuCl, $AlCl_3$ b) paraformaldehyde, NEt_3, $MgCl_2$ c) $SOCl_2$, 2,4-dialkylphenol

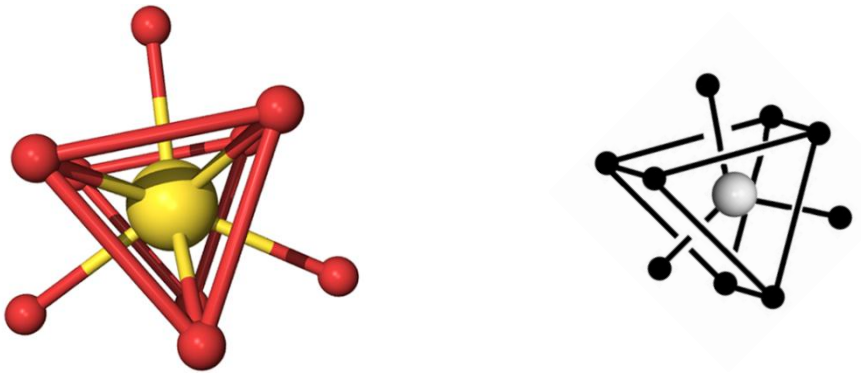

Figure 4-5. General depiction of a nona-aqua lanthanide complex (left) and the measured twist angle of the two triangular planes (right).

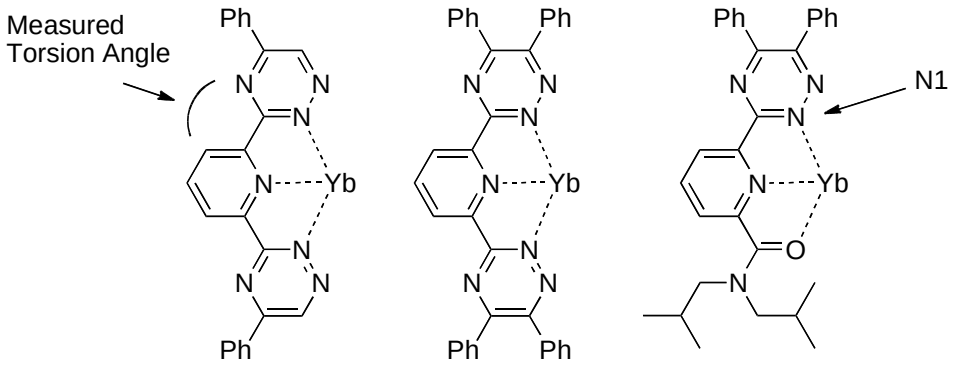

Figure 4-6. Representations of compounds 4-18, 4-19, and 4-20. Only one binding arm is shown for clarity. N1 refers to the nitrogen in the 1 position of the triazine, bound to the metal. N_{py} is the pyridine nitrogen.

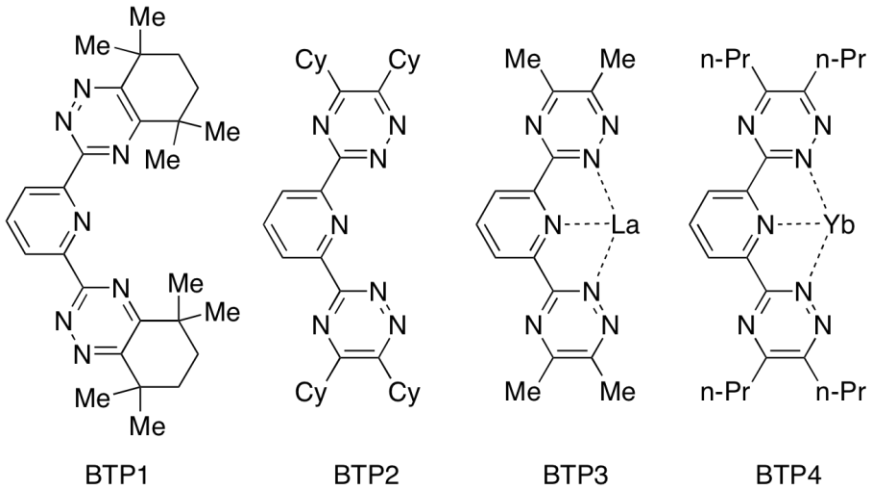

Figure 4-7. Representations of structures previously reported in the literature. For compounds BTP3[96] and BTP4[97], only one binding arm is shown for clarity.[93,95,96,97]

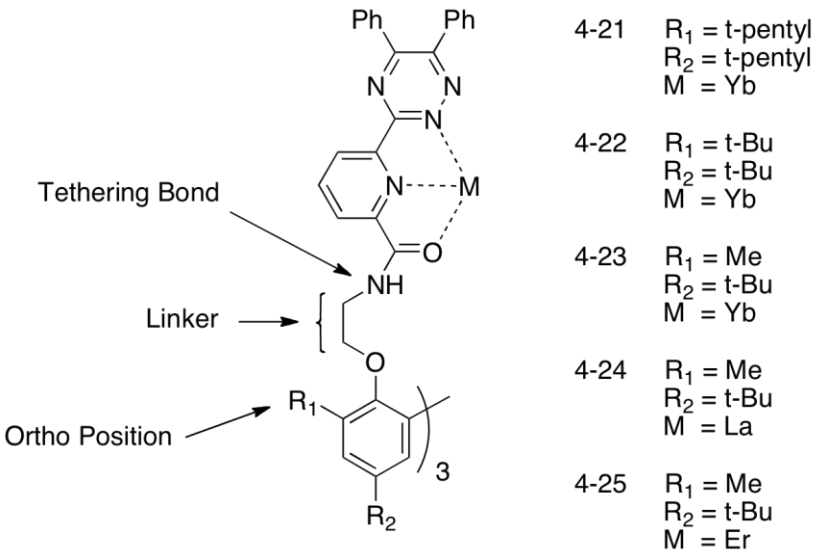

Figure 4-8. Representations of nonadentate picolinamide-triazine based ligand systems discussed.

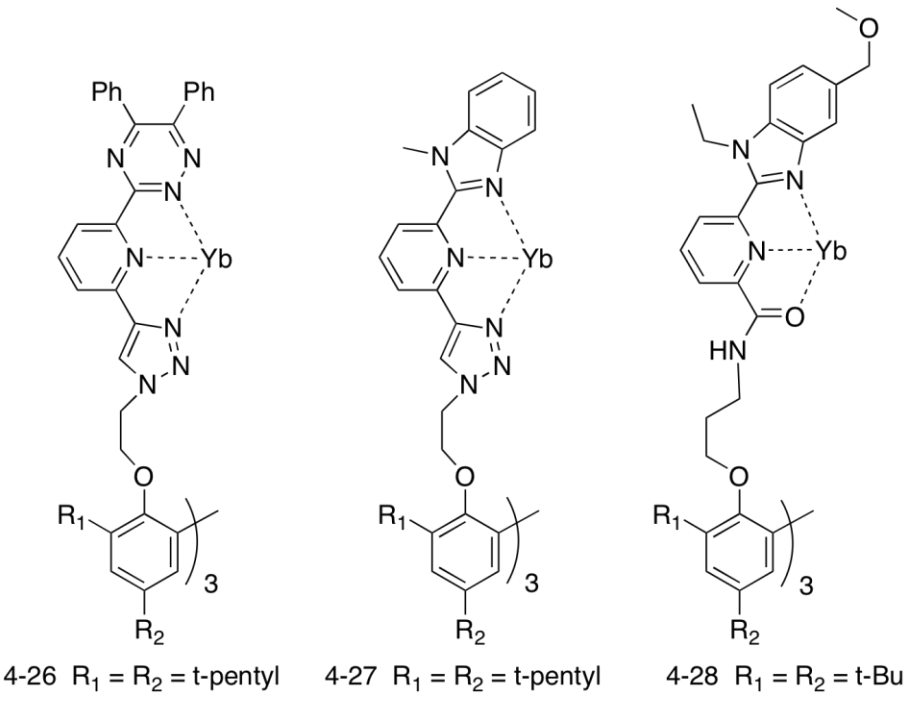

Figure 4-9. Representations of compounds 4-26, 4-27, and 4-28.

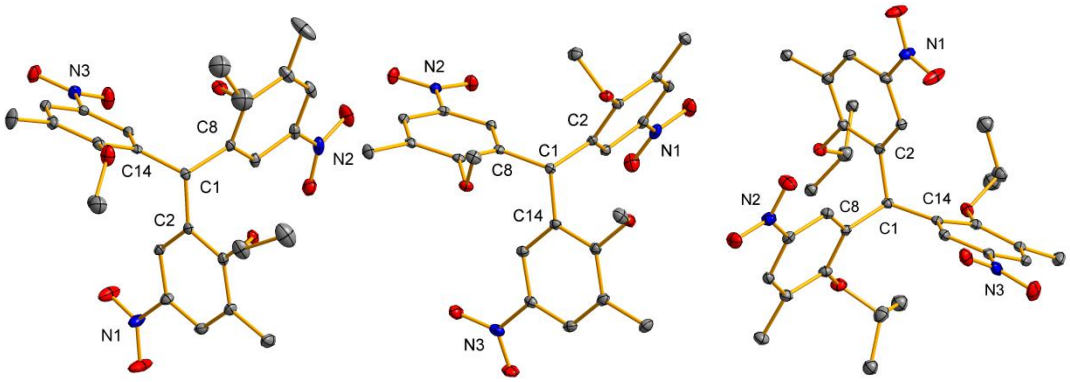

Figure 4-10. Solid-state structures of compounds 4-4 (left), 4-5 (middle), and 4-6 (right). 30% probability ellipsoids. Hydrogens omitted for clarity.

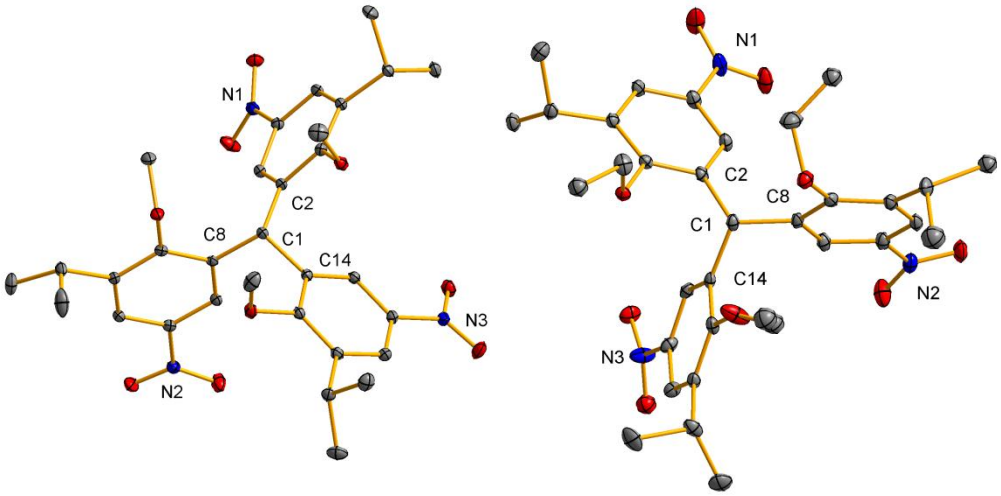

Figure 4-11. Solid-state structures of compounds 4-7 (left) and 4-8 (right). 30% probability ellipsoids. Hydrogens omitted for clarity.

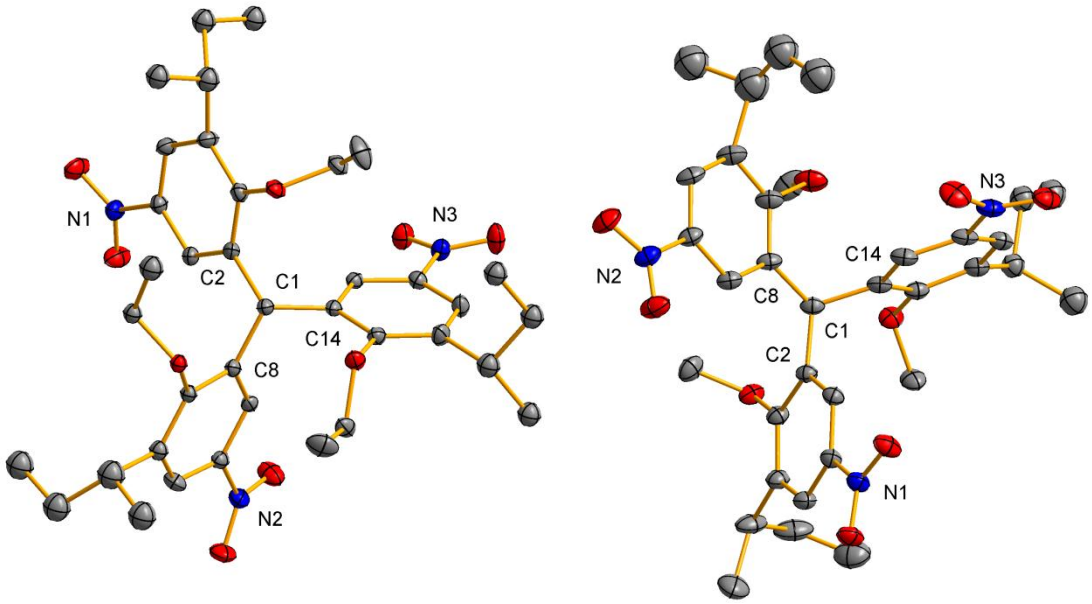

Figure 4-12. Solid-state structures of compounds 4-9 (left) and 4-10 (right). 30% probability ellipsoids. Hydrogens omitted for clarity.

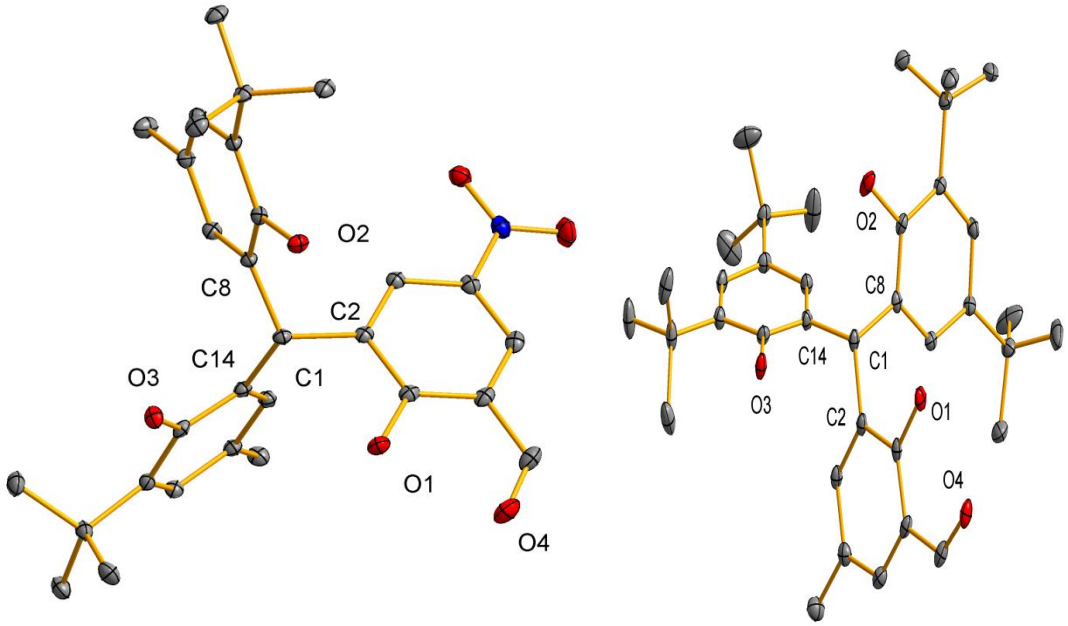

Figure 4-13. Solid-state structures of compounds 4-11 (left) and 4-12 (right). 30% probability ellipsoids. Hydrogens omitted for clarity.

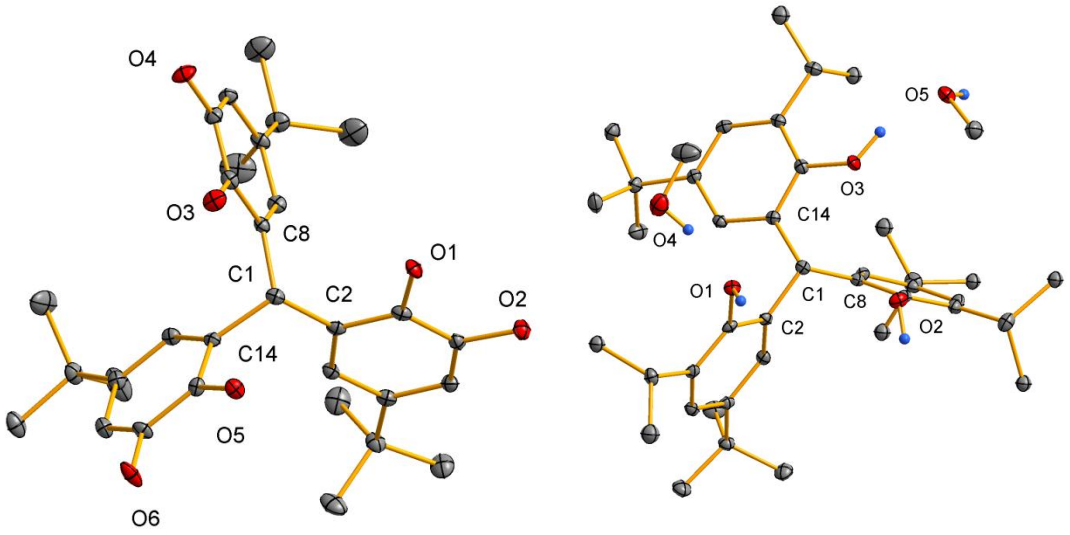

Figure 4-14. Solid-state structures of compounds 4-13 (left) and 4-2 (right). 30% probability ellipsoids. Hydrogens omitted for clarity.

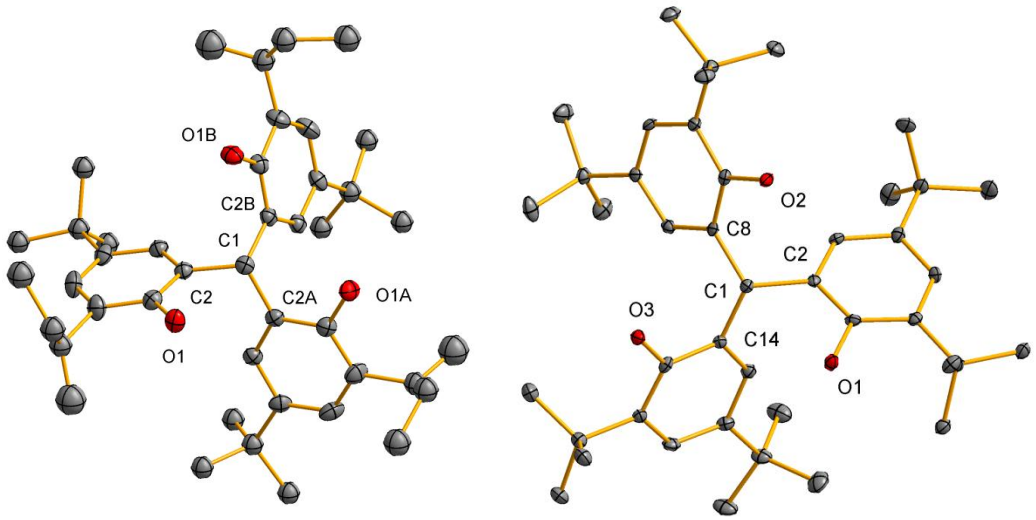

Figure 4-15. Solid-state structures of compounds 4-3 (left) and 4-14 (right). 30% probability ellipsoids. Hydrogens omitted for clarity.

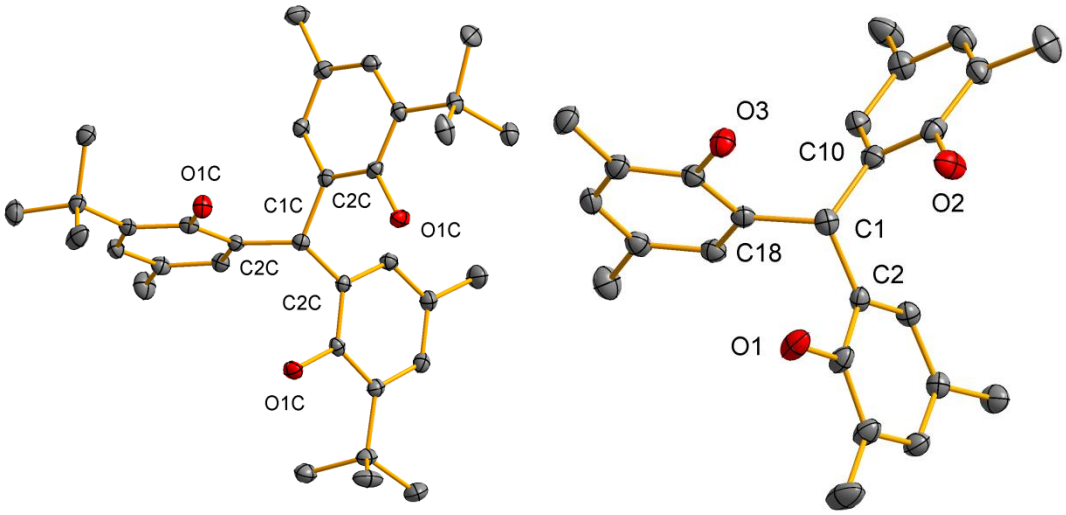

Figure 4-16. Solid-state structures of compounds 4-16 (left) and 4-17 (right). 30% probability ellipsoids. Hydrogens omitted for clarity.[51]

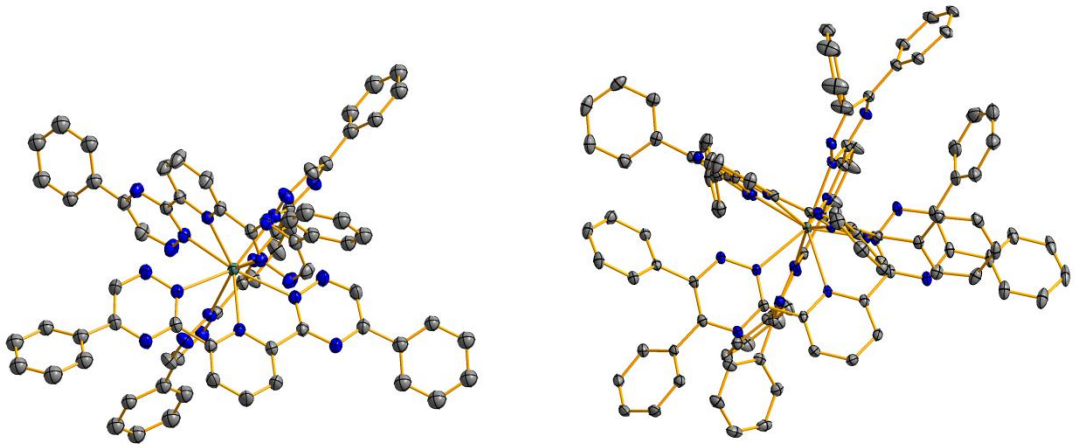

Figure 4-17. Solid-state structures of compounds 4-18 (left) and 4-19 (right). 50% probability ellipsoids, hydrogens and counter ions omitted for clarity.

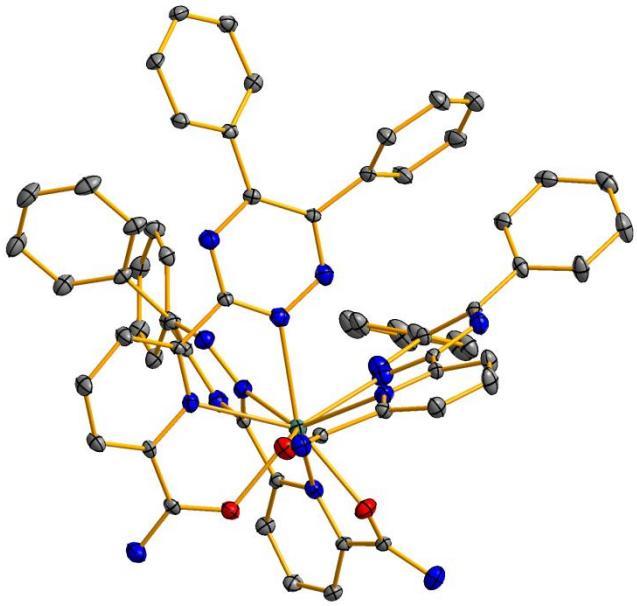

Figure 4-18. Solid-state structures of compound 4-20. Iso-butyl groups omitted for clarity. 50% probability ellipsoids, hydrogens and counter ions omitted for clarity.

APPENDIX

^{1}H-NMR SPECTRA OF COMPOUNDS

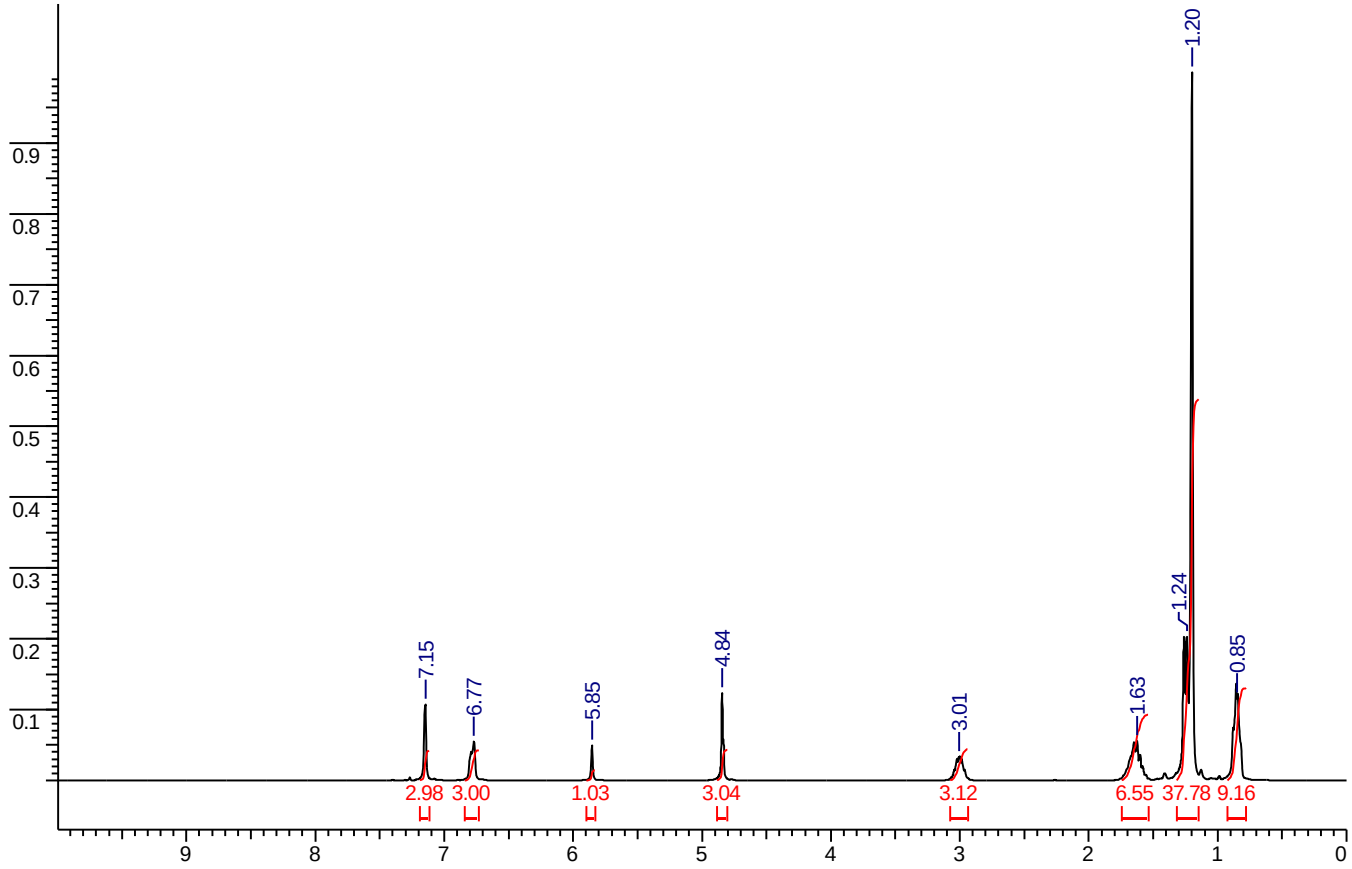

Figure A-1. ^{1}H-NMR Spectrum of compound 3-1

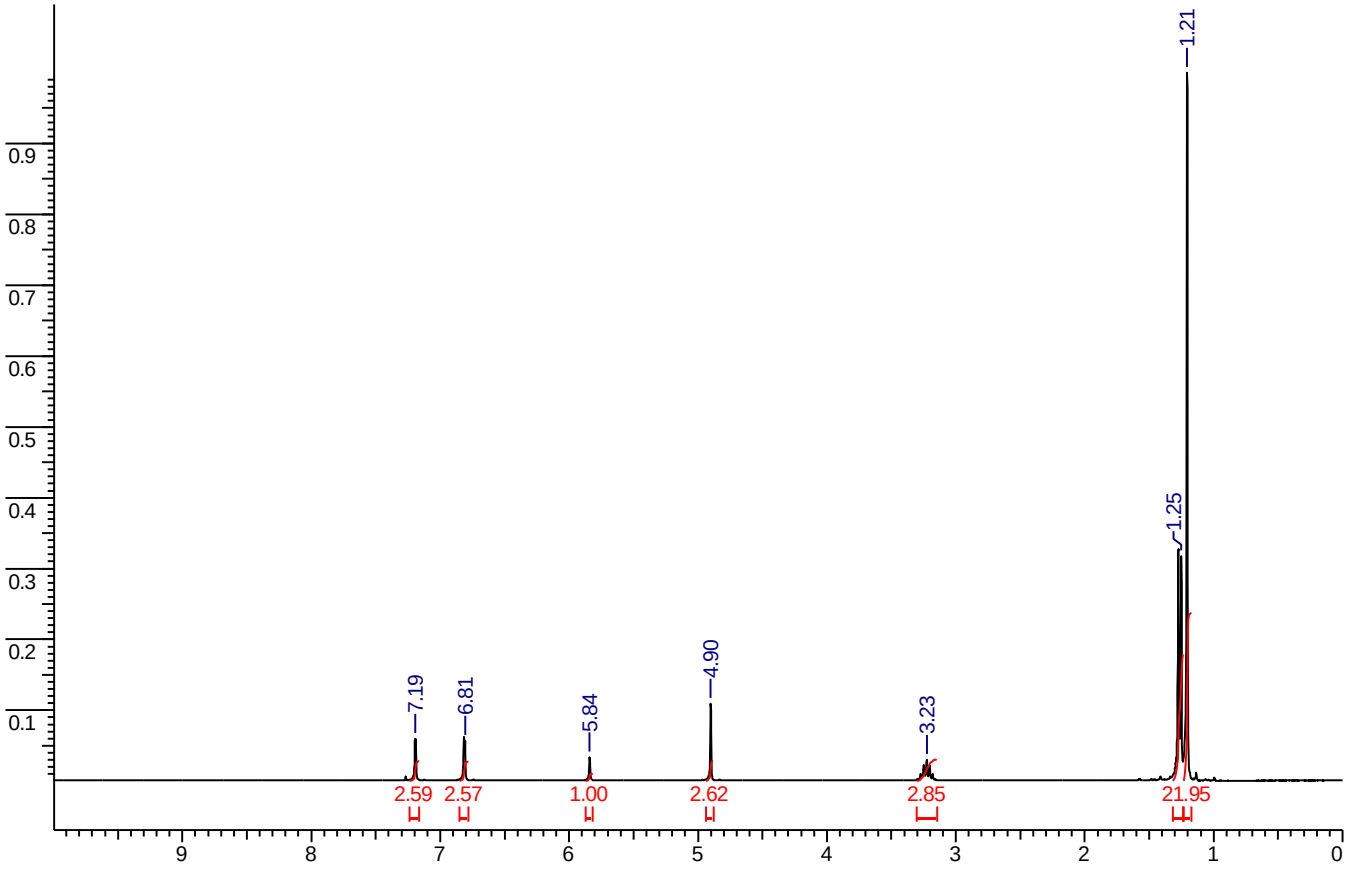

Figure A-2. ^{1}H-NMR Spectrum of compound 3-2

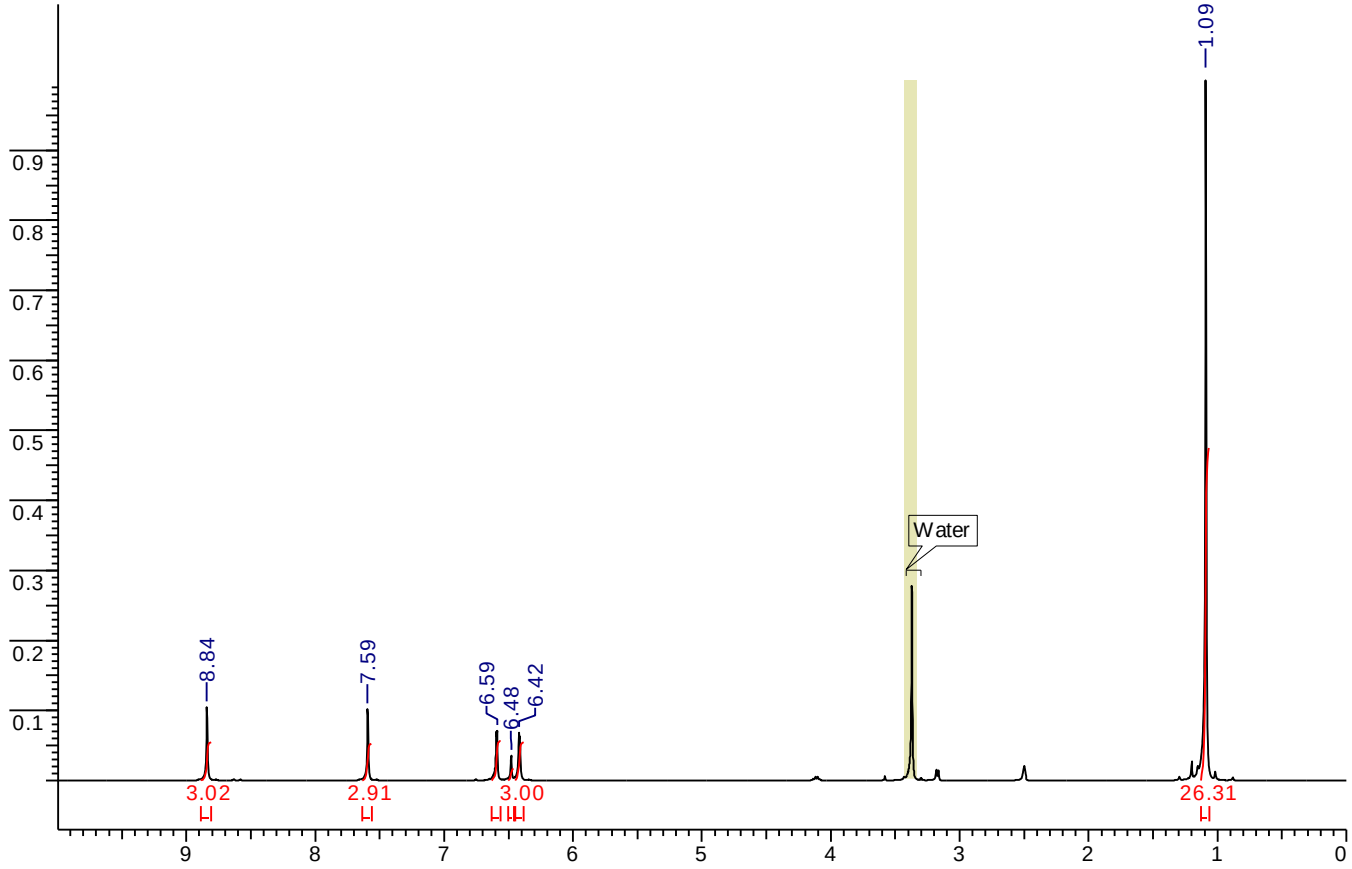

Figure A-3. ^{1}H-NMR Spectrum of compound 3-3

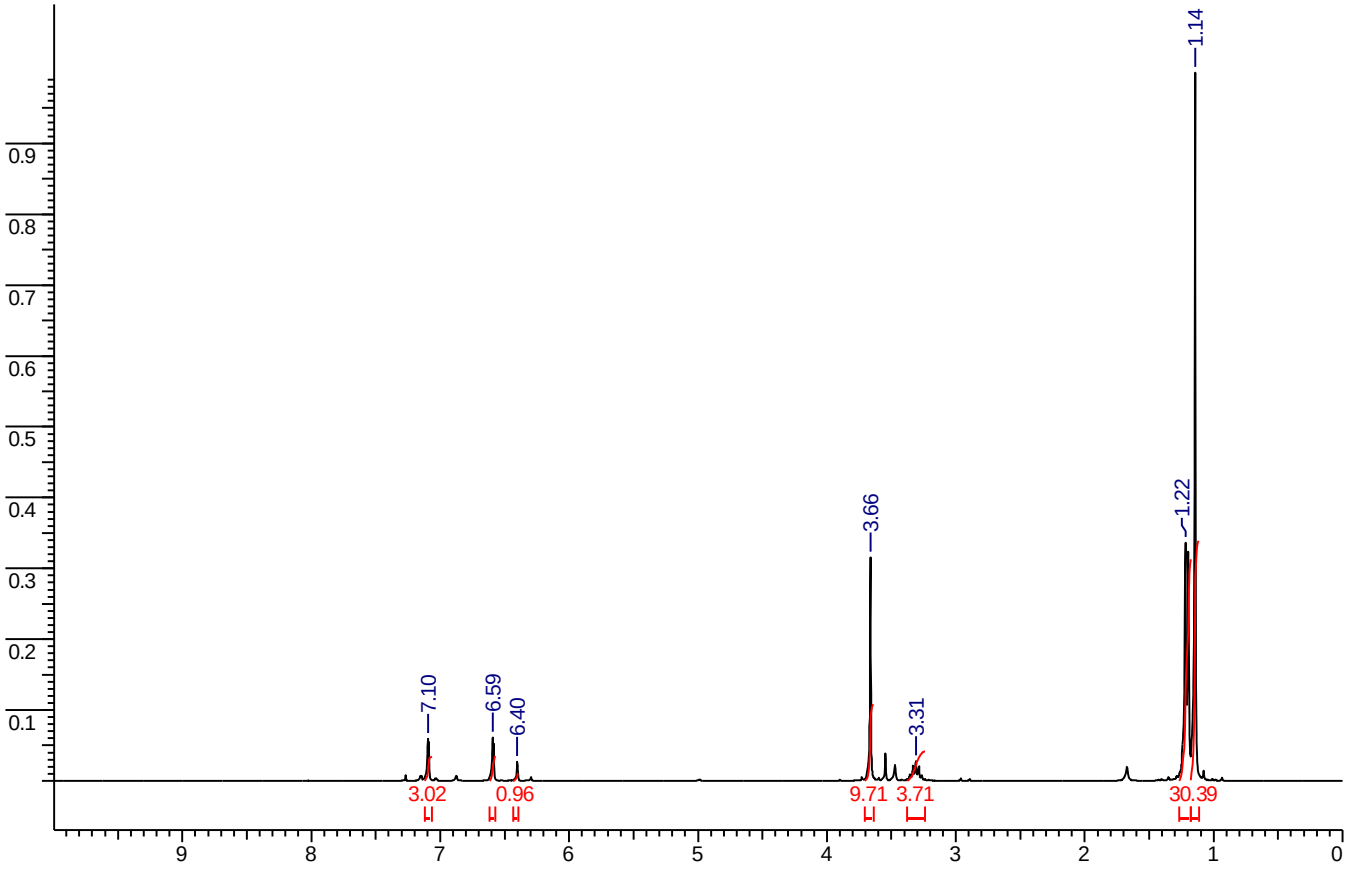

Figure A-4. ^{1}H-NMR Spectrum of compound 3-4

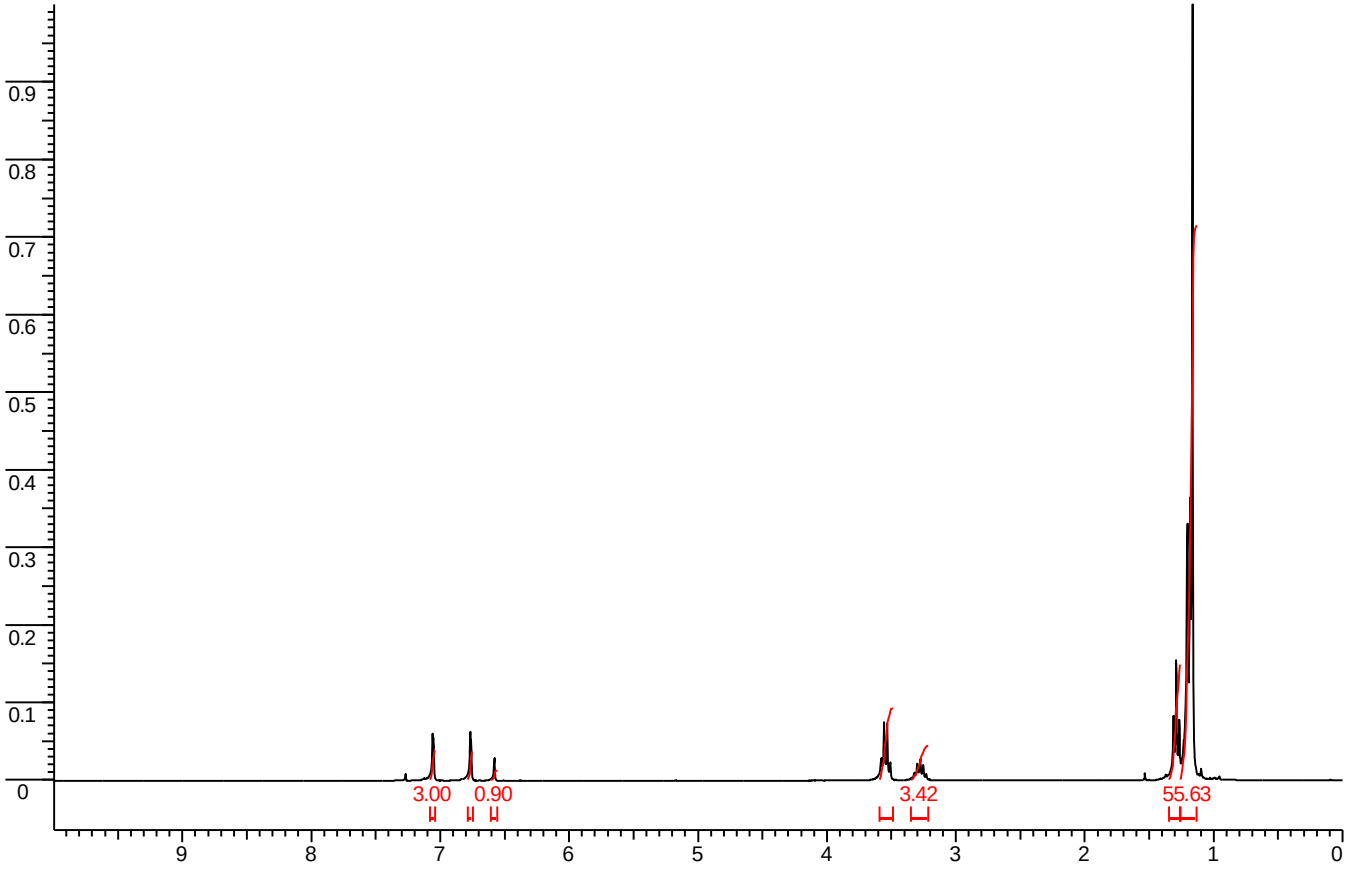

Figure A-5. ^{1}H-NMR Spectrum of compound 3-5

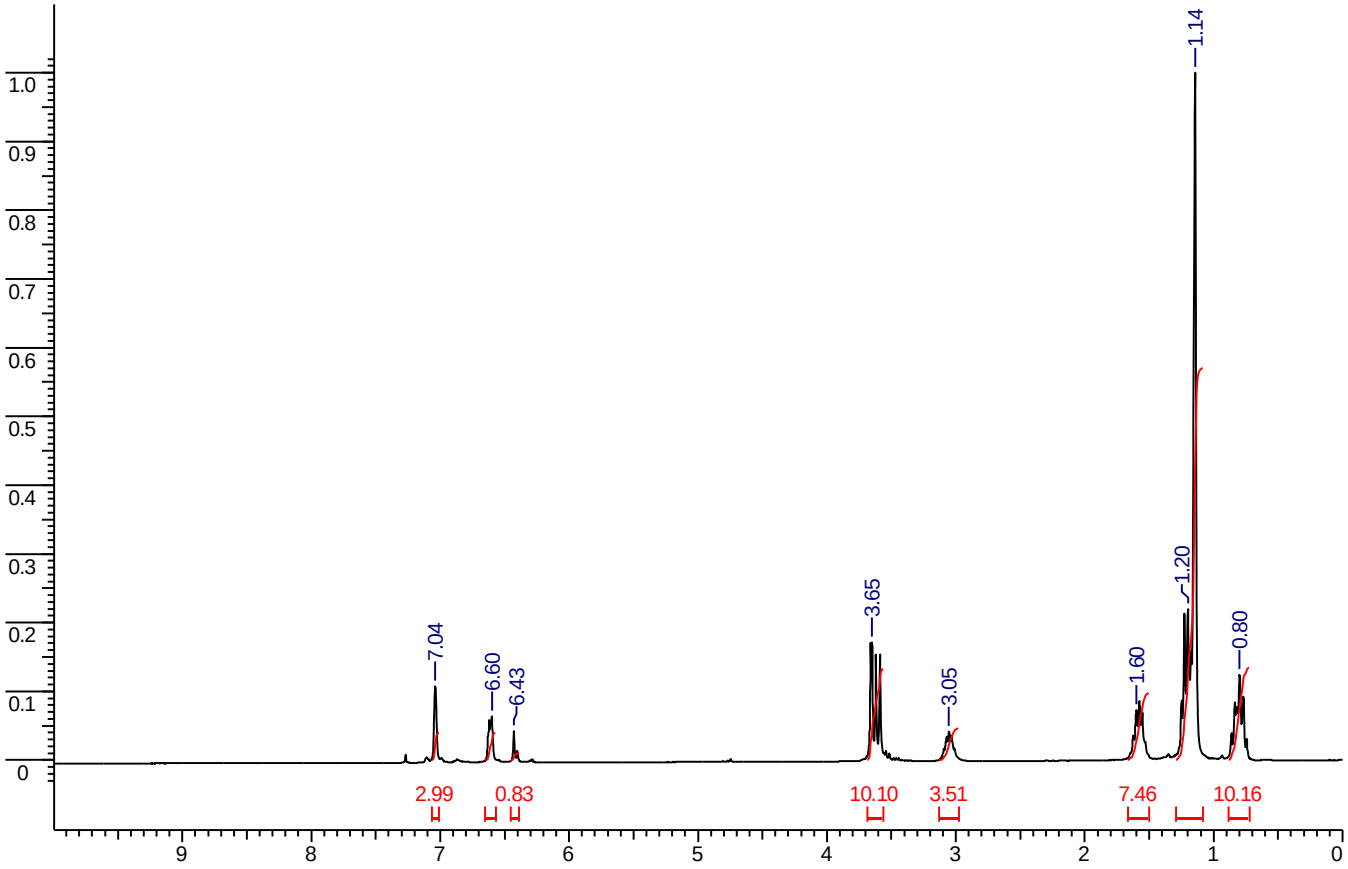

Figure A-6. ^{1}H-NMR Spectrum of compound 3-6

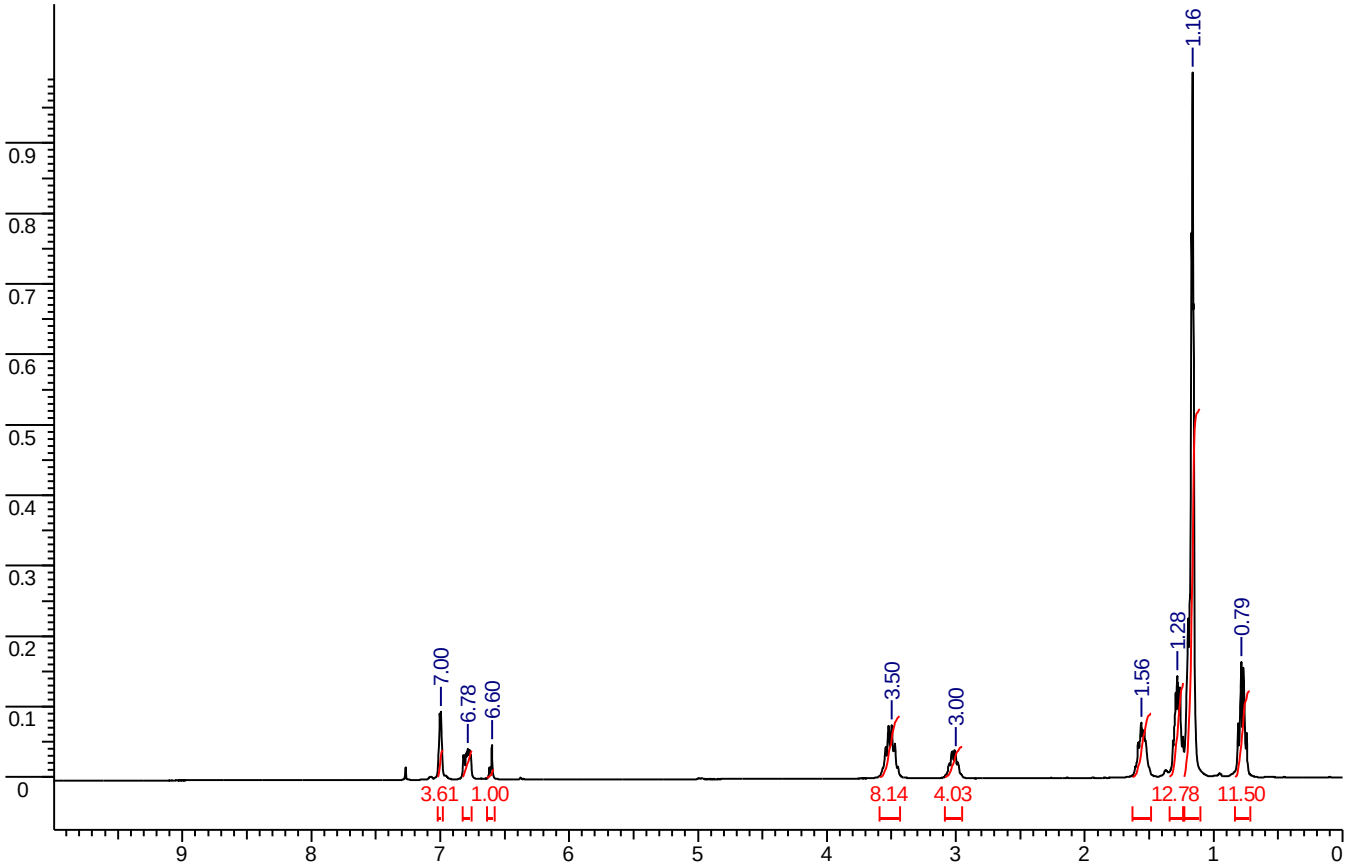

Figure A-7. ^{1}H-NMR Spectrum of compound 3-7

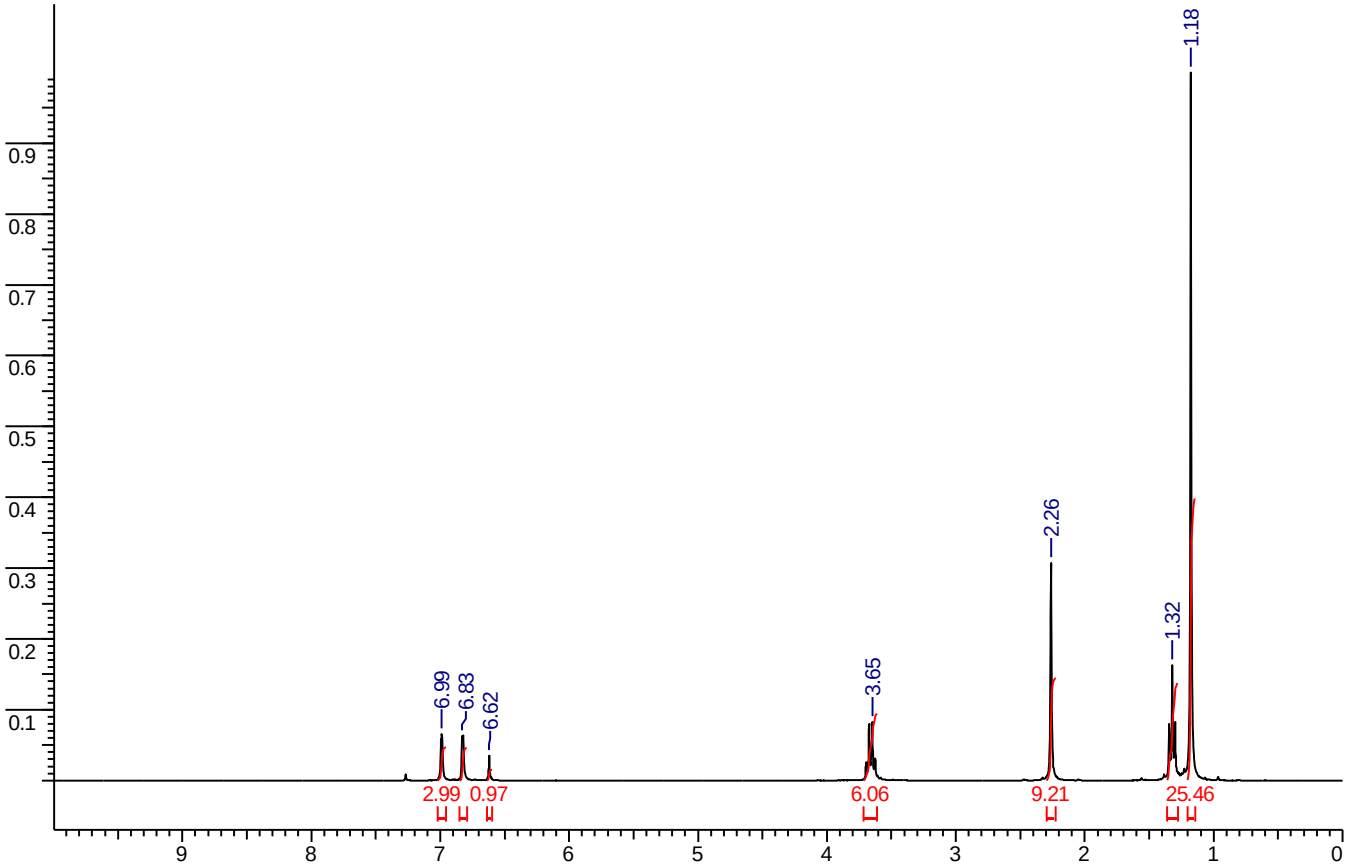

Figure A-8. ^{1}H-NMR Spectrum of compound 3-8

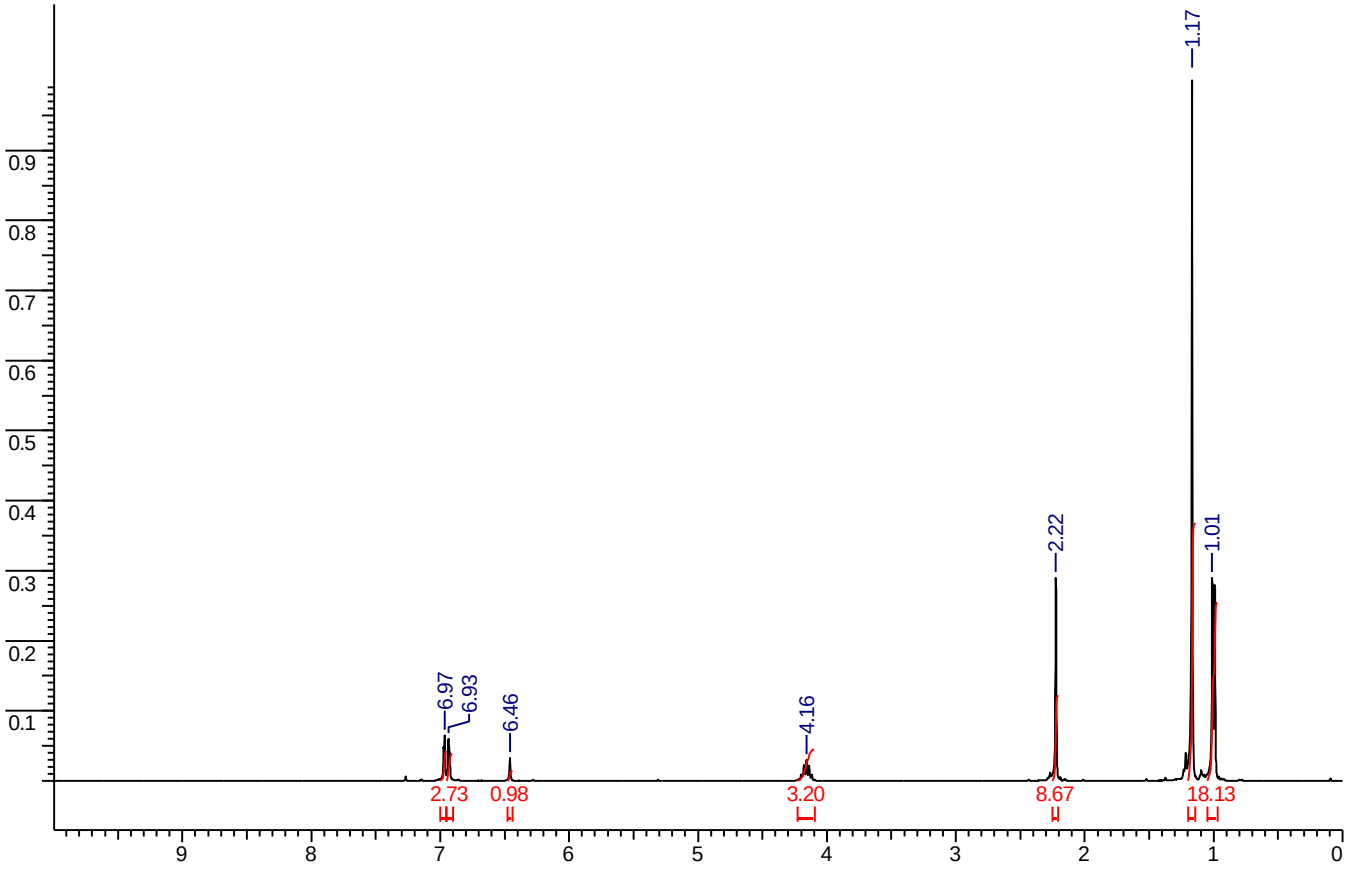

Figure A-9. ^{1}H-NMR Spectrum of compound 3-9

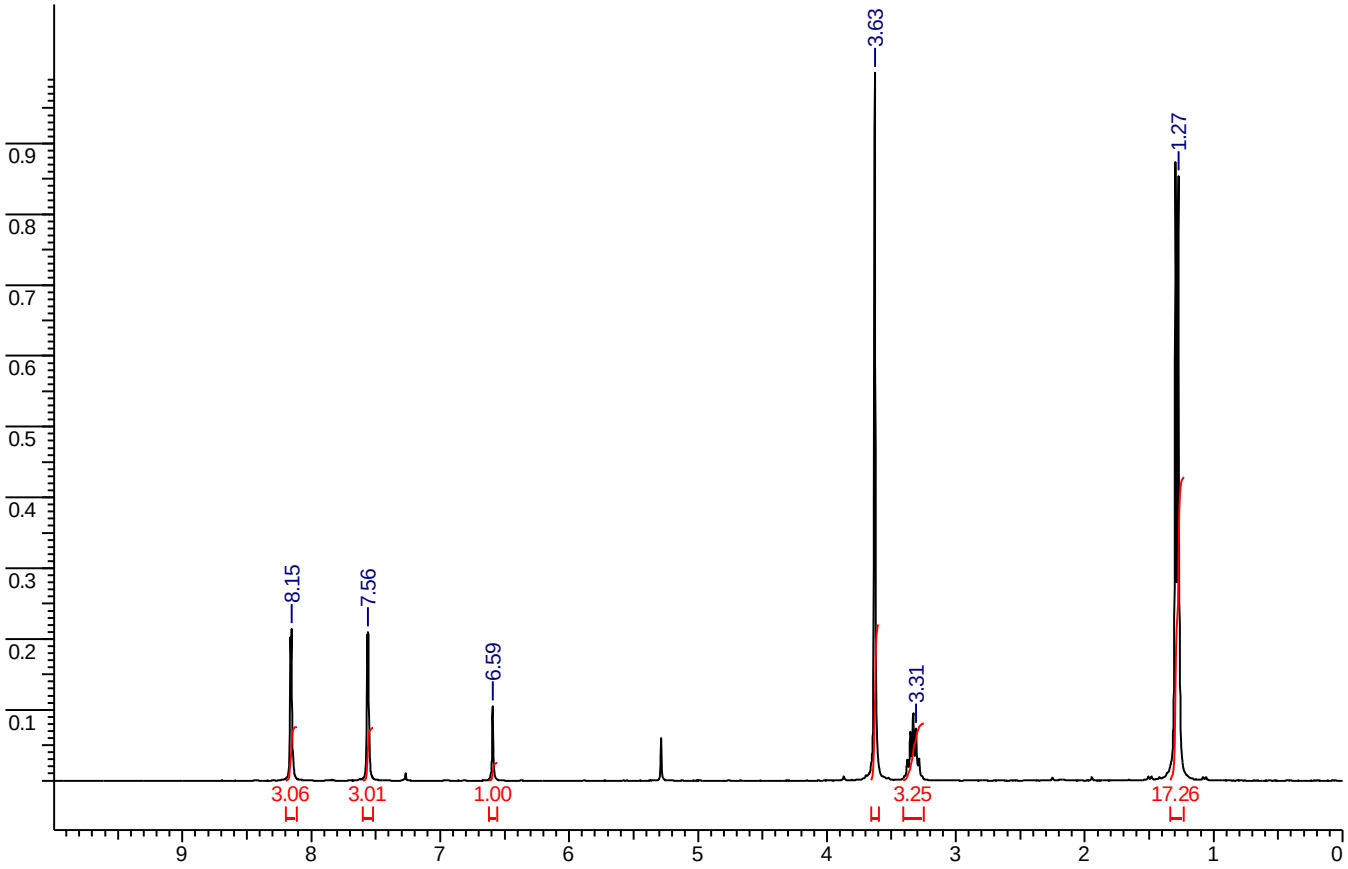

Figure A-10. ^{1}H-NMR Spectrum of compound 3-10

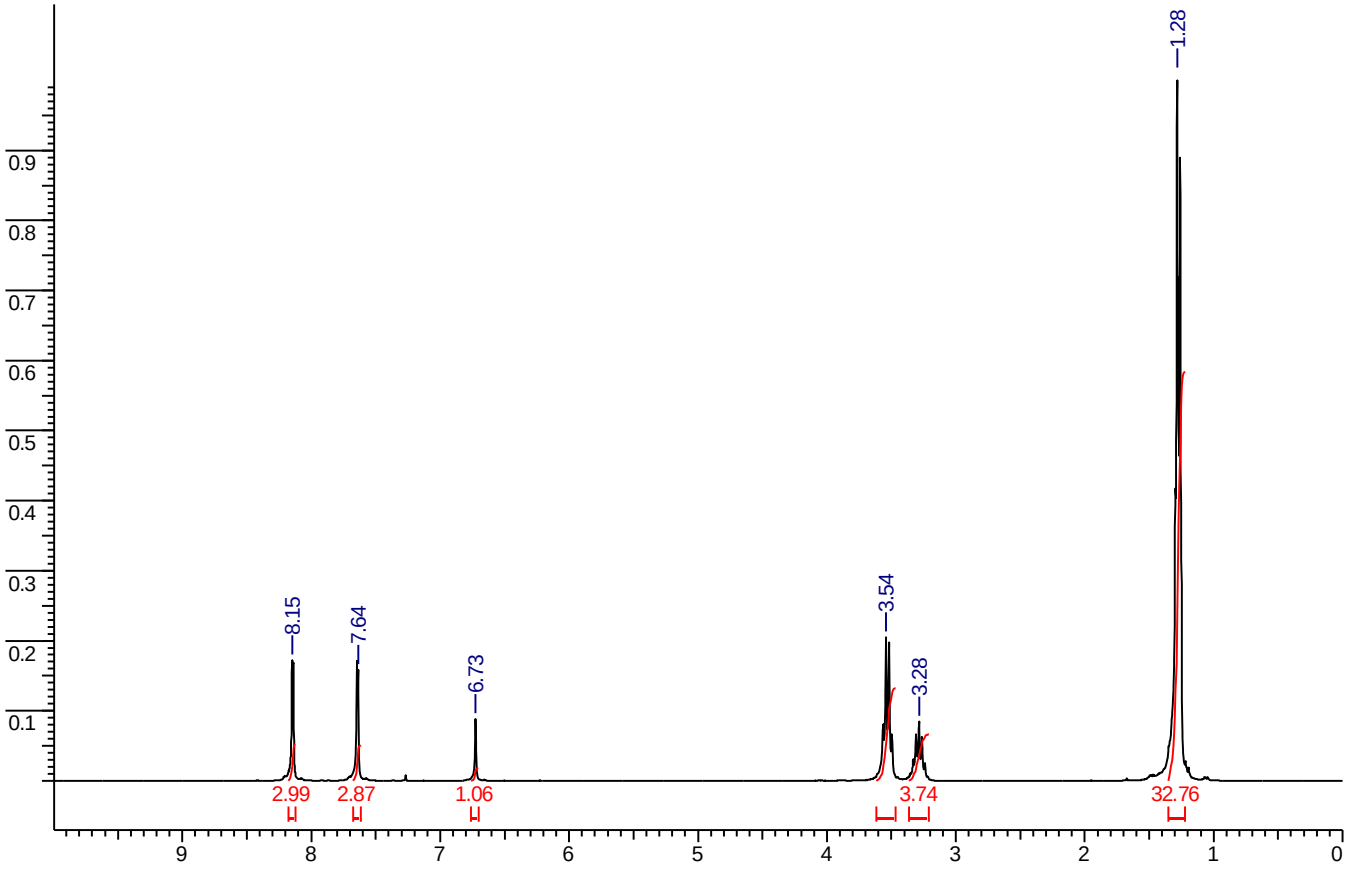

Figure A-11. ^{1}H-NMR Spectrum of compound 3-11

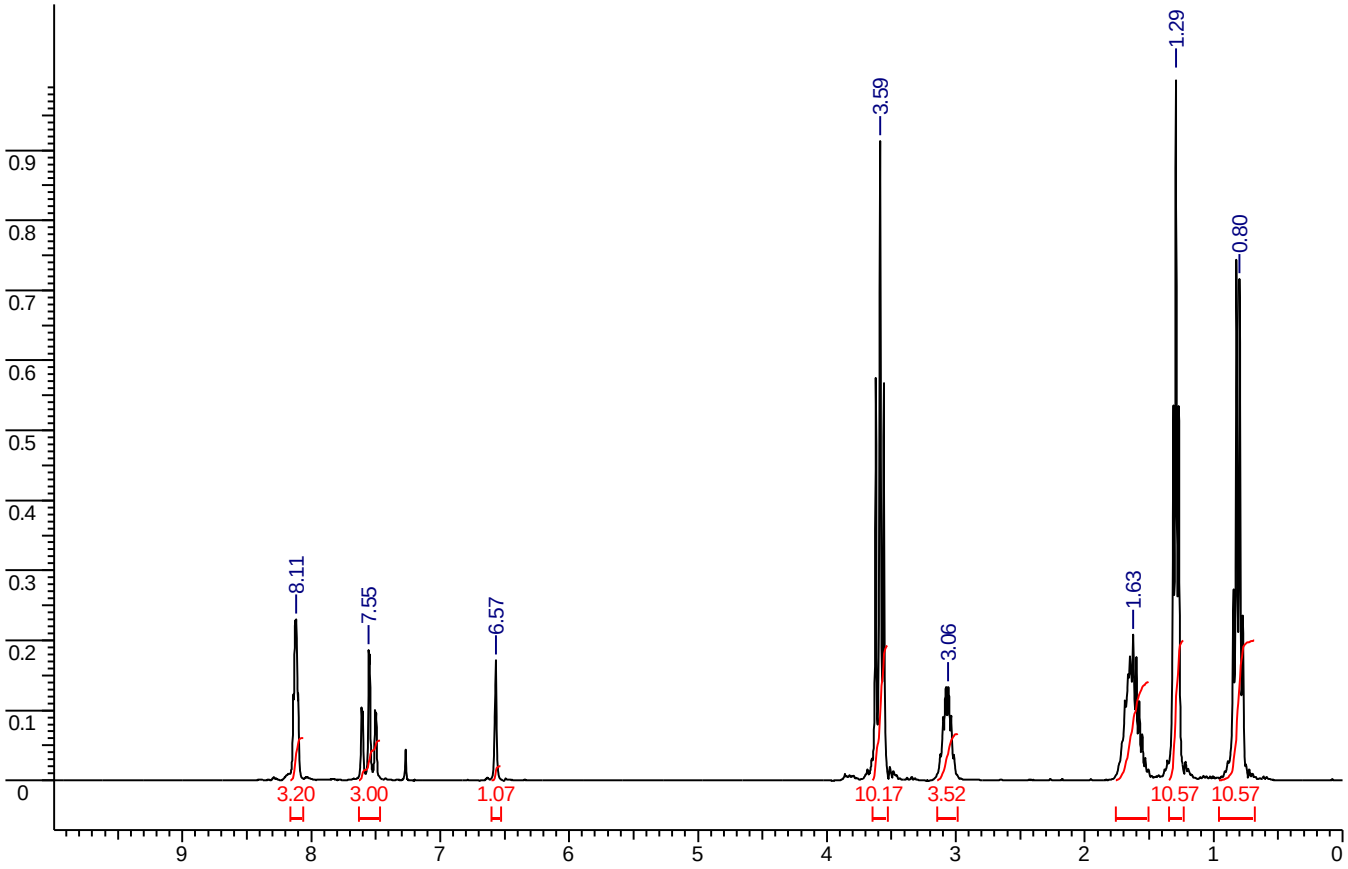

Figure A-12. ^{1}H-NMR Spectrum of compound 3-12

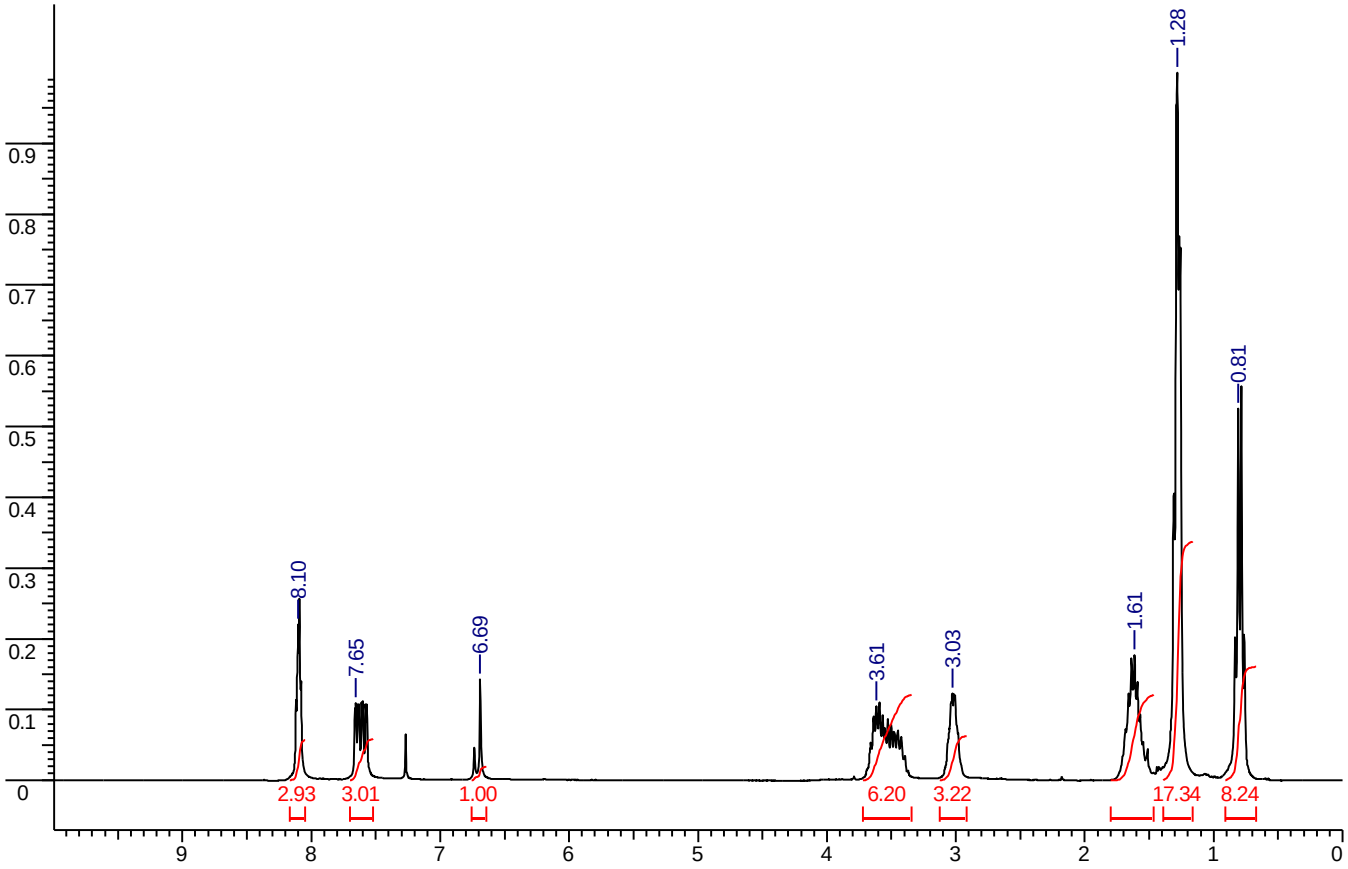

Figure A-13. ^{1}H-NMR Spectrum of compound 3-13

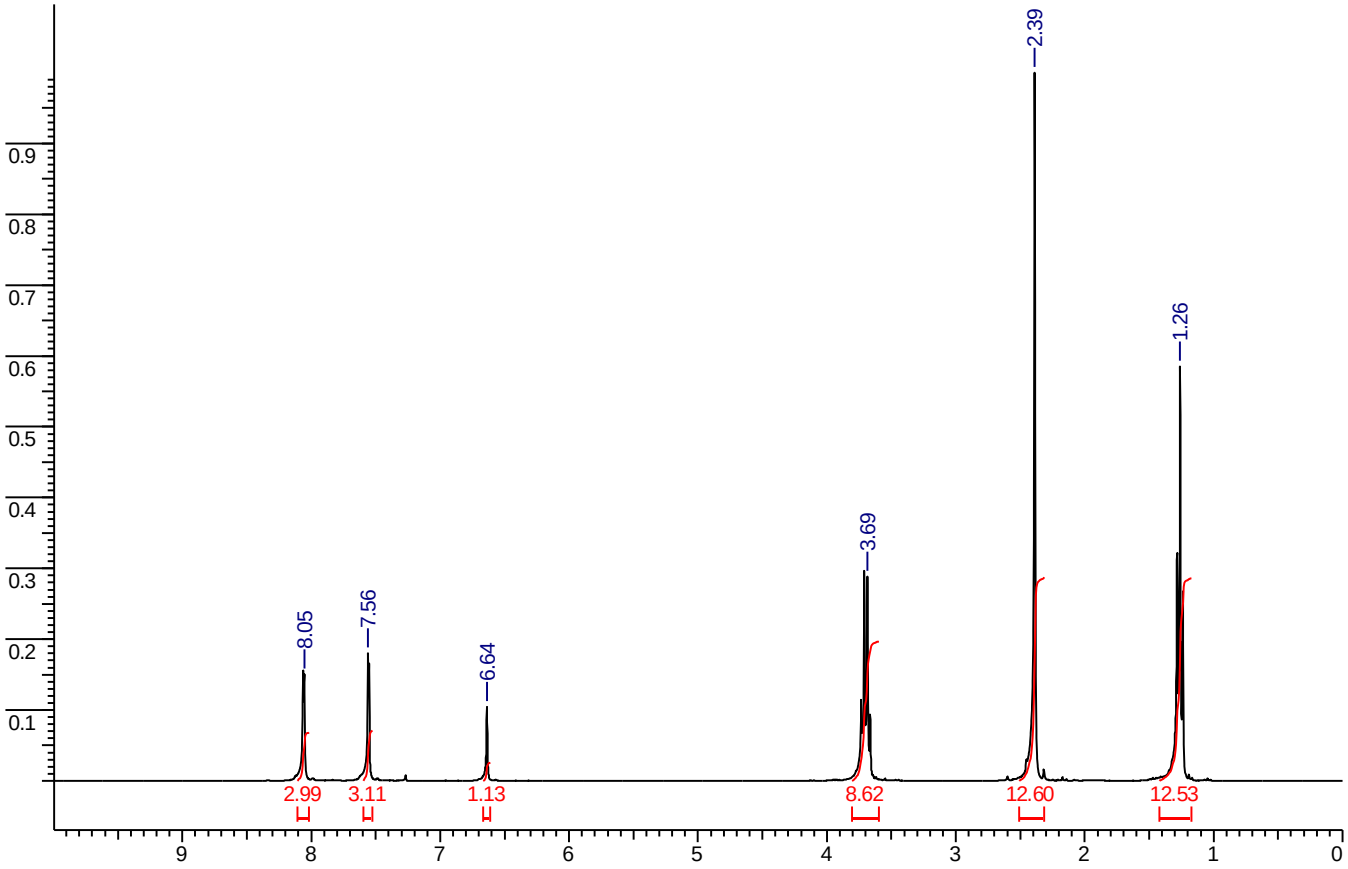

Figure A-14. ^{1}H-NMR Spectrum of compound 3-14

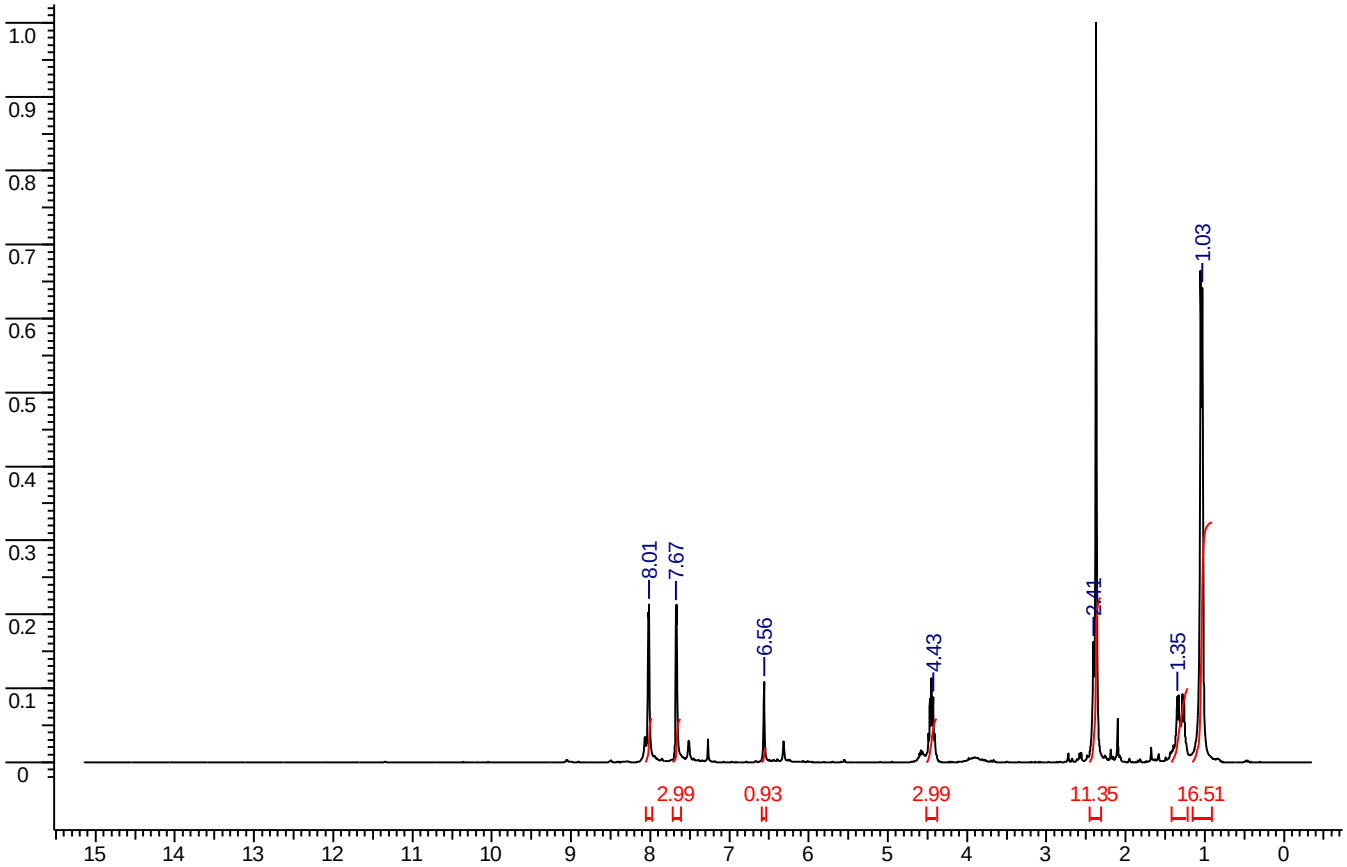

Figure A-15. ^{1}H-NMR Spectrum of compound 3-15

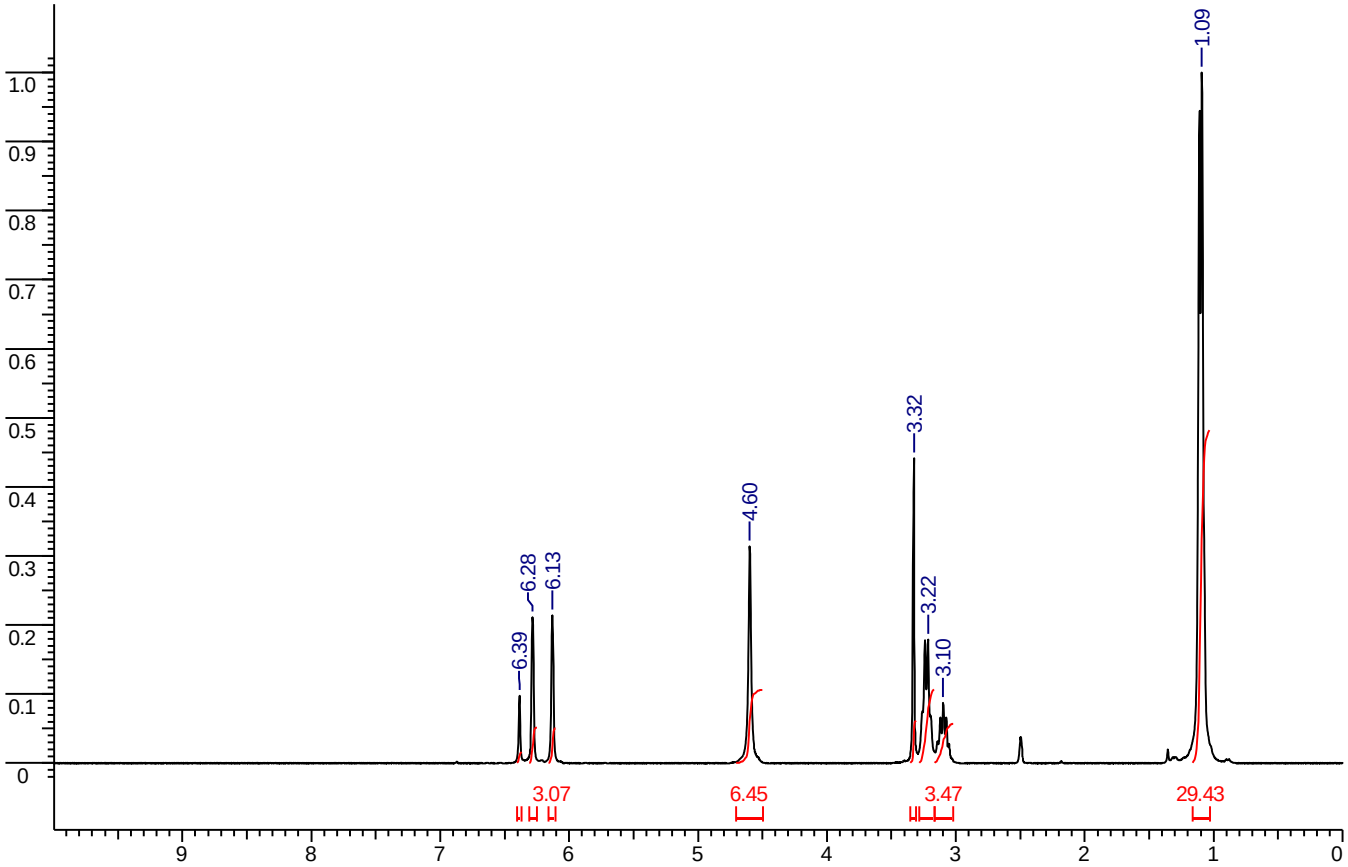

Figure A-16. ^{1}H-NMR Spectrum of compound 3-16

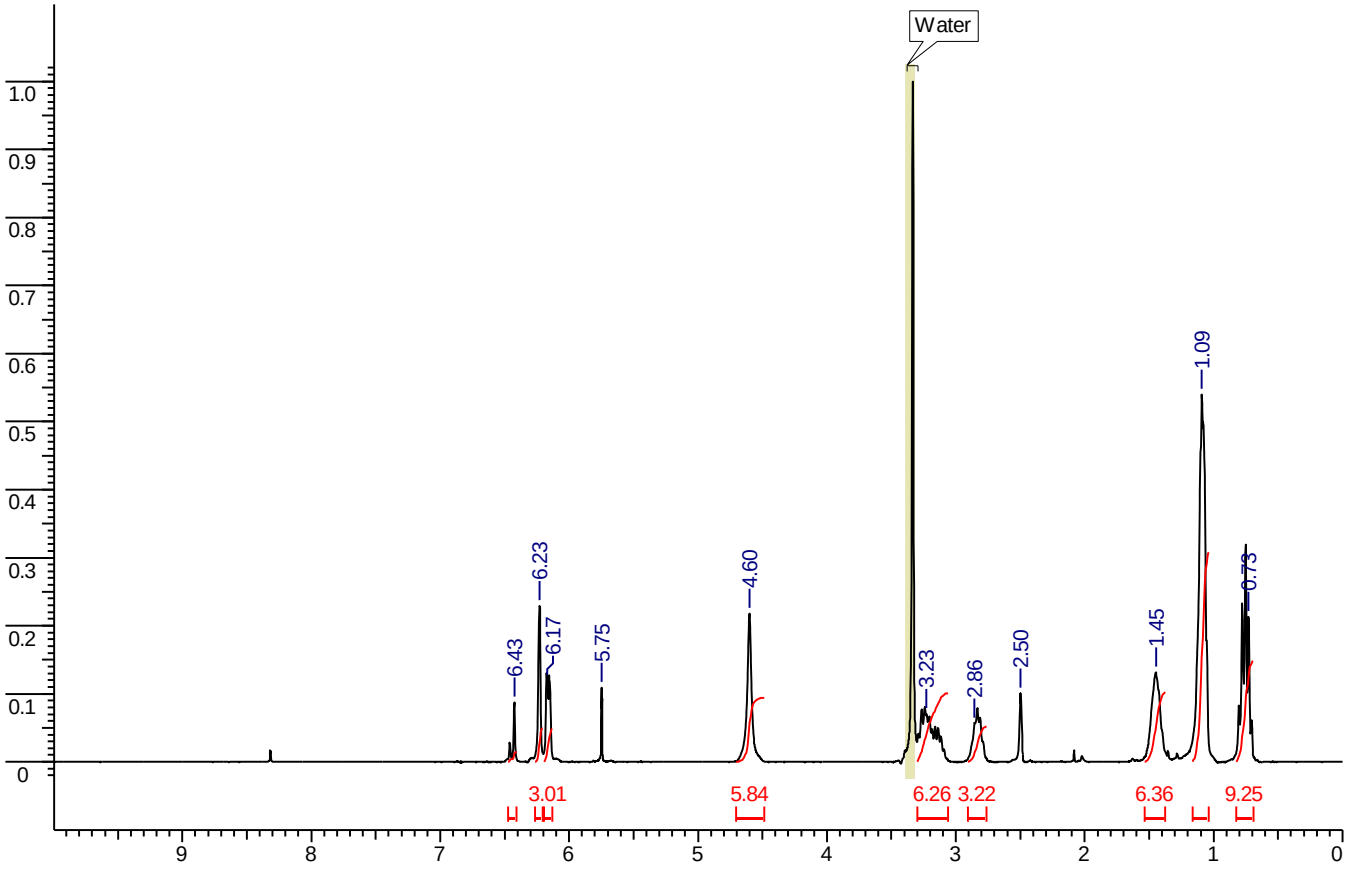

Figure A-17. ^{1}H-NMR Spectrum of compound 3-17

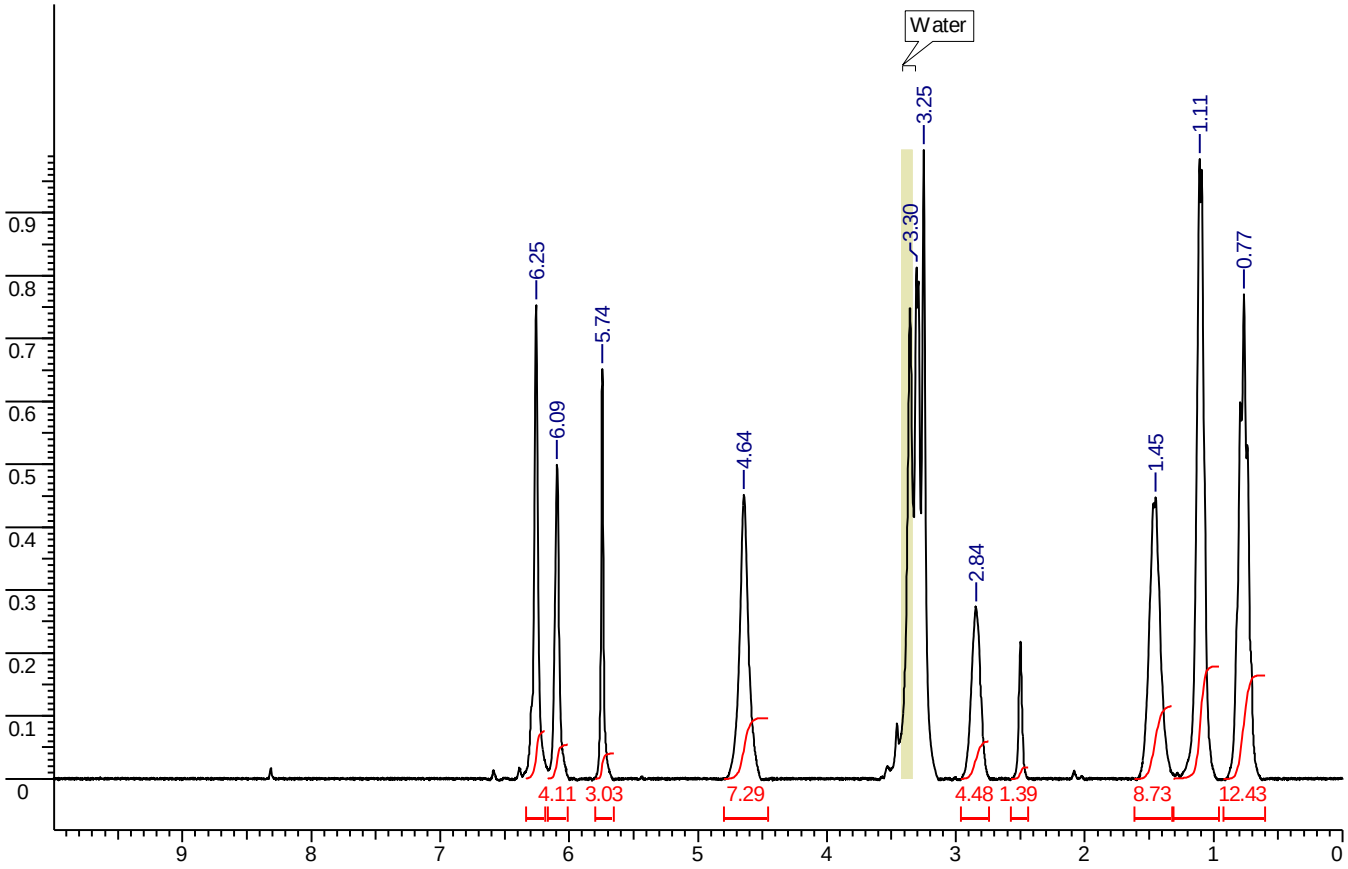

Figure A-18. ^{1}H-NMR Spectrum of compound 3-18

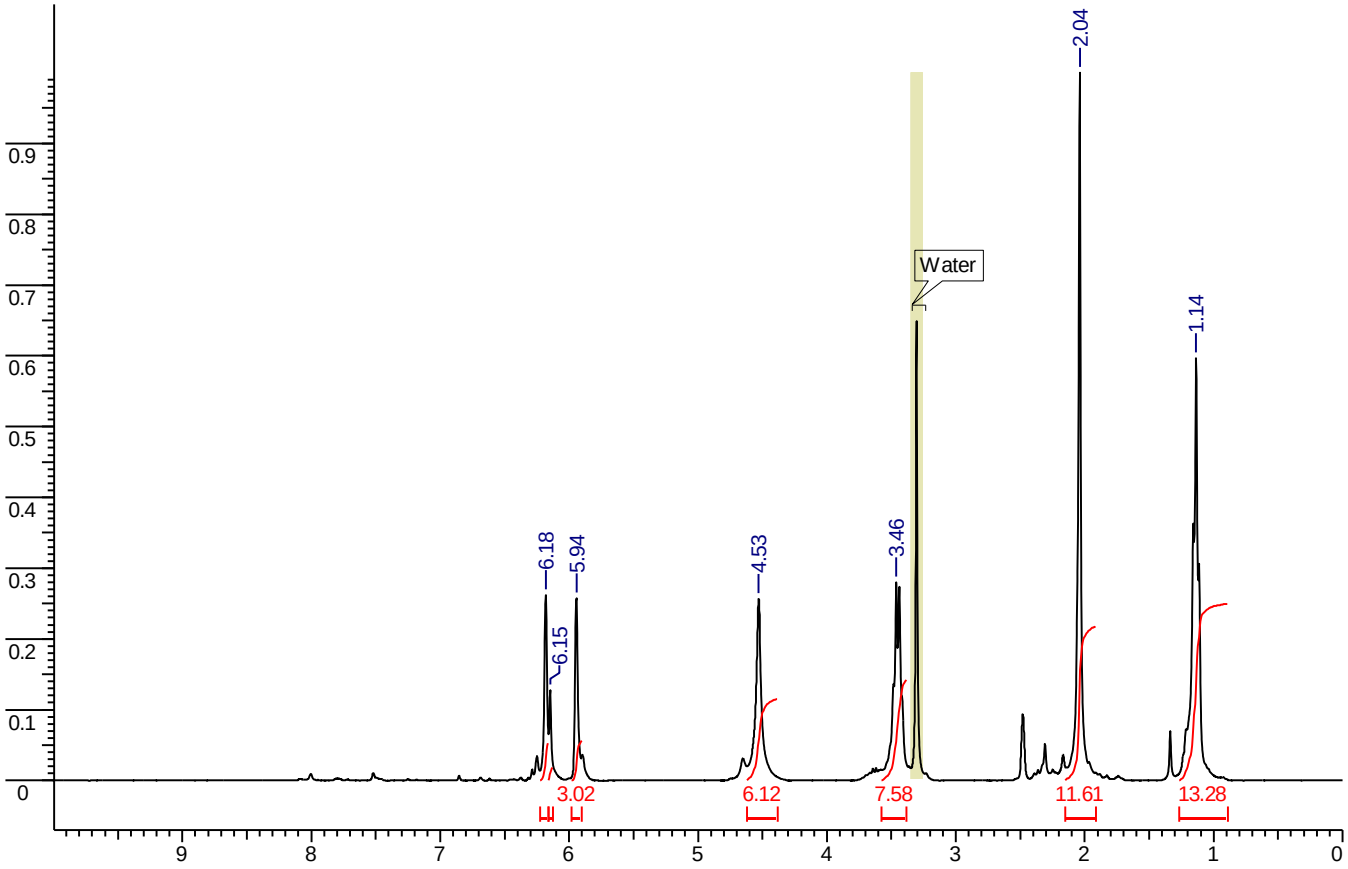

Figure A-19. ^{1}H-NMR Spectrum of compound 3-19

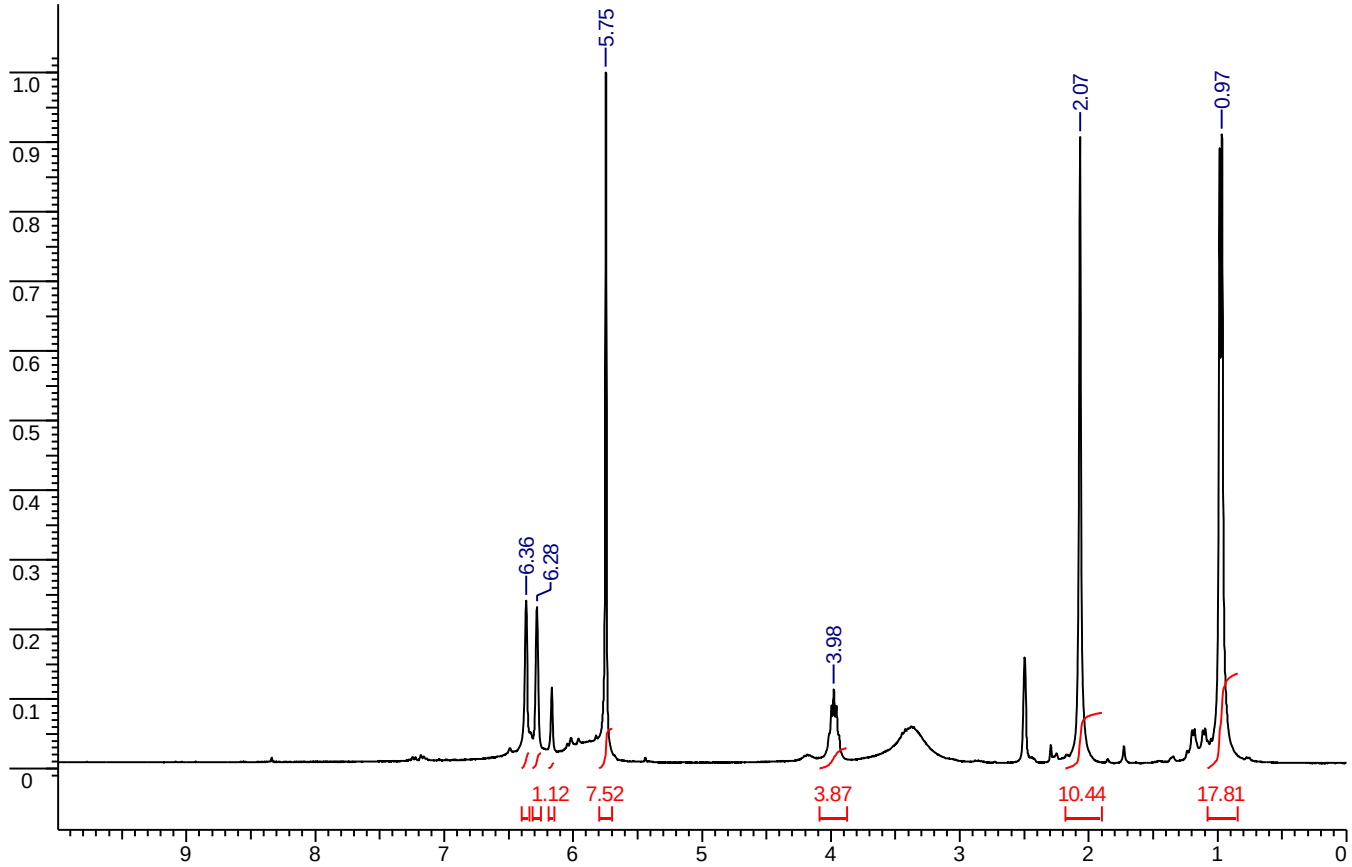

Figure A-20. ^{1}H-NMR Spectrum of compound 3-20

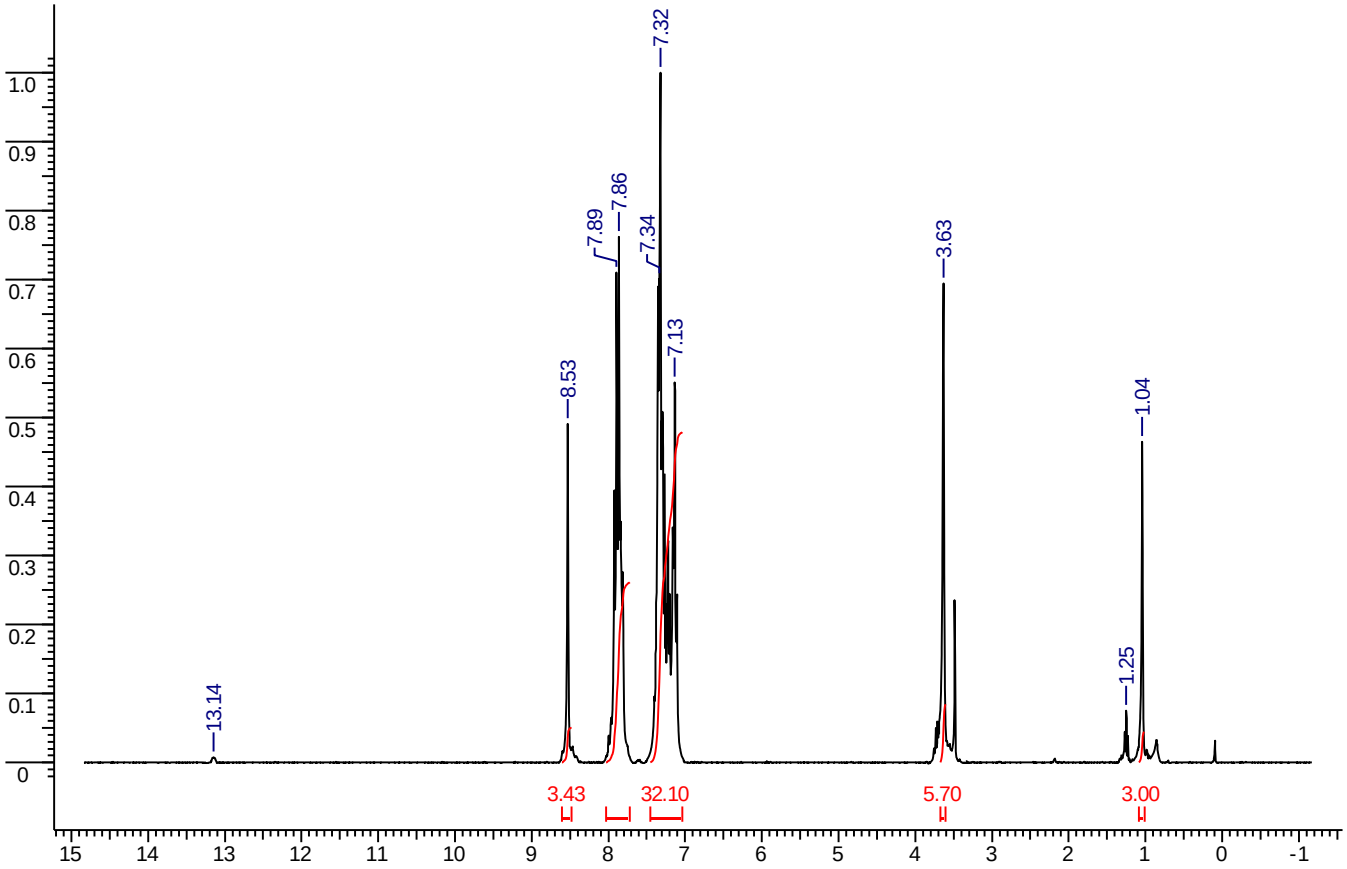

Figure A-21. ^{1}H-NMR Spectrum of compound 2-1

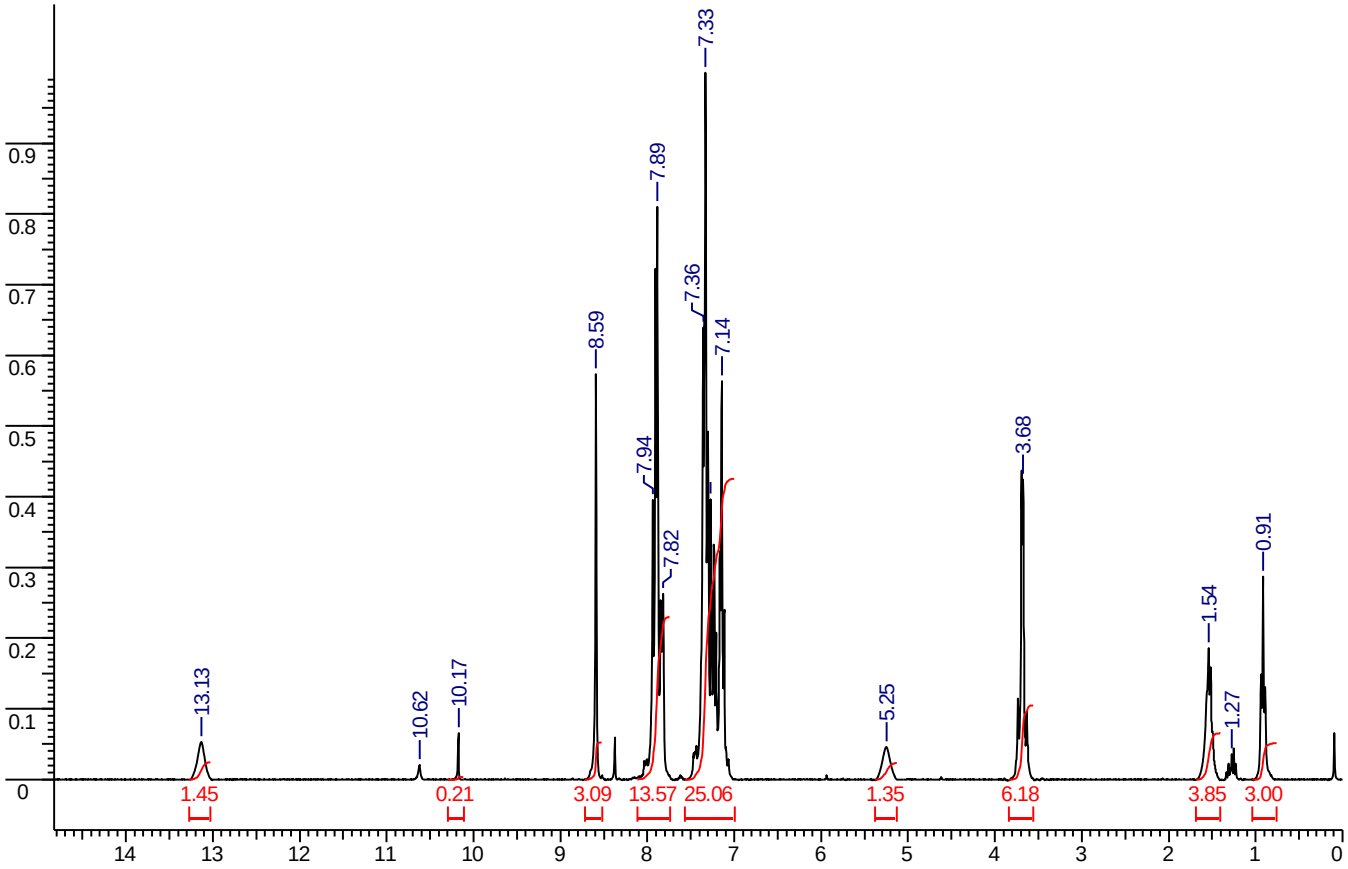

Figure A-22. ^{1}H-NMR Spectrum of compound 2-2

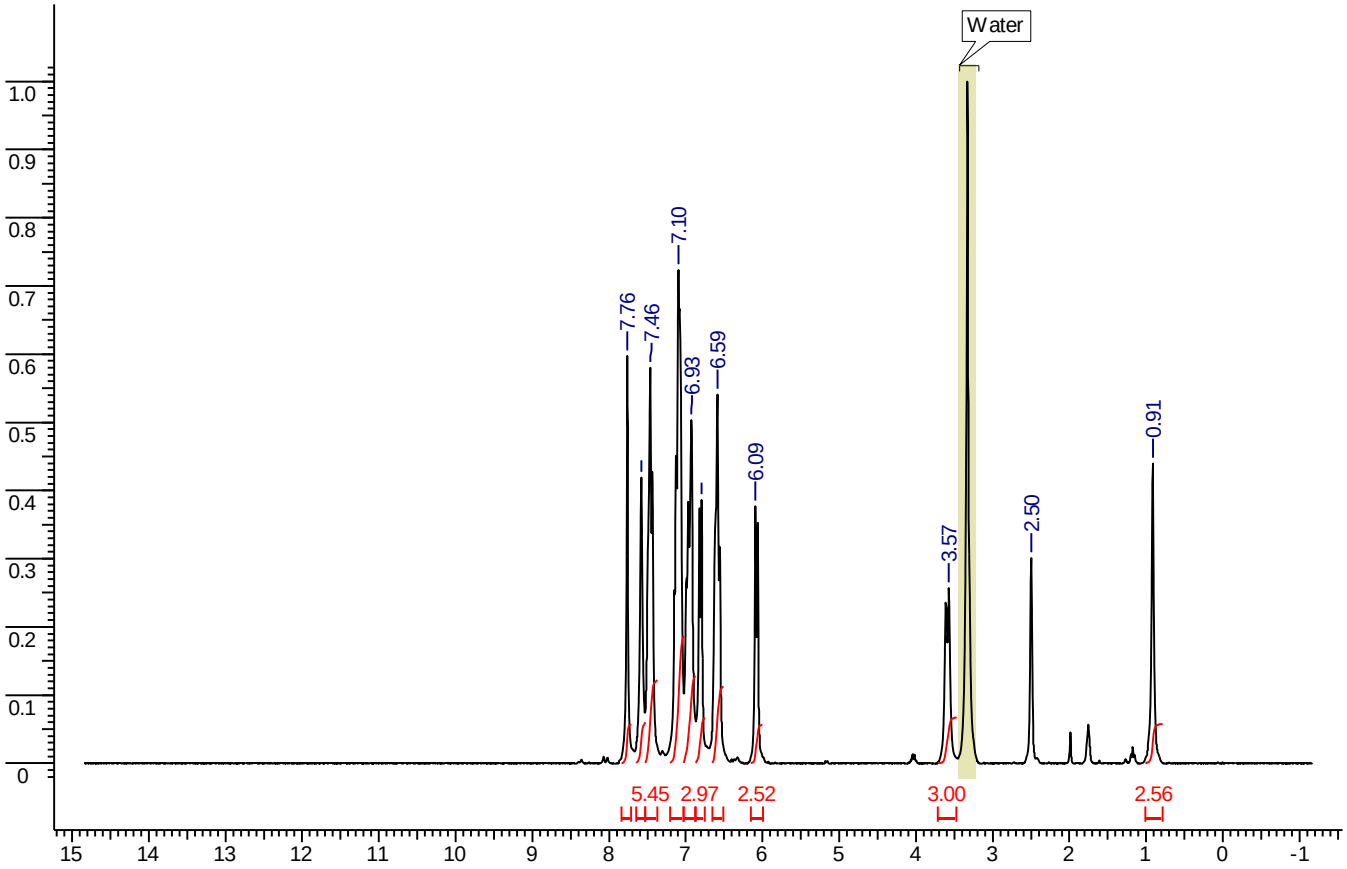

Figure A-23. ^{1}H-NMR Spectrum of compound 2-3

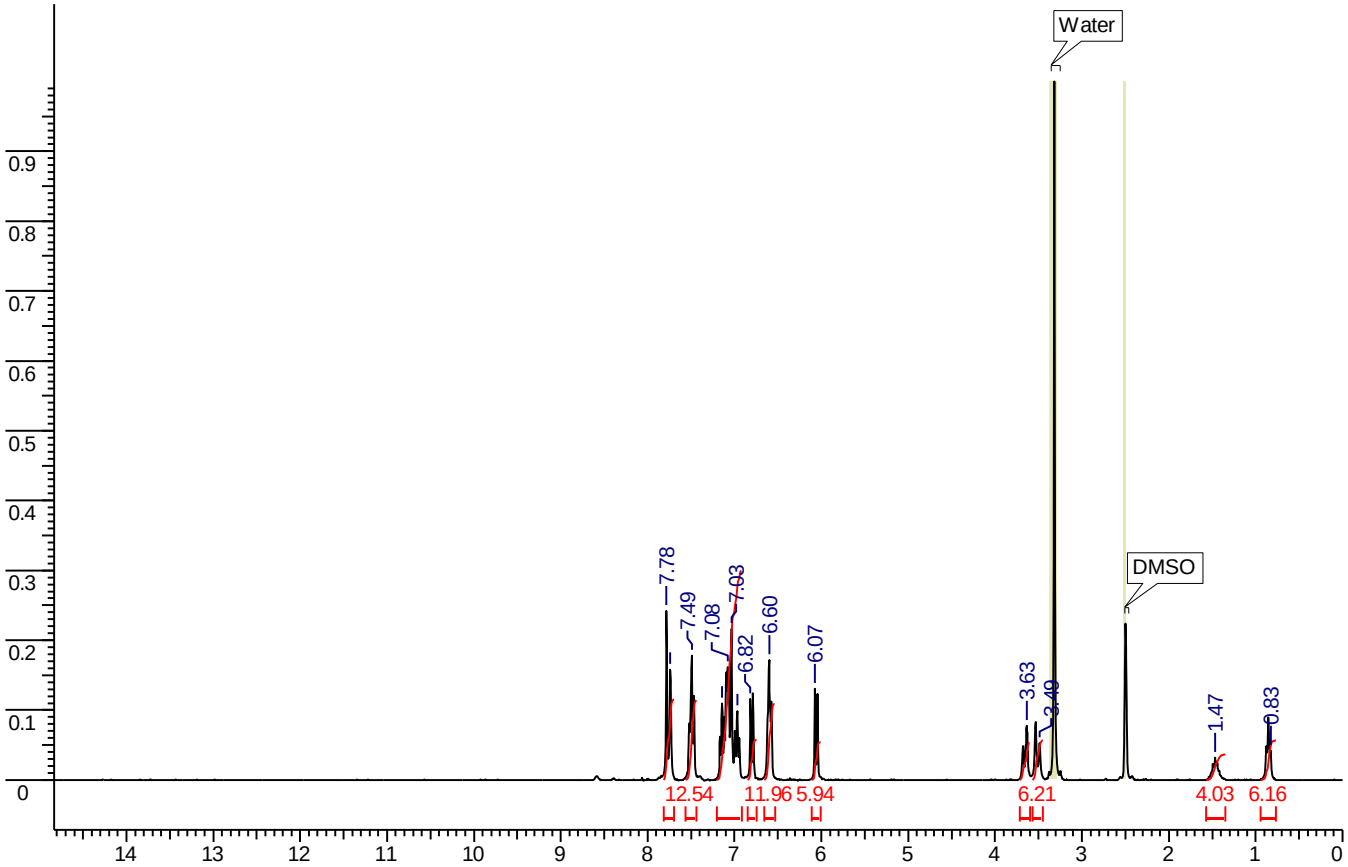

Figure A-24. ^{1}H-NMR Spectrum of compound 2-4

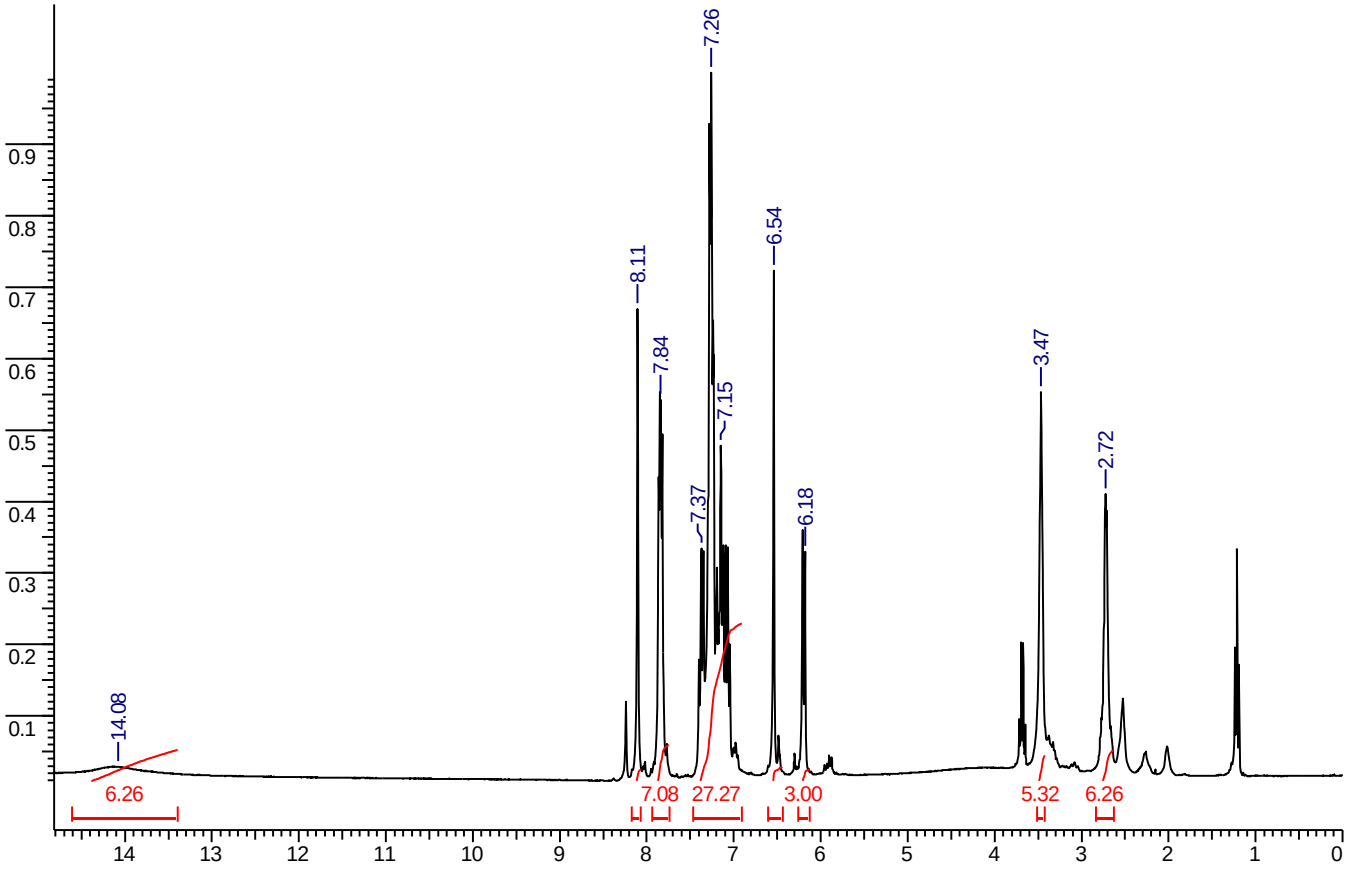

Figure A-25. ^{1}H-NMR Spectrum of compound 2-5

LIST OF REFERENCES

(1) Corma, A.; Garcia, H. *Chem. Rev.* **2002**, *102*, 3837-3892.

(2) Corma, A.; Garcia, H. *Chem. Rev.* **2003**, *103*, 4307-4365.

(3) Johnson, N. B.; Lennon, I. C.; Moran, P. H.; Ramsden, J. A. *Acc. Chem. Res.* **2007**, *40*, 1291-1299.

(4) Dalko, P. I.; Moisan, L. *Angew. Chem. Int. Ed Engl.* **2004**, *43*, 5138-5175.

(5) Pearson, R. G. *J. Am. Chem. Soc.* **1963**, *85*, 3533.

(6) Wulfsburg, G. *Inorganic Chemistry;* University Science Books: Sausilito, CA, 2000.

(7) Quintanar, L.; Stoj, C.; Taylor, A. B.; Hart, P. J.; Kosman, D. J.; Solomon, E. I. *Acc. Chem. Res.* **2007**, *40*, 445-452.

(8) Carey, F. A. In *Organic Chemistry;* McGraw-Hill: New York, NY, 2003.

(9) Grubbs, R. H. "Robert H. Grubbs - Nobel Lecture". Nobelprize.org. http://nobelprize.org/nobel_prizes/chemistry/laureates/2005/grubbs-lecture.html.(accessed 08/03, 2010).

(10) Groves, J., K. *Chem. Soc. Rev.* **1972**, *1*, 73.

(11) Poulsen, T. B.; Jorgensen, K. A. *Chem. Rev.* **2008**, *108*, 2903-2915.

(12) Yamamoto, H. In *Lewis Acid Reagents: A Practical Approach;* Oxford University Press: New York, NY, 1999;

(13) Corey, E. J. *Angew. Chem. Int. Ed Engl.* **2002**, *41*, 1650-1667.

(14) Kagan, H. B.; Riant, O. *Chem. Rev.* **1992**, *92*, 1007-1019.

(15) Jensen, W. B. *Chem. Rev.* **1978**, *78*, 1-22.

(16) Wuest, J. D. *Acc. Chem. Res.* **1999**, *32*, 81-89.

(17) Dias, L. C. *J. Braz. Chem. Soc.* **1997**, *8*, 289-332.

(18) Yoon, T. P.; Jacobsen, E. N. *Science* **2003**, *299*, 1691-1693.

(19) Pfaltz, A.; Drury, W. J.,3rd *Proc. Natl. Acad. Sci. U. S. A.* **2004**, *101*, 5723-5726.

(20) Chen, Y.; Yekta, S.; Yudin, A. K. *Chem. Rev.* **2003**, *103*, 3155-3212.

(21) Berthod, M.; Mignani, G.; Woodward, G.; Lemaire, M. *Chem. Rev.* **2005**, *105*, 1801-1836.

(22) Ikariya, T.; Murata, K.; Noyori, R. *Org. Biomol. Chem.* **2006**, *4*, 393-406.

(23) Mizuno, N.; Misono, M. *Chem. Rev.* **1998**, *98*, 199-218.

(24) Paull, D. H.; Abraham, C. J.; Scerba, M. T.; Alden-Danforth, E.; Lectka, T. *Acc. Chem. Res.* **2008**, *41*, 655-663.

(25) Mahato, S. B. *J. Indian Chem. Soc.* **2000**, *77*, 175-191.

(26) Sartori, G.; Maggi, R. *Chem. Rev.* **2006**, *106*, 1077-1104.

(27) Bandini, M.; Melloni, A.; Tommasi, S.; Umani-Ronchi, A. *Synlett* **2005**, *8*, 1222.

(28) Buckley, T. F.; Rapoport, H. *J. Am. Chem. Soc.* **1980**, *102*, 3056.

(29) Kokotalio, G. T.; Schlenker, J. L.; Dwyer, F. G.; Walyocsik, E. W. *Zeolites* **1985**, *5*, 349.

(30) Bigi, F.; Casiraghi, G.; Casnati, G.; Sartori, G.; Fava, G. G.; Belicchi, M. F. *J. Org. Chem.* **1985**, *50*, 5018.

(31) Zhou, J.; Tang, Y. *J. Am. Chem. Soc.* **2002**, *124*, 9030-9031.

(32) Hashimoto, S.; Komeshima, N.; Koga, K. *J. Chem. Soc. Chem. Commun.* **1979**, , 437.

(33) Bao, J.; Wullf, W. D.; Rheingold, A. L. *J. Am. Chem. Soc.* **1993**, *115*, 3814.

(34) Krause, N.; Hoffman-Röder, A. *Synthesis* **2001**, *2*, 171-196.

(35) Rossiter, B. E.; Swingle, N. M. *Chem. Rev.* **1992**, *92*, 806.

(36) Sibi, M. P.; Manyem, S. *Tetrahedron* **2000**, , 8033-8061.

(37) Vaugeois, J.; Simard, M.; Wuest, J. D. *Coord. Chem. Rev.* **1995**, *145*, 55-73.

(38) Wedge, T. J.; Hawthorne, M. F. *Coord. Chem. Rev.* **2003**, *240*, 128.

(39) Piers, W. E.; Irvine, G. J.; Williams, V. C. *Eur. J. Inorg. Chem.* **2000**, , 2131-2142.

(40) Shur, V. B.; Tikhonova, I. A. *Russian Chem. B+,* **2003**, *12*, 2539-2554.

(41) Biallas, M. J.; Shriver, D. F. *J. Am. Chem. Soc.* **1966**, *88*, 375-376.

(42) Beauchamp, A. L.; Olivier, M. J.; Wuest, J. D.; Zacharie, B. *J. Am. Chem. Soc.* **1986**, *108*, 73-77.

(43) Peters, M. W. **2002**. Bio-inspired Transition Metal Complexes and Actinide-Selective Extractants using Triphenoxymethane-based C_3-symmetric Ligand Systems. Doctoral Dissertation, University of Florida, Gainesville.

(44) Bourget-Merle, L.; Lappert, M. F.; Severn, J. R. *Chem. Rev.* **2002**, *102*, 3031-3066.

(45) Edelmann, F. T. *Coord. Chem. Rev.* **1994**, *137*, 403-481.

(46) Barker, J.; Kilner, M. *Coord. Chem. Rev.* **1994**, *133*, 219-300.

(47) Bailey, P. J.; Pace, S. *Coord. Chem. Rev.* **2001**, *214*, 91-141.

(48) Holm, R.; Kennepohl, P.; Solomon, E. I. *Chem. Rev.* **1996**, *96*, 2239-2314.

(49) Solomon, E. I.; Sarangi, R.; Woertink, J. S.; Augustine, A. J.; Yoon, J.; Ghosh, S. *Acc. Chem. Res.* **2007**, *40*, 581-591.

(50) Mirica, L. M.; Ottenwaelder, X.; Stack, T. D. *Chem. Rev.* **2004**, *104*, 1013-1045.

(51) Dinger, M. B.; Scott, M. J. *Eur. J. Org. Chem* **2000**, 2467-2478.

(52) Knochel, P.; Grenouillat, N. *Encyclopedia of Reagents for Organic Synthesis* **2006**, 1-46.

(53) Hayashi, S.; Hirao, A.; Imai, A.; Nakamura, H.; Murata, Y.; Ohashi, K.; Nakata, E. *J. Med. Chem.* **2009**, *52*, 610-625.

(54) Sundberg, R. J.; Pitts, W. J. *J. Org. Chem.* **1991**, *56*, 3048-3054.

(55) Khan, F. A.; Dash, J.; Sudheer, C.; Gupta, R. K. *Tett. Letters* **2003**, *44*, 7783-7787.

(56) MOPAC2009, James J. P. Stewart, Stewart Computational Chemistry, Colorado Springs, CO, USA, HTTP://OpenMOPAC.net (2008).

(57) Rosevear, J.; Wilshire, J. F. K. *Aust. J. Chem.* **1985**, *38*, 1163-1176.

(58) Sberegaeva, A., Ozbeck, O., Scott, M.J. *In press*

(59) Maruoka, K. *Bull. Chem. Soc. Jpn.* **2009**, *82*, 917-930.

(60) Hoefelmeyer, J. D.; Schulte, M.; Tschinkl, M.; Gabbaï, F. P. *Coord. Chem. Rev.* **2002**, *235*, 93-103.

(61) Gabbai, F. P. *Angew. Chem. Int. Ed Engl.* **2003**, *42*, 2218-2221.

(62) Hudnall, T. W.; Chiu, C. W.; Gabbai, F. P. *Acc. Chem. Res.* **2009**, *42*, 388-397.

(63) Hudnall, T. W.; Gabbai, F. P. *J. Am. Chem. Soc.* **2007**, *129*, 11978-11986.

(64) Yamamoto, H.; Futatsugi, K. *Angew. Chem. Int. Ed Engl.* **2005**, *44*, 1924-1942.

(65) Pohnert, G. *J. Prakt. Chem.* **1999**, *341*, 406-409.

(66) Healy, M. D.; Power, M. B.; Barron, A. R. *Coord. Chem. Rev.* **1994**, *130*, 63-135.

(67) Maruoka, K.; Itoh, T.; Sakurai, M.; Nonoshita, K.; Yamamoto, H. *J. Am. Chem. Soc.* **1988**, , 3588-3597.

(68) Starowieyski, K. B.; Pasynkiewicz, S.; Skowroñska-Ptasiñska, M. *J. Organomet. Chem.* **1975**, *90*, C43.

(69) Ooi, T.; Kondo, Y.; Maruoka, K. *Angew. Chem. Int. Ed Engl.* , *37*, 3039-3041.

(70) Saito, S.; Yamamoto, H. *Chemm. Comm.* **1997**, , 1585-1592.

(71) Leung, W.; Zhang, Q.; Yi, X. *Coord. Chem. Rev.* **2007**, *251*, 2266-2279.

(72) Kläui, W. *Angew. Chem. Int. Ed Engl.* **1990**, *29*, 627-637.

(73) Lam, T. C. H.; Mak, W.; Wong, W.; Kwong, H.; Sung, H. H. Y.; Lo, S. M. F.; Williams, I. D.; Leung, W. *Organometallics* **2004**, *23*, 1247-1252.

(74) Zieleniuk, C. 2009. Anion Binding and Catalytic Studies of Metal Salen Complexes. Doctoral Dissertation, University of Florida, Gainesville.

(75) Blackman, A. G. *Polyhedron* **2005**, *24*, 1-39.

(76) Ishihara, K.; Kobayashi, J.; Inanaga, K.; Yamamoto, H. *Synlett* **2001**, *3*, 394-396.

(77) Yamamoto, H. *Proc. Jpn. Acad., Ser. B* **2008**, *84*, 134-146.

(78) Linderman, R. J.; Jaber, M.; Griedel, B. D. *J. Org. Chem.* **1994**, *59*, 6499-6500.

(79) Suresh, P.; Simurugan, S.; Pati, H. N. *Chem. Lett.* **2007**, *36*, 1332-1333.

(80) Fleischer, E. B.; Gebala, A. E.; Levey, A.; Tasker, P. A. *J. Org. Chem.* **1971**, *36*, 3042-3044.

(81) Viguir, R.; Serratrice, G.; Dupraz, A.; Dupuy, C. *Eur. J. Inorg. Chem.* **2001**, 1789-1795.

(82) Gaussian 09, Revision **A.1**, Frisch, M. J.; Trucks, G. W.; Schlegel, H. B.; Scuseria, G. E.; Robb, M. A.; Cheeseman, J. R.; Scalmani, G.; Barone, V.; Mennucci, B.; Petersson, G. A.; Nakatsuji, H.; Caricato, M.; Li, X.; Hratchian, H. P.; Izmaylov, A. F.; Bloino, J.; Zheng, G.; Sonnenberg, J. L.; Hada, M.; Ehara, M.; Toyota, K.; Fukuda, R.; Hasegawa, J.; Ishida, M.; Nakajima, T.; Honda, Y.; Kitao, O.; Nakai, H.; Vreven, T.; Montgomery, Jr., J. A.; Peralta, J. E.; Ogliaro, F.; Bearpark, M.; Heyd, J. J.; Brothers, E.; Kudin, K. N.; Staroverov, V. N.; Kobayashi, R.; Normand, J.; Raghavachari, K.; Rendell, A.; Burant, J. C.; Iyengar, S. S.; Tomasi, J.; Cossi, M.; Rega, N.; Millam, N. J.; Klene, M.; Knox, J. E.; Cross, J. B.; Bakken, V.; Adamo, C.; Jaramillo, J.; Gomperts, R.; Stratmann, R. E.; Yazyev, O.; Austin, A. J.; Cammi, R.; Pomelli, C.; Ochterski, J. W.; Martin, R. L.; Morokuma, K.; Zakrzewski, V. G.; Voth, G. A.; Salvador, P.; Dannenberg, J. J.; Dapprich, S.; Daniels, A. D.; Farkas, Ö.; Foresman, J. B.; Ortiz, J. V.; Cioslowski, J.; Fox, D. J. Gaussian, Inc., Wallingford CT, 2009.

(83) Ooi, T., Takahasi, M., Yamada, M., Tayama, E., Omoto, K., Maruoka, K. *J. Am. Chem. Soc.* **2004**, *126*, 1150-1160

(84) Dam, H., Reinhoudt, D., Verboom, W. *Chem. Soc. Rev.* **2007**, 36, 367-377

(85) Baaden, M., Berny, F., Madic, C., Schurhammer, R., Wipff, G. *Solvent Extr. Ion Exc.* **2003**, 21, 199-220.

(86) MItra, R., Peters, M., Scott, M. *Dalton Trans.* **2007**, 3924-3935

(87) Matoka, K., Sah, A., Paters, M., Srinivasan, P., Gelis, A., Regalbuto, M., Scott, M. *Inorg. Chem.* **2007**, 46, 10549-10563

(88) Libra, E., Scott, M. *Chem. Comm.* **2006**, 1485-1487

(89) Lindoy, L., Meehan, G., Svenstrup, N. *Synthesis* **1998**, 7, 1029-1032

(90) Sameni, S., Jeunesse, C., Matt, D., Harrowfield, J. *Chem Soc. Rev.* **2009**, 38, 2117-2146

(91) Lumetta, G., Gelis, A., Vandergraft, G. *Solvent Extr. Ion Exc.* **2010**, 28, 287-312

(92) Hudson, M., Boucher, C., Braekers, D., Desreux, J., Drew, M., Foreman, M., Harwood, L., Hill, C., Madic, C., Marken, F., Youns, T. *New J. Chem.* **2006**, 30, 1171-1183

(93) Sluis, P., Spek, A. *Acta Crystallogr.* **1990**, A46, 194-201

(94) Berthet, J., Miquel, Y., Iveson, P., Nierlich, M., Thuery, P., Madic, C., Ephritikhine, M. *Dalton Trans.* **2002**, 3265-3272

(95) Roblou, E., Ait-Haddou, H., Sasaki, I., Daran, J. *Acta Crystallogr.* **2003**, E59, o1175-o1177

(96) Drew, M., Guillaneux, D., Hudson, M., Iveson, P., Russell, M., Madic, C. *Inorg. Chem. Comm.* **2001**, 4, 12-15

BIOGRAPHICAL SKETCH

Patrick was born in the beach town of Morehead City, North Carolina in the spring of 1983. As a young boy, he spent most of his time playing outdoors with his favorite toys, namely his CO_2 powered BB gun and the go-kart his dad built him; no restrictor plate. The countless time spent at the beach fishing, playing, and exploring left a lasting impression on Patrick, and to this day the beach holds that special place of rest for him. In the summer between second and third grade, Patrick and his family moved to High Point, NC where they live currently.

Living closer to the mountains held even more fascination for Patrick. Having thoroughly explored the beaches as a child, now the vastness of the wilderness held his fascination. His family lived far outside the city, surrounded by acres of forest. BB gun in hand and with his intrepid exploring partner Daniel, his brother, the two spent most of their days wandering the woods making forts, drawing maps, and hiding “treasure.”

The summer after his fifteenth birthday meant the end of his leisurely days. Patrick started working as a pharmacy technician at Target. He vividly recalls reading the drug bottle labels and noting some strange geometrical designs drawn on the side of them, apparently indicating some sort of inherent structure to the chemical names which he could barely pronounce at the time. His high school chemistry teacher did not provide much insight into the drawings, merely stating they just represented atoms and how they were put together. Patrick’s interests in high school wandered to engineering, and thus he applied and was accepted into the mechanical engineering program at North Carolina State University in the fall of 2001.

Patrick’s first year at college was tumultuous to say the least. He applied and was accepted into the mechanical engineering program, but quickly switched to the

biomedical engineering programs within the first weeks of school. This change would prove to be the most life altering decision of his life as the curriculum called for two semesters of organic chemistry. Intimidated by the floating rumors in the student body, Patrick did not know what to expect from the weird world of chemistry which he had no real background in. Fortunately for him, organic chemistry just “clicked” for him. By the end of the first semester, he could now look back and interpret the strange drawings he remembered from his days in the pharmacy. From here on he sought to learn more about chemistry and how it affected the world around him.

Patrick graduated cum laude from NC State in the spring of 2005. His undergraduate research had led him to the field of polymer chemistry and he decided to come to the University of Florida to join the Wagner group. Fortunately, the summer prior to graduate school found Patrick without a job. Dr. Michael Scott at UF offered Patrick a position in his lab to work. Therefore, the day after his graduation from college, Patrick packed up and moved down to Florida. Working in the lab with the Scott group proved to be a wonderful experience for him, and he decided to switch from polymers to inorganic chemistry as a specialty. After graduation, Patrick will be moving to Oak Ridge, Tennessee to continue his studies as a post-doctoral fellow at the Oak Ridge National Laboratories under the supervision of Dr. Sheng Dai.